Studies on polysaccharide hydrolase-mediated transglycosylation and itsmechanism

THESIS

Studies on polysaccharide hydrolase-mediated transglycosylation and its mechanism

Takeshi Hattori

Graduate School of

Science and Technology, Educational Division

Department of Bioscience

Shizuoka University

January 2013

THESIS

Studies on polysaccharide hydrolase-mediated transglycosylation and its mechanism

（多糖水解酵素を介した糖転移反応とその機作に関する研究）

服部　武史

静岡大学

大学院自然科学系教育部

バイオサイエンス専攻

２０１３年１月

Contents

General Introduction

Oligosaccharides and polysaccharides are key biomolecules in essentially all living organisms. They have multiple functions including serving as structural components of cell walls, energy storage, cell recognition, regulation of signaling, cell differentiation, cell proliferation, immune response, bacterial and viral infection.[1,2] These compounds are structurally composed of monosaccharide residues linked through glycosidic linkages, which have very complicated structures owing to not only a variety of the monosaccharide structures but also the differences in regio- and stereotypes of the glycosidic linkages.[3-5] The structural diversity is greatly exceeding the diversity of proteins (oligopeptides) and nucleic acids (oligonucleotides).[6] Hence, the complexity of their structures makes the development of efficient and general synthetic routes difficult and major challenge. In past decades, the need for new carbohydrate materials and the development of glycomics have provided a boost to carbohydrate chemistry. Chemical methods for obtaining oligosaccharides have been developed.[7] However, they involve various elaborate procedures for protection, glycosylation, and deprotection strategies often lead to low yields and increased costs, particularly with longer oligosaccharides. Furthermore, perfect control of the regio- and stereochemistry of glycosylation is still a difficult problem. Enzymatic synthesis is alternative approach for obtaining the biomolecules. The method requires no elaborate procedures such as protection and deprotection of corresponding substrates and the reaction takes place under mild conditions. In general, living organisms synthesize oligosaccharides and polysaccharides from uridine diphosphate sugar substrates through glycosyltransferases-catalyzed reactions.[8, 9] These enzymes catalyze efficient and specific transfer of a monosaccharide from a sugar nucleotide donor to an acceptor and have been used as catalysts for *in vitro* synthesis of carbohydrates. But both the enzymes and the sugar nucleotides are expensive and the reactions are often subject to feedback inhibition from the nucleoside phosphate that is generated during the reaction. On the other hand, glycosidases have been also used to prepare oligosaccharides *via* transglycosylation[10-12] and condensation reactions.[13] The glycosidase-catalyzed syntheses have attracted much attention in recent years, as the widespread glycosidases are usually easy

to obtain, capable of taking readily available and relatively inexpensive donor substrates. Therefore, glycosidases have been considered a powerful tool for the practical synthesis of oligosaccharides.[14, 15] *Exo*-glycosidases, which transfer non-reducing terminal mono-saccharide from a donor to an acceptor, have been applied to the synthesis of oligosaccharides through transglycosylation reaction. However, contrary to glycosyltransferases, *exo*-glycosidases exhibit a rather poor regioselectivity. In general, the translgycosylation reaction mostly results in complex mixtures and the primary hydroxyl group reacts preferentially to the secondary ones, yielding 1,6-linked products.[10] On the other hand, *endo*-glycosidases also used as a tool for the synthesis of oligosaccharides. *Endo*-glycosidases are one of the general types of glycosidases and hydrolyze internal glycosidic bonds of oligosaccharide and polysaccharide chains, resulting in the release not of monosaccharides, but oligosaccharides. The enzymes often exhibit strict regioselectivity for the proper hydroxyl group of the acceptor on the glycosidic linkage formed by their tranglycosylation reactions.

In this study, enzymatic syntheses of short-chain glycans and glycosides have been developed *via* a non-biosynthetic pathway through polysaccharide hydrolase (*endo*-glycosidase)-mediated transglycosylations. The strategy is very simple as follows: (1) utilization of non-modified and commercially available *endo*-glycosidases, (2) utilization of non-activated substrates, (3) enzymatic transglycosylation in aqueous system for stringent regio- and stereoselection, which is an example of 'green chemistry'. Furthermore, the synthetic short-chain glycans and glycosides were used for explaining the hydrolytic mechanism of *endo*-glycosidase on glycan.

Abbreviations

GlcNAc: *N*-acetyl-D-glucosamine

*p*NP: *p*-nitrophenyl

Glc: D-glucose

Gen_2: gentiobiose

Gen_3: gentiotriose

Gen_4: gentiotetraose

Gen_5: gentiopentaose

Gen_6: gentiohexaose

Gen_7: gentioheptaose

Gen_8: gentiooctaose

Gen_9: gentiononaose

Glc β-*O*Me: methyl β-D-glucoside

Gen_2 β-*O*Me: methyl β-gentiobioside

Gen_3 β-*O*Me: methyl β-gentiotrioside

Gen_4 β-*O*Me: methyl β-gentiotetraoside

Gen_5 β-*O*Me: methyl β-gentiopentaoside

Gen_6 β-*O*Me: methyl β-gentiohexaoside

Glc β-*p*NP: *p*-nitrophenyl β-D-glucoside

Gen_2 β- *p*NP: *p*-nitrophenyl β-gentiobioside

Gen_3 β- *p*NP: *p*-nitrophenyl β-gentiotrioside

Gen_4 β- *p*NP: *p*-nitrophenyl β-gentiotetraoside

Gen_5 β-*p*NP: *p*-nitrophenyl β-gentiopentaoside

Gen_6 β-*p*NP: *p*-nitrophenyl β-gentiohexaoside

MALDI-TOF mass: matrix-assisted laser desorption ionization–time of flight mass spectrometry

NMR: nuclear magnetic resonance

XRD: X-ray diffraction

HPLC: high performance liquid chromatography

HPAEC-PAD: High-pH anion-exchange chromatography with pulsed amperometric detection

CP/MAS: cross polarization/magic angle spinning

ESI-MS: electrospray ionization mass spectrometry

DP: degree of polymerization

Chapter I

Enzymatic synthesis of an α-chitin-like substance *via* lysozyme-mediated transglycosylation

1. Introduction

Chitin, a linear polymer of β-(1→4)-linked GlcNAc, is most abundant bioresource after cellulose. The biopolymer serves as crucial structural component in many life forms throughout the natural world. Chitin has been of interest due to its remarkable biological activities and utilities.[1,2] Recently, the self-assembly and hierarchical features of the chitin molecules have attracted considerable interest in the field of biomaterials.[3,4] The specific intra/intermolecular hydrogen bonds and stereoregular packing of chitin chain assemblies result in high chemical resistance and poor solubility in commonly used solvents. Hence, standard synthetic methods are unsuitable for producing these biopolymers.

It is known that the natural chitin is partially N-deacetylated in the glycan chain, but the degree of deacetylation varies depending upon its biological origin.[5] Generally, chitin is synthesized *via* a biosynthetic pathway mediated by chitin synthase (EC 2.4.1.16). Chitin synthases using uridine diphosphate *N*-acetyl-D-glucosamine (UDP-GlcNAc) as substrate produce chain lengths of 100 or more GlcNAc residues.[6] Therefore, *in vitro* synthesis of chitin using a glycosyl hydrolase is a alternative approach to prepare chitin. The use of a glycosyl hydrolase as a catalyst for the selective synthesis of complicated polysaccharides has become a hot topic in glycotechnology.[7,8] Kobayashi *et al.*[9,10] have reported the *in vitro* synthesis of artificial chitin by utilizing an enzymatic glycosylation of a chitobiose oxazoline derivative catalyzed by chitinase. The excellent method was achieved by using activated substrate. We used ammonium sulfate to successfully generate $(GlcNAc)_6$ and $(GlcNAc)_7$ from $(GlcNAc)_2$/$(GlcNAc)_4$ by utilizing chitinolytic enzymes.[11,12] However, this represents a limited synthesis of higher chitinoligomers up to DP 7 from the lower oligomers. If we would represent *in vitro* synthetic method obtaining more elongated chitinoligomers, it may lead to elucidation of process of chitin to highly ordered crystal structure.

The present paper describes the enzymatic synthesis of highly ordered chitin-like substance *via* a non-biosynthetic pathway through lysozyme-mediated transglycosylation. Our strategy is very simple as follows: 1) utilization of non-modified and commercially available lysozyme, 2) utilization of non-

activated substrate, 3) enzymatic transglycosylation in aqueous system for stringent regio-/stereo selection and green chemistry. Our method enables the production of non-deacetylated chitin without special techniques. The resulting chitin substance was then characterized by MALDI-TOF mass spectrometry, solid-state ^{13}C NMR spectroscopy, and XRD analysis.

2. Results

2.1. Lysozyme-mediated transglycosylation with $(GlcNAc)_3$

A transglycosylation was carried out with high concentration of $(GlcNAc)_3$ (32 mM) as an initial substrate and hen-egg white lysozyme (1,000 kU). When the enzyme was incubated with $(GlcNAc)_3$, the initially homogenous solution gradually became turbid, and eventually formed a gel-like precipitate, which was centrifuged, suspended in 50% ethanol containing urea and dithiothreitol, and washed with 50% ethanol. The time needed to generate a precipitate from $(GlcNAc)_3$ upon incubation at 40 °C was examined by measuring the turbidity of the solution as shown in Figure 1. Reaction mixtures containing different concentrations of ammonium sulfate were initially studied. The increase in turbidity was greater as the salt concentration in the reaction mixture increased and the total yield of product also went up when the reaction was performed at higher salt levels. The time required for the turbidity to reach a maximum value at 30, 20, 10 and 0% ammonium sulfate was 96, 72, 48 and 24 h, whereas the maximum product yield was 12.9 mg (32.3%), 8.1 mg (20.3%), 4.4 mg (11.0%) and 3.1 mg (7.8%), respectively, as in Table 1. In each case the concentration of product reached a maximum and then gradually decreased with extended reaction time. The maximal precipitates obtained at different salt concentrations were treated with $NaBH_4$ to give a series of chitooligosyl alditols. The aqueous suspension became completely clear during this reaction. The reduced products were then analyzed by HPLC. Reduction of the products was necessary because it is very difficult to analyze the original chitin oligosaccharides of DP > 8, which are slightly soluble in water. Figure 2 shows the elution pattern of the reduced products at different salt concentrations. The chromatogram showed eight peaks (G_6 -G_{13}), corresponding to a DP 6-13 of the sugar alcohols of $(GlcNAc)_6$-$(GlcNAc)_{13}$. At 30% salt, two main

peaks at G_7 and G_8 corresponding to $(GlcNAc)_7$ and $(GlcNAc)_8$ respectively, appeared with two minor peaks at G_6 and G_9. In addition, the change in composition with time in a water-soluble part was analyzed by the same method as in Figure 3. In the initial stage, once $(GlcNAc)_4$ reaches its maximum, the amount rapidly decreases during the subsequent reaction with utilization of $(GlcNAc)_3$ substrate. In the absence of salt, peaks G_{10}-G_{13} also appeared, corresponding to $(GlcNAc)_{10}$-$(GlcNAc)_{13}$, respectively. Thus, a chitinoligomer with a maximum of DP 13 was generated in this reaction. In addition, the maximum products at different salt concentrations were also directly applied to MALDI-TOF mass spectrometry as shown in Figure 4. At 30% salt, two main peaks with *m/z* values of 1463 and 1666 were observed as molecular ions corresponding to $[M + Na]^+$ species of $(HexNAc)_7$ and $(HexNAc)_8$, respectively. Two minor peaks were also present with an *m/z* of 1260 and 1869, corresponding to $(HexNAc)_6$ and $(HexNAc)_9$, respectively. Additional peaks also gradually emerged as the salt level was reduced with *m/z* values of 2072, 2275, 2478, 2681 and 2884 corresponding to $(HexNAc)_{10\sim14}$. The spectrum clearly shows that the synthetic products correspond to a sugar-linked substance. Notably, each signal in the series differs by a mass value corresponding to the molecular weight of an anhydrous *N*-acetylglucosamine molecule. Our findings clearly show that the addition of ammonium sulfate to the reaction mixture resulted in the preferred formation of $(GlcNAc)_7$ and $(GlcNAc)_8$. However, when the reaction was performed in the absence of salt a broad distribution of products was generated i.e., up to DP 14. The precipitate produced by the lysozyme-mediated reaction was identified as a chitin-like substance as described below. It should be noted that the peak intensities corresponding to the respective DP values as determined by MALDI-TOF mass spectrometry are very similar to those arising from the elution profiles of the HPLC analyses (Figures 2 and 4). This observation suggests that mass spectrometry can be used as a quick guide for determining the proportion of oligomer corresponding to DP in the product.

2.2. Preparation of chitin-like substance

The enzyme reaction without ammonium sulfate was in fact carried out on a synthetic scale with 1 g of $(GlcNAc)_3$ to yield 120 mg precipitate. The structure of the resulting precipitate was analyzed by MALDI-TOF mass spectrometry, cross polarization/magnetic angle spinning (CP/MAS) solid-state ^{13}C NMR, and XRD analyses (Figures 5-7). In MALDI-TOF mass spectrometry, a series of peaks corresponding to $(HexNAc)_{6\sim15}$ were observed as molecular ions. Analysis of the results confirmed the formation of a more extended chitooligomer with a DP as high as 15 (Figure 5). The solid-state ^{13}C NMR and XRD patterns of the precipitate were very similar to that of natural α-chitin, in which all the glycan chains adopt an anti-parallel arrangement.[13,14] Thus, the NMR spectrum showed the six signals at 104.5, 83.5, 76.1, 73.8, 61.3, and 55.5 ppm corresponding to the carbons C1, C4, C5, C3, C6 and C2 of GlcNAc unit, respectively (Figure 6). Signals of the carbonyl carbon and the methyl carbon were observed at 173.8 and 23.2 ppm respectively. These results clearly indicate that glycosidic bond formation occurs in a regio- and stereo-selective manner between GlcNAc units during the polymerization to afford a stereoregular chitin product with β-(1→4) linkages. XRD analysis of the precipitate also showed sharp peaks at $2\theta = 9.28$ and 19.16 (Figure 7). This signature is characteristic of α-chitin and is readily distinguishable from β-chitin, in which all the chitin chains adopt a parallel arrangement.[13-15] The sharp peaks indicated that the precipitate has a highly ordered α-chitin structure with high crystallinity.

3. Discussion

There are several ways to manipulate enzymatic reactions of glycosidases to favor synthesis over hydrolysis, e.g., the use of high salt concentrations or organic solvents.[16] Previously we have used ammonium sulfate to promote the formation of $(GlcNAc)_6$ and $(GlcNAc)_7$ from $(GlcNAc)_2$ and synthesized *p*NP-$(GlcNAc)_5$ from $(GlcNAc)_5$ and *p*NP-GlcNAc in 50% DMSO using hen-egg white lysozyme-mediated transglycosylation.[12,17] Rupley[18] has reported that the rate of hydrolysis of $(GlcNAc)_2$ compared with $(GlcNAc)_3$ (at 1.0) was 0.003, whereas those on $(GlcNAc)_4$, $(GlcNAc)_5$ and $(GlcNAc)_6$ were 8, 4,000 and 30,000, respectively. $(GlcNAc)_2$ itself is cleaved only very slowly because

it is bound largely in a nonproductive mode. The lysozyme-mediated transglycosylation of $(GlcNAc)_2$ in aqueous media required both a high temperature and high enzyme concentration.[12] Thus, the reaction at 70 °C provided $(GlcNAc)_6$ and $(GlcNAc)_7$ as major products, but that at 40 °C was little proceeded. In contrast, the transglycosylation reaction of $(GlcNAc)_3$ as an initial substrate occurred at much milder conditions than that of $(GlcNAc)_2$ as mentioned below. For these reason, we employed $(GlcNAc)_3$ as an initial substrate to raise reaction efficiency in the present study. In different concentration of salt, turbidities of all reactions reached a maximum and then gradually decreased with extended reaction time. This is caused by depletion of soluble lower substrates that involve in further elongation reaction and gradual hydrolysis of insoluble transglycosylation products. When an high concentration of $(GlcNAc)_3$ substrate was reacted at 40 °C with a large amount of hen-egg white lysozyme in the absence of ammonium sulfate, a more extended chitinoligomer product of up to DP 6-15 was generated. In contrast, the reaction at 30% ammonium sulfate resulted in a relatively narrow distribution of products i.e., preferred formation of chitinoligomer of DP 7 and 8. The yield and corresponding DP distribution of synthesized chitinoligomers were found to be highly dependent on the salt concentration of the reaction mixture. The mechanism of preferred formation of $(GlcNAc)_7$ and $(GlcNAc)_8$ from $(GlcNAc)_3$ at a high salt concentration was estimated as in Scheme 1. Thus, $(GlcNAc)_4$ formation through transfer of the *N*-acetylglucosaminyl residue to $(GlcNAc)_3$ is a rate-limiting step in the overall process of transglycosylation, because as enough amount of the tetramer build up, the formation of the heptamer and octamer is initiated. In this case, once $(GlcNAc)_4$ reaches its maximum, the amount rapidly decreases during the subsequent reaction. As a result, the sugar chain-elongation reaction from the trimer proceeds in sequence to produce $(GlcNAc)_5$ and $(GlcNAc)_6$, which may act as main carriers in a series of reactions for formation of heptamer and octamer. Finally, when $(GlcNAc)_7$ and $(GlcNAc)_8$ are produced by transglycosylation, most of them precipitate out to separate the desired compounds during the reaction. Because the heptamer and octamer are only slightly soluble in the described medium, there is less probability that is attacked by the enzyme. On the other hand, the reaction in the absence of the salt is shown to produce a more extended chtinoligomer. It suggests that, once $(GlcNAc)_7$ and

$(GlcNAc)_8$ produced, they are attacked by the enzyme to act as carriers for formation of the more extended higher oligomers. The transglycosylation process might be reinforced by the solubility of higher chitinoligomer in the medium because the heptamer shows about 0.1 % solubility in the absence of ammonium sulfate and only slightly soluble in a medium containing 30% salt.

As a result, the chain-elongation reaction without the salt was used for the synthesis of the chitin-like substance. Solid-state ^{13}C NMR analysis revealed the substance was chitin-like polymer and the lysozyme-mediated transglycosylation occurred in regio-/stereo-selective manner. The synthetic chitin-like substance was shown to adopt a highly ordered α-chitin structure by solid-state ^{13}C NMR and XRD analyses. The sharp peak in both analyses indicates that the artificial chitin had a higher level of crystallinity than native α-chitin. The ^{13}C NMR and XRD pattern were also very similar to that of a crystal product of α-chitin generated by chitinase-catalyzed polymerization of a chitobiose oxazoline derivarive.[10] The elongation reaction in an aqueous medium produces a more extended chitinoligomer before crystallization occur to give a highly ordered α-chitin-like substance as a result of self-assembly *via* oligomer-oligomer interactions during precipitation. The present method allows the production of the perfectly *N*-acetylated chitins. In general, it is very difficult to obtain such chitin, because native chitins normally requires an acid or alkaline treatment, causing the generation of partially N-deacetylated chitins.[19] In a similar reaction, we have recently reported the synthesis of gentiooligosaccharides (DP 9) from gentiotriose using β-(1→6)-glucanase from *Penicillium multicolor*.[20] In this study, one-pot synthesis of artificial chitin was achieved by means of endo-glycosidase, lysozyme-catalyzed polymerization of trisaccharide. Further studies are necessary to understand exactly how crystallization can occur in the abiogenic production of the glycans. The present finding may provide clues for determining the shape of crystals and molecular organization into a higher-ordered structure, but also for further understanding of *in vivo* biosynthesis mechanism leading to native chitin formations.

In conclusions, lysozyme-mediated transglycosylation using the corresponding unactivated trisaccharide as starting substance resulted in the production of a significant amount of higher chitin oligosaccharides with a DP of up to 15. In addition, once produced in a higher oligomer form, the oligosaccharides immediately assemble to adopt a highly ordered α-chitin-like substance with quite high crystallinity. Thus, we have developed a novel enzymatic synthetic method for obtaining artificial chitin.

4. Experimental

4.1. Materials

$(GlcNAc)_3$ and crab chitin were kindly provided by Yaizu Suisan Kagaku Industry Co., Ltd. (Shizuoka, Japan). The hen-egg white lysozyme recrystallized six times was purchased from Seikagaku Biobusiness Co. (Tokyo, Japan). All other commonly used chemicals were obtained from commercial sources.

4.2. Analytical methods

MALDI-TOF mass spectra were obtained using on an AutoFlex (Bruker Daltonics, Bremen, Germany). The spectra were measured in the positive reflection mode with 10 mg/mL 2,5-dihydroxybenzoic acid in H_2O/ethanol 70:30 as the matrix solution. The sample solutions were mixed with the matrix solution (1:4 v/v) and then a 1 μL droplet was applied to a stainless target plate and dried at room temperature. A mass calibration procedure was employed prior to the analysis of samples using peptide calibration standard II (Bruker Daltonics). HPLC analysis was performed using a Hitachi L-7000 HPLC system (Hitachi, Tokyo, Japan) equipped with a Unison UK-C18 column (4.6 × 250 mm, 3 μm; Imtakt Corporation, Kyoto, Japan) at 45 °C. Bound substance was eluted using the following gradient: 0-20 min, ratio of eluent A (deionized water) was decreased to 85.0% (v/v) from 99.9% (v/v), ratio of eluent B (methanol) was increased to 15.0% (v/v) from 0.1% (v/v); 20-35 min, 99.9% (v/v) eluent A, and 0.1% eluent B. The elution was monitored at 210 nm and the flow rate was 0.7 mL/min. The solid-state ^{13}C NMR experiment was carried out on a Chemagnetics CMX Infinity 400 MHz (9.05

T) wide-bore magnet spectrometer operating at room temperature. A double resonance magic-angle spinning (MAS) probe equipped with a 4-mm spinning module was used. The sample was restricted to approximately 20 mg in the rotor to increase the ratio frequency field homogeneity. Spectra were acquired with cross-polarization MAS (CPMAS) techniques using a contact time of 100 μs for synthetic chitin samples. The recycle delay was set to 4.0 s. Total number of acquisitions were collected 50,000 times for chitin. Proton decoupling fields of ca. 83 kHz were employed in these experiments together with a spinning speed of 12.0 Hz. Spectra were calibrated through the methyl carbon resonance of hexamethylbenzene as an external reference at 17.35 ppm. XRD were obtained with Cu-Kα from a powder XRD generator (JDX3530; Japan Electronic Organization Co. Ltd., Tokyo Japan) operating at 30 kV and 30 mA.

4.3. Enzyme assay

Lysozyme activity was determined by measuring turbidity changes in bacterial cell suspensions of *Micrococcus lysodeikticus* (0.2 mg/mL) in 100 mM phosphate buffer pH 7.0 at 30°C as previously reported by Saint-Blancard.[21] Absorbance of the suspension was measured at 450 nm, and a decrease in absorbance of 0.001 was defined as 1 unit of lysozyme activity.

4.4. Analysis of lysozyme-mediated transglycosylation

Analysis of the time course of transglycosylation and characterization of the resulting products was performed by five different methods as outlined below.

4.4.1. Turbidity

The lysozyme-mediated reaction mixture (20 μL) was mixed with H_2O (180 μL). The solution was homogenized by sonication and the absorbance at 660 nm was measured.

4.4.2. HPLC

Artificial chitin solution (50 μL, 5 mg/mL) was mixed with sodium borohydride solution (50 μL, 10 mg/mL) and reduced for 30 min with sonication at room temperature. The reaction was quenched by addition of 1 M HCl (15 μL) to the reaction mixture. The mixture was then incubated for 15 min with sonication immediately prior to analysis by HPLC (described above).

4.4.3. MALDI-TOF mass spectrometry, solid-state ^{13}C NMR spectroscopy, and XRD

Synthetic chitin was directly analyzed by MALDI-TOF mass spectrometry, solid-state ^{13}C NMR spectroscopy, and XRD without derivatization.

4.5. Identification of chitooligosyl alditol

Chitooligosyl alditols were identified in the chitin obtained from the enzyme reaction by first reducing the sample and then analyzing by HPLC according to the procedure mentioned earlier. The eluate was collected for 5 ~ 25 minutes. The collected solution was then concentrated, lyophilized and applied to MALDI-TOF mass analysis as described in the analytical methods. The corresponding chitooligosyl alditols were observed as molecular ions arising from the $[M + Na]^+$ ions (data not shown). Mass of the each molecular ion was increased by 2 amu compared to the corresponding untreated artificial chitin. This result confirms the addition of two protons to the anomeric carbon atom arising from reduction of the reducing terminals in the artificial chitin.

4.6. Transglycosylation with $(GlcNAc)_3$ by lysozyme

$(GlcNAc)_3$ (40 mg) was dissolved in 2 mL of 0.1 M acetate buffer (pH 3.8) containing various concentrations of ammonium sulfate (0 ~ 30% w/v). Each solution was added to 10 mg (1,000 kU) of hen-egg white lysozyme. The mixture was then incubated at 40 °C until the turbidity of the reaction mixture had reached a maximum value. The precipitates which formed in the reaction mixtures were centrifuged off, suspended in 8 mL of 8 M urea in ethanol/40 mM Tris-HCl buffer (pH 8.5) 1:1 containing 10 mM dithiothreitol, and then kept for 1 h at 37 °C. The mixtures were again clarified by centrifugation. The precipitates were washed 5 times with 5 mL of H_2O/ethanol 1:1, suspended in an appropriate volume of H_2O and lyophilized. The resulting products were directly analyzed by MALDI-TOF mass spectrometry, solid-state ^{13}C NMR spectroscopy and XRD. HPLC analysis of the products was performed after reducing the samples as mentioned above.

For analysis of water-soluble part of the reaction at 30% ammonium sulfate, the reaction mixture was filtrated with 0.45 μm filter. The filtrate (10 μl) was diluted with H_2O (40 μl) and then analyzed by HPLC after reducing.

4.7. *In vitro* preparation of chitin-like substance

Chitin was synthesized as follows. $(GlcNAc)_3$ (1.0 g) was dissolved in 50 mL of 0.1 M acetate buffer (pH 3.8) and then added to 250 mg (25,000 kU) of hen-egg white lysozyme. The solution was kept for 24 h at 40 °C without addition of salt. The precipitate formed in the reaction mixture was centrifuged, washed 3 times with 25 mL of H_2O/ethanol 1:1 at 4 °C and then dried *in vacuo* to afford 120 mg of substance. The artificial chitin was directly applied to MALDI-TOF mass spectroscopy, solid-state ^{13}C NMR spectroscopy, and XRD.

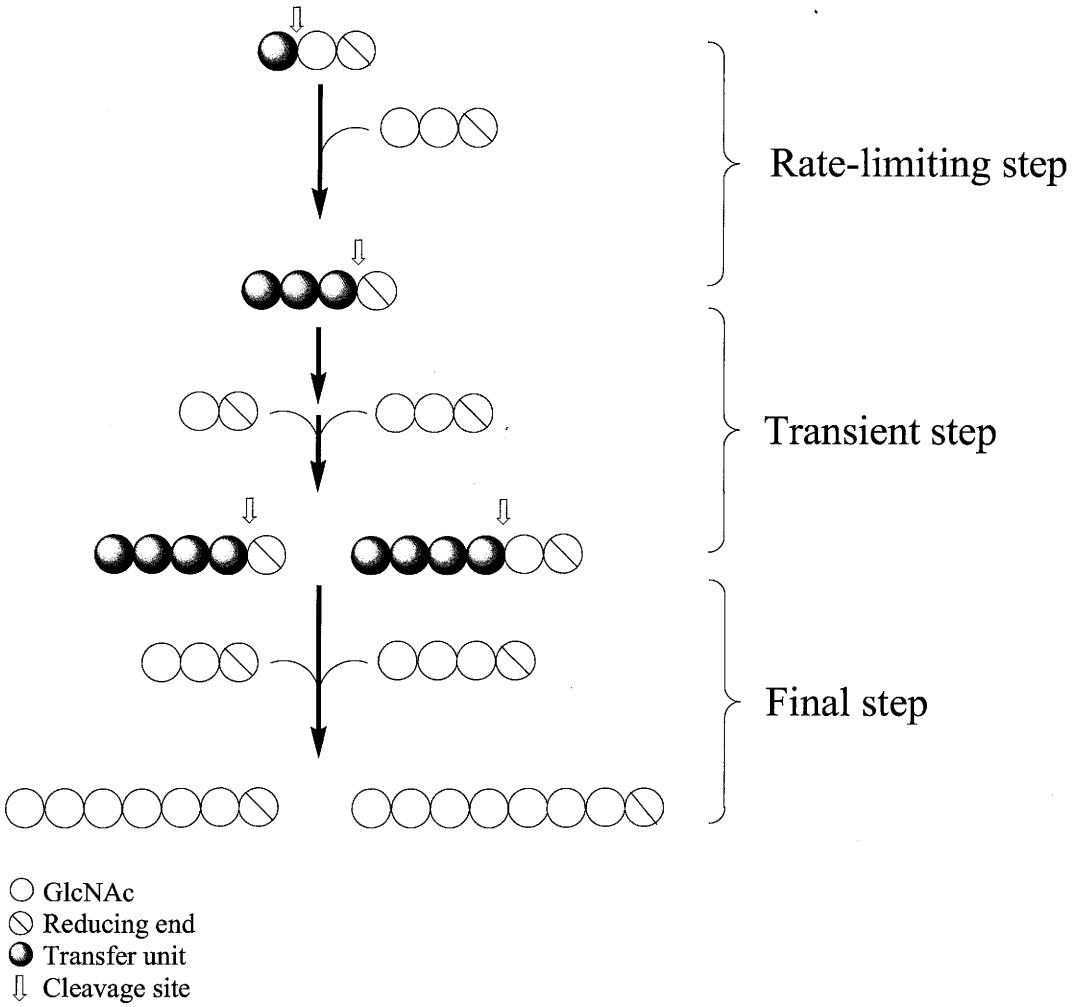

Scheme 1. Proposed mechanism of the preferred formation of $(GlcNAc)_7$ and $(GlcNAc)_8$ from $(GlcNAc)_3$ in aqueous system containing 30% ammonium sulfate.

Table 1. Transglycosylation reaction using $(GlcNAc)_3$ as an initial substrate in aqueous system containing various concentrations of ammonium sulfate. The reaction was carried out at 40 °C. The yield is given as 50% ethanol-insoluble part

$(NH_4)_2SO_4$ (%)	time (h)	yield (%)
0	24	7.8
10	48	11.0
20	72	20.3
30	96	32.3

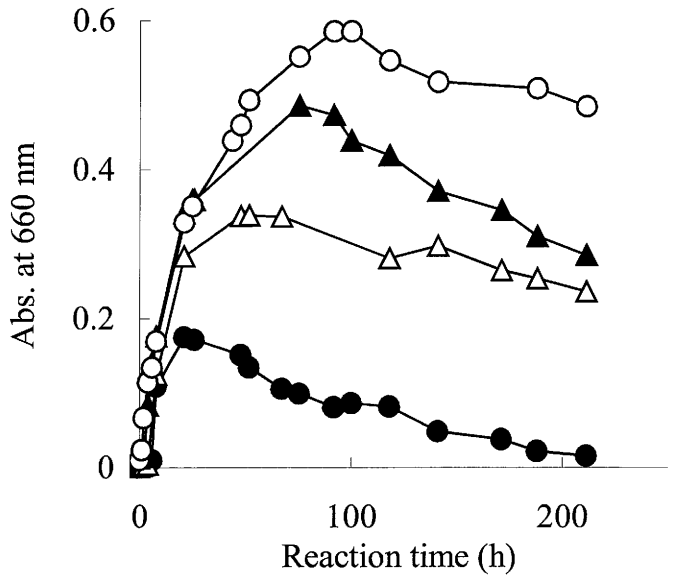

Figure 1. Time course of the turbidity assay for the lysozyme-mediated reaction using $(GlcNAc)_3$ as the initial substrate. The reactions were carried out at 40 °C in different concentrations of ammonium sulfate. Filled circle, 0%; open triangle, 10%; filled triangle, 20%; open circle, 30%.

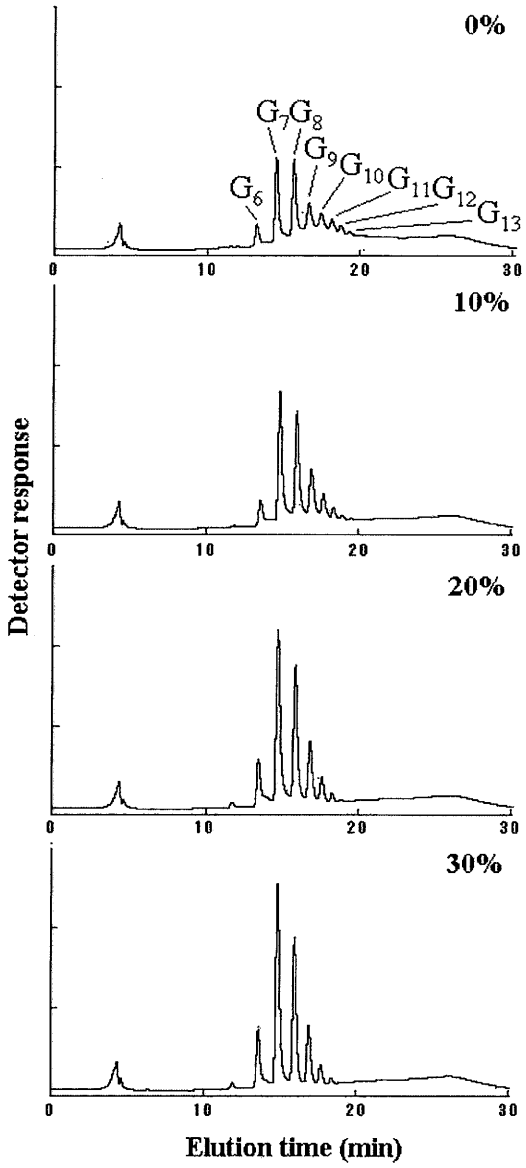

Figure 2. HPLC profiles of the transglycosylation products using $(GlcNAc)_3$ at 0, 10, 20 and 30% ammonium sulfate. The reaction products were washed with 50% ethanol, lyophilized, and reduced with $NaBH_4$ for HPLC analysis. The elution positions of G_6-G_{13} corresponding to a series of chitooligosyl alditols (DP 6 ~ 13) are shown.

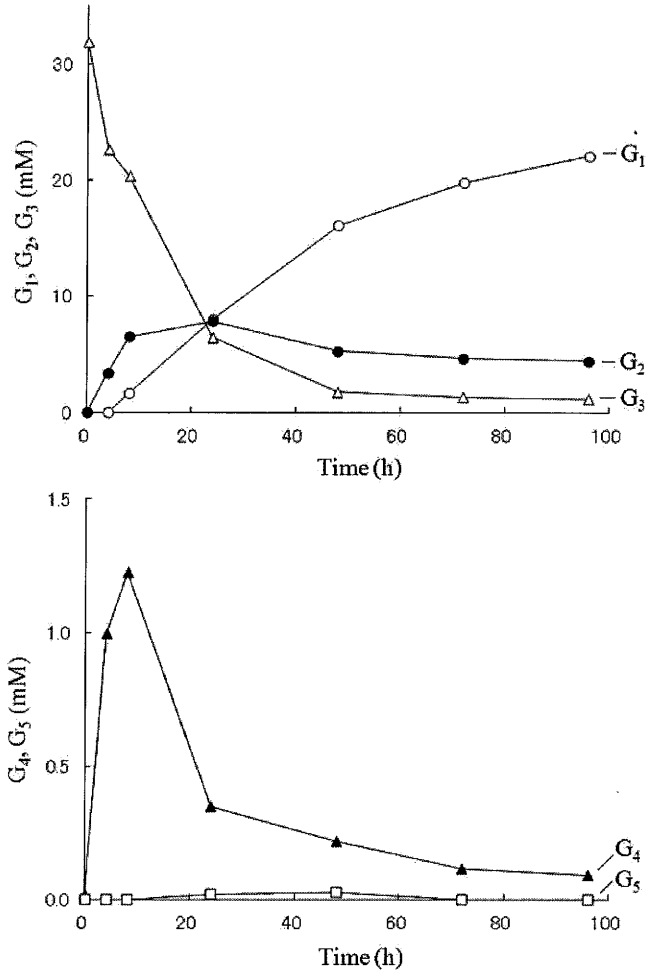

Figure 3. Formation of products of the lysozyme-mediated reaction on $(GlcNAc)_3$. The enzyme reaction was performed with 30% ammonium sulfate at 40 °C and a water-soluble part was analyzed by HPLC after reducing with $NaBH_4$. G_1 and G_2-G_5 indicate *N*-acetylglucosaminitol and a series of chitooligosyl alditols (DP 2 ~ 5), respectively.

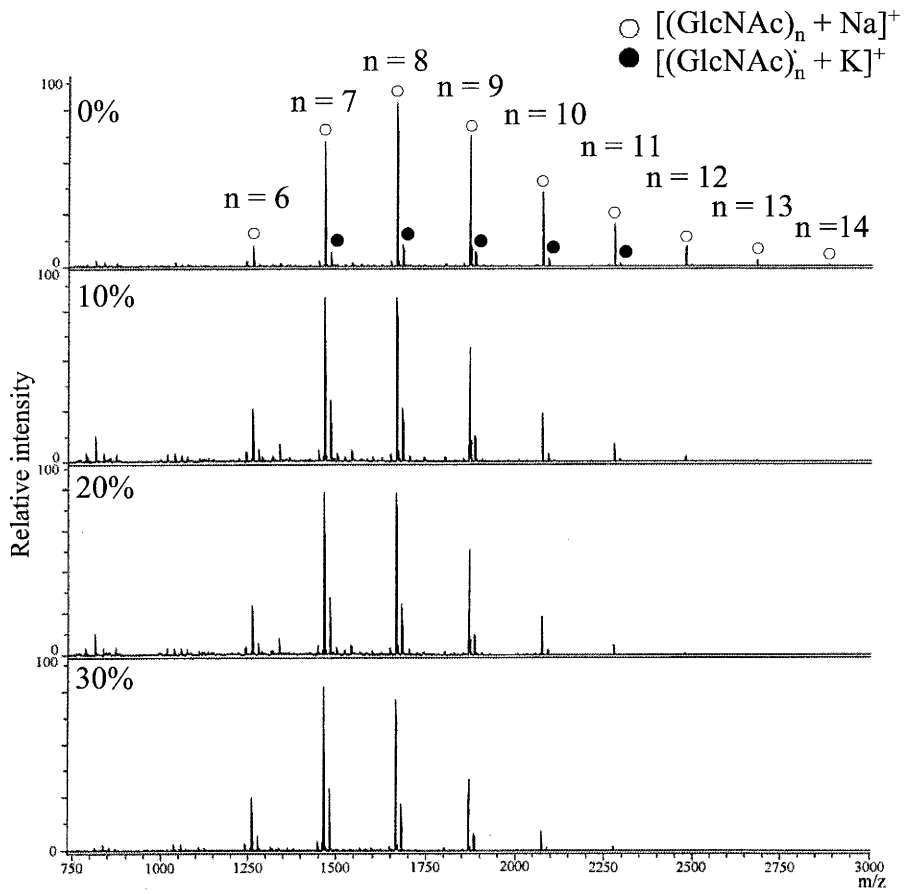

Figure 4. MALDI TOF-mass spectra of the lysozyme-mediated translycosylation products using $(GlcNAc)_3$ at 0, 10, 20, and 30% ammonium sulfate.

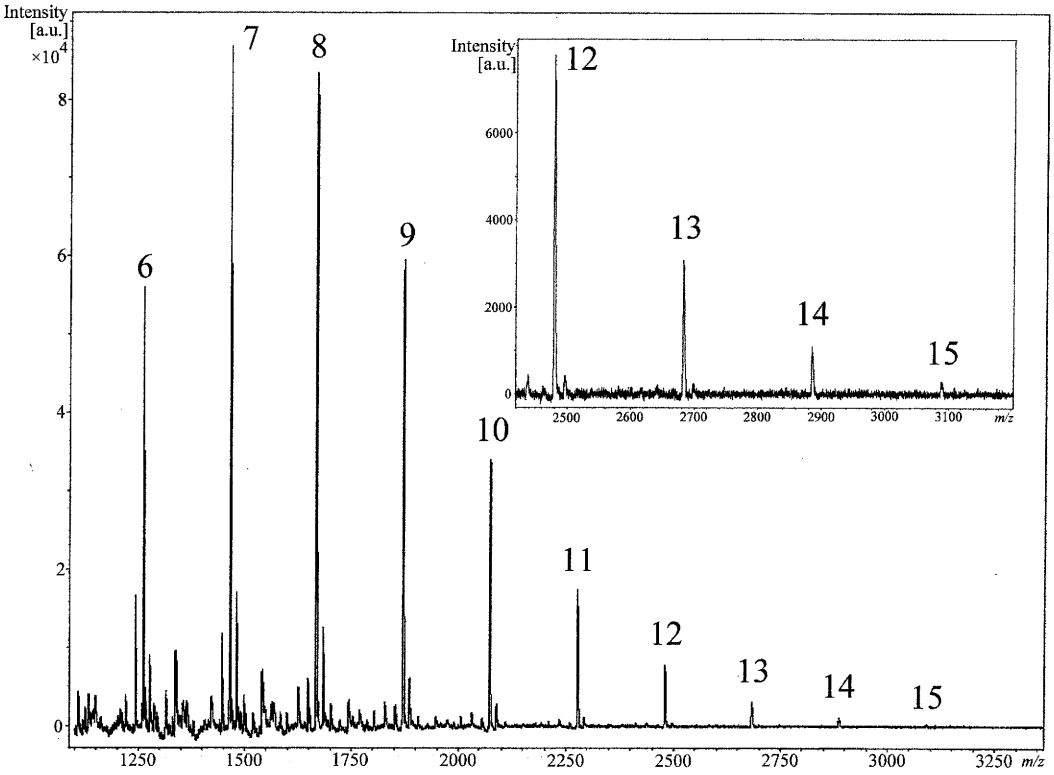

Figure 5. MALDI-TOF mass spectum of the precipitate obtained by lysozyme-mediated transglycosylation.

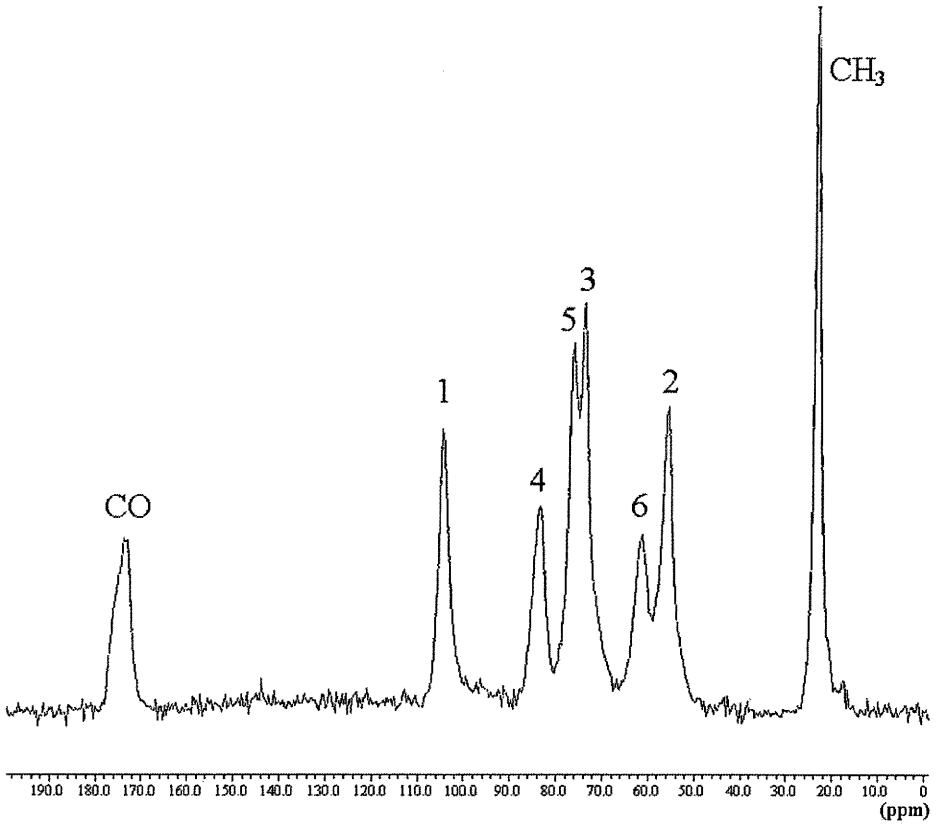

Figure 6. 1D CP/MAS ^{13}C NMR spectrum of the chitin-like substance obtained by lysozyme-mediated transglycosylation.

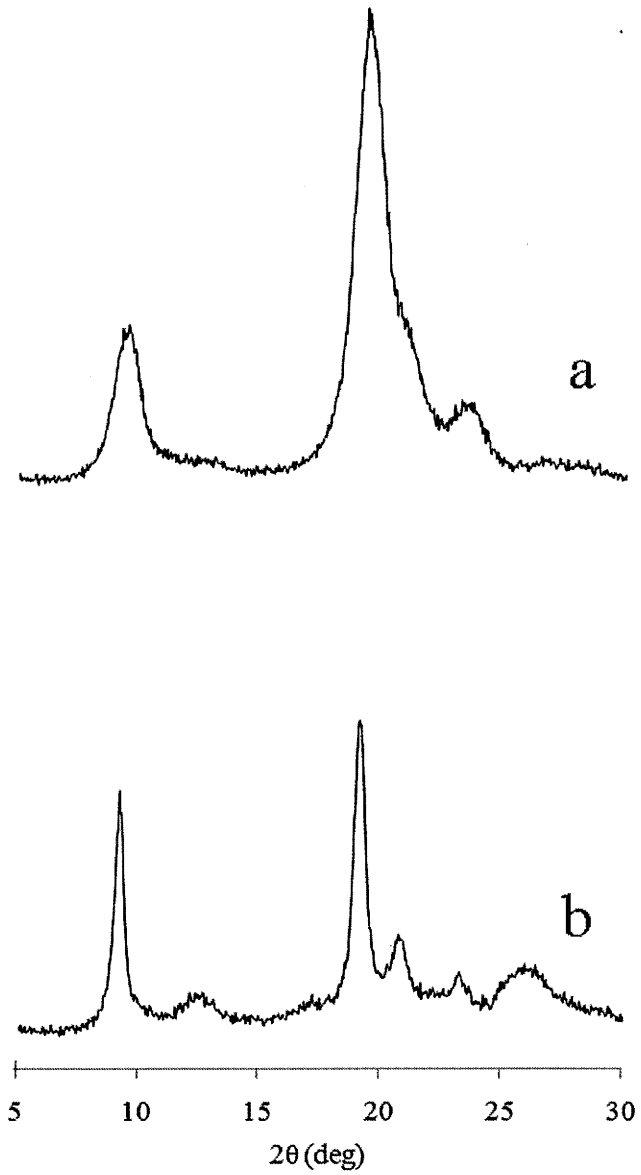

Figure 7. XRD patterns of (a) crab α-chitin and (b) chitin-like substance.

Chapter II

Enzymatic synthesis of cellulose II-like substance *via* cellulolytic enzyme-mediated transglycosylation in an aqueous medium

1. Introduction

Cellulose, which is the most ubiquitous and abundant biopolymer on earth, possesses a linear chain of β-(1→4)-glycosidic linked D-glucose units. This homo-polysaccharide serves as a crucial structural component in many life forms throughout the natural world.[1] Despite its relative chemical simplicity, the physical and morphological structure of native cellulose in higher plants is complex and heterogeneous.[2,3] Furthermore, cellulose chains are intimately associated with other polysaccharides and lignin in plant cell walls, resulting in even more complex morphologies.[4] Recently, the self-assembly and hierarchical features of the cellulose molecule have attracted considerable interest in the field of biomaterials.[5,6] The specific intra/intermolecular hydrogen bonds and stereoregular packing of cellulose chain assembly result in significant chemical resistance and poor solubility in commonly used solvents.[7] Hence, standard synthetic methods are unsuitable for producing the biopolymer.

So far, *in vitro* syntheses of cellulose using cellulose synthase (EC 2.4.1.12) as a catalyst have been reported.[8-13] These synthetic products from uridine diphosphate glucose always result in the formation of cellulose II, in which all the glycan chains adopt an anti-parallel arrangement.[14,15] Cellulose II is normally obtained by mercerization of cellulose I,[16] in which the cellulose chains adopt a parallel arrangement, or regeneration from cellulose I dissolved in solvent. The anomalous cellulose II has been also produced by microbes.[16,17] Recently, the use of a glycosyl hydrolase as catalyst for the selective synthesis of complicated polysaccharides has become a hot topic in glycotechnology.[18] The first *in vitro* synthesis of cellulose was reported as an enzymatic polymerization using β-cellobiosyl fluoride as substrate in an acetonitrile/acetate system.[19] This synthetic cellulose displayed the characteristic structure of cellulose II. The polymerization reaction of β-cellobiosyl fluoride catalyzed by a mutant cellulase has also been investigated.[20] As an alternative approach, the *in vitro* synthesis of cellulose I by means of a partially purified cellulase-catalyzed polymerization of β-cellobiosyl fluoride has also been reported.[21] However, introduction of fluoride onto anomeric center of cellobiose requires laborious synthetic process including protection and deprotection of the hydroxyl group. In contrast, the use of

cellobiose or cellotriose as a substrate is attractive for the synthesis, because it is easy to obtain their oligomers by partial acid hydrolysis of cellulose. Egusa and co-workers have recently reported the enzymatic polymerization of cellobiose to longer-chain cellulose.[22,23] This synthesis was successfully achieved by using a cellulase/surfactant complex in a non-aqueous medium. Hiraishi and co-workers prepared cellooligosaccharide with an average DP of 9 by cellodextrin phosphorylase and the product showed a cellulose II crystalline structure.[24]

The present paper describes the enzymatic synthesis of cellotriose to cellulose II-like substance *via* a non-biosynthetic pathway through EG I-mediated transglycosylation in an aqueous medium. The enzyme reaction was performed by using non-modified substrate and enzyme in an aqueous system without special techniques. The resulting cellulose substance was then characterized by MALDI-TOF mass spectrometry, solid-state ^{13}C NMR spectroscopy, and XRD analyses.

2. Results

2.1. EG I-mediated transglycosylation with cellobiose and cellotriose

In the present study, EG I from *H. jecorina* was used to catalyze a transglycosylation reaction with either cellobiose or cellotriose as substrate. When cellobiose was incubated with a large amount of EG I, water-soluble oligomers (G_3~G_6) were detected by HPAEC-PAD analysis (data not shown) but no water-insoluble product was obtained. The reaction solution using cellobiose as an initial substrate at 16 h was further analyzed by MALDI-TOF mass spectrometry, which showed a DP value of 7 had been achieved (Fig. 1A). Three main peaks with *m/z* values of 689, 851 and 1013 were observed as molecular ions corresponding to $[M+Na]^+$ species of $(Hex)_4$, $(Hex)_5$ and $(Hex)_6$, respectively. A minor peak was also present with *m/z* value of 1175 as molecular ion corresponding to $(Hex)_7$. MALDI-TOF mass analysis clearly shows that the synthetic products correspond to a sugar-linked substance with repeated signals at intervals corresponding to the molecular weight of an anhydrous glucose molecule. By

contrast, when the reaction was performed using cellotriose as substrate, the initially homogenous solution gradually became turbid and eventually formed a precipitate. The time required for the turbidity to reach a maximum was 1 h (data not shown). However, the aqueous suspension became completely clear with prolonged reaction time. The precipitate generated after 1 h was analyzed by MALDI-TOF mass spectrometry and the results are shown in Figure 1B. A series of peaks with a wide range of *m/z* values were observed corresponding to molecular ion $[M+Na]^+$ species of $(Hex)_{4\sim16}$ (i.e., up to DP 16). The precipitate produced by the EG I-mediated reaction was subsequently identified as β-(1→4)-glucan (see later results). In addition, we also analyzed the change in composition of the water-soluble fraction of the reaction mix by HPAEC-PAD (Fig. 2). The concentration of cellotetraose reached a maximum value after approximately 1 h but then the level rapidly decreased with extended reaction time. Furthermore, this sharp decrease in the concentration of cellotetraose was closely correlated with the rapid utilization of cellotriose substrate. The sequential generation of cellopentaose and cellohexaose was then observed, although the concentration of these two molecules gradually decreased with extended reaction. It is notable that cellooligomers of DP > 7, which are only slightly soluble in water, were not detected under the present reaction conditions.

2.2. Preparation of cellulose-like substance

The EG I-mediated transglycosylation using cellotriose as the initial substrate gave a maximum yield of water-insoluble product after a reaction time of 1 h. When the enzyme was incubated for 1 h with cellotriose (100 mg) the initially homogenous solution gradually became turbid and eventually formed a gel-like precipitate, which was centrifuged and washed three times with 50% methanol to afford 30 mg of product. The structure of the resulting precipitate was determined by MALDI-TOF mass spectrometry and solid-state ^{13}C NMR spectroscopy. MALDI-TOF mass analysis revealed a broad distribution of products i.e., up to DP 16 (Fig. 1B). The CP/MAS solid-state NMR spectrum of the precipitate was compatible with that of the structure of cellulose II, which was biosynthesized as a ^{13}C-enriched

cellulose by *Acetobacter xylinum*.[25-27] From the earlier data, each signal was easily assigned to the corresponding carbon atom of the glucose unit (Fig. 3). Thus, the spectrum enabled us to assign all carbon resonance lines of two kinds of anhydroglucose residues in the structure of cellulose II as previously reported.[26] The results of the ^{13}C resonance assignment of the two-anhydroglucose residues A and B in cellulose II are listed in Table 1. These data clearly indicate that glycosidic bond formation catalyzed by EG I occurs in a regio- and stereoselective manner between glucose units during the polymerization to afford a stereoregular cellulose product with β-(1→4) linkages. XRD analysis gave sharp peaks at 2θ = 12.22, 19.96 and 22.08, which are characteristic of type II cellulose (Fig. 4). The sharp peaks also indicate that the precipitate adopts a highly ordered structure with a high level of crystallinity.

3. Discussion

We have already reported that an endo-glycosidase from *H. jecorina* (EG I), which is a type of cellulase, catalyzes two types of reactions, condensation and transglycosylation.[28,29] In the present study, we demonstrate an alternative approach for the *in vitro* synthesis of a cellulose-like substance through the enzyme-mediated transglycosylation *via* a non-biosynthetic route. Interestingly, the reaction of EG I with cellotriose led to the synthesis of a more extended cellooligomer i.e., up to DP 16. A significant amount of water-insoluble product precipitated out from the reaction system. The results shown in Figure 2 suggest that this gradual clearing of the reaction mixture is caused by depletion of soluble lower oligomers, which are involved in the elongation reaction, and a steady hydrolysis of insoluble transglycosylation products. An outline of the chain-elongation reaction from cellotriose is shown in Scheme 1. Thus, cellotetraose formation through transfer of a glucosyl residue to cellotriose is the rate-limiting step in the overall process of transglycosylation. The accumulation of a sufficient amount of tetramer then initiates the formation of pentamer and hexamer in sequence. Biely and co-workers have reported that bond cleavage of [1-^{3}H]cellotriose by EG I tends to occur at the glucosidic linkage at the

non-reducing end of the glucose unit to generate [1-^{3}H]cellobiose as the major product.[30] These findings suggest that the glucose unit at the non-reducing end of cellotriose, which serves as both donor and acceptor, is transferred to another cellotriose molecule to generate cellotetraose. Consequently, the sugar chain-elongation reaction from the tetrasaccharide proceeds in sequence to produce the pentamer and hexamer, which in turn act as chain carriers in a series of reactions to form heptamer or above. Finally, when higher oligomers of DP > 7 are produced by transglycosylation, most of them precipitate out from the reaction system. Indeed, the hexamer displayed only about 0.4% solubility in the medium. EG I is well known to possess a more open substrate binding groove at the active site.[31] It makes possible to accommodate the resulting longer chain cellooligosaccharides. The resulting water-insoluble product was then analyzed by solid-state ^{13}C NMR. The spectrum resembled that of cellulose II, which consists of the corresponding monomers joined exclusively in a β-(1→4)-linked chain with stringent regio-/stereo selection.[25,26] Various cellulose allomorphs have been identified by their characteristic XRD patterns.[32-35] The results from XRD analysis of the water insoluble product were also consistent with a cellulose II structure displaying a high degree of crystallinity. Our results suggest that once the higher oligomers with a DP of up to 16 are produced in solution, multiple oligomeric chains spontaneously unite to form a highly ordered cellulose II-like structure as a result of self-assembly *via* oligomer-oligomer interactions during precipitation. Cellulose II is easily obtained by mercerization of native cellulose.[36] Kobayashi and co-workers have reported the synthesis of cellulose II having a DP of up to 22 *via* a transglycosylation reaction catalyzed by cellulase using β-D-cellobiosyl fluoride as substrate.[20] In another report, the successful synthesis of longer-chain cellulose II has also been achieved by using a cellulose/surfactant complex in non-aqueous media, possibly through reverse hydrolysis.[22,23]

Hiraishi and co-workers have reported an enzymatic synthesis of oligosaccharides with an average DP of 9 using cellodextrin phosphorylase, which quickly forms a highly ordered cellulose II structure regardless of the length of the oligomer chains.[24]

In conclusion, one-pot synthesis of cellulose II-like substance was achieved by means of an endo-glucanase, cellulase-catalyzed polymerization of non-modified cellotriose in an aqueous system. The enzyme produced a significant amount of higher cellulose oligosaccharides with a DP of up to 16. In addition, once produced in a higher oligomer form, the oligosaccharides immediately assemble to adopt a cellulose II with a high level of crystallinity. The present findings may assist in determining the shape of crystals and molecular organization of higher-ordered structures as well as the mechanism for the *in vivo* biosynthesis of native cellulose.

4. Experimental

4.1. Materials

Cellobiose and cellotriose were kindly provided from Yaizu Suisan Kagaku Industry Co., Ltd. (Shizuoka, Japan). Avicel PH-101 was a gift from Asahi Kasei Chemical Industry Co., Ltd. (Tokyo, Japan). Mercerized cellulose was prepared by immersion of Avicel PH-101 into 18% NaOH aqueous solution for 5 days at 20°C. Cellulase (GODO TCD-H3, crude enzyme) from *H. jecorina* was a kind gift from Godo Shusei Co., Ltd (Tokyo, Japan). EG I was purified by β-lactosylamidine-based affinity chromatography and ion exchange chromatography on a Mono P column (GE Healthcare, Piscataway, NJ) starting from the crude enzyme as described previously.[37] *p*-Nitrophenyl β-lactoside (Lac-β-*p*NP) was prepared by our previously described methods.[28,29] All other commonly used chemicals were obtained from commercial sources.

4.2. Analytical methods

MALDI-TOF mass spectra were obtained using on an AutoFlex (Bruker Daltonics, Bremen, Germany). The spectra were measured in the positive reflection mode with 10 mg/mL 2,5-dihydroxybenzoic acid in H_2O/ethanol 70:30 as the matrix solution. The sample solutions were mixed

with the matrix solution (1:4 v/v) and then a 1 μL droplet was applied to a stainless target plate and dried at room temperature. A mass calibration procedure was employed prior to the analysis of samples using peptide calibration standard II (Bruker Daltonics). The solid-state ^{13}C NMR experiments were carried out on a Chemagnetics CMX Infinity 400 MHz (9.05 T) wide-bore magnet spectrometer operating at room temperature. A double resonance magic-angle spinning (MAS) probe equipped with a 4-mm spinning module was used. The sample was restricted to approximately 20 mg in the rotor to increase the ratio frequency field homogeneity. Spectra were acquired with cross-polarization MAS (CP/MAS) techniques using a contact time of 100 μs for artificial cellulose samples. The recycle delay was set to 4.0 s. The total number of acquisitions collected for artificial cellulose was 50,000. Proton decoupling fields of ca. 83 kHz were employed in these experiments together with a spinning speed of 12.0 kHz. Spectra were calibrated through the methyl carbon resonance of hexamethylbenzene as an external reference at 17.35 ppm. High-pH anion-exchange chromatography with pulsed amperometric detection (HPAEC-PAD) analysis was carried out using a DIONEX DX-500 system (Dionex, Sunnyvale, CA) fitted with a PAD (ED-40) and a CarboPac PA1 column (4.0 × 250 mm). The column was pre-equilibrated in 60% (v/v) deionized water (eluent A) and 40% (v/v) 0.2 M NaOH (eluent B). Bound substance was then eluted using the following gradient: 0-40 min, linear decrease in ratio of eluent A from 60% (v/v) to 45% (v/v) with increase of eluent C (0.1 M NaOH, 1.0 M sodium acetate) from 0 % (v/v) to 15 % (v/v) with eluent B remaining constant at 40% (v/v); 40-50 min, 100% (v/v) eluent C; 50-60 min, 60% (v/v) eluent A and 40% (v/v) eluent B. The flow rate was 1.0 mL/min. XRD were obtained with Cu-Kα from a powder XRD generator (JDX3530; Japan Electronic Organization Co. Ltd., Tokyo Japan) operating at 30 kV and 30 mA.

4.3. Enzyme assay

EG I activity was colorimetrically determined with Lac-β-*p*NP as a substrate according to our previous method.[35] A mixture containing 25 μL of 10 mM substrates Lac-β-*p*NP in 50 mM acetate

buffer (pH 4.0, 50 μL volume) and an appropriate amount of enzyme (25 μL) was incubated in a 96-well microplate for 20 min at 40°C. One-tenth of the reaction mixture was removed at 5-min intervals and immediately transferred to a microplate containing 190 μL of 1 M Na_2CO_3 to stop the reaction. The amount of *p*NP liberated was determined by measuring the absorbance at 405 nm using a microplate reader (Ultrospec Visible Plate Reader II 96, GE Healthcare Bio-Sciences, Little Chalfont, UK). One unit of activity was defined as the amount of enzyme releasing 1 μmol of *p*NP per min.

4.4. Analysis of EG I-mediated transglycosylation

Analysis of the time course of transglycosylation and characterization of the resulting products was performed by four different methods as outlined below.

4.4.1. HPAEC-PAD

To a solution (200 μL) of cellobiose (110 mg) or cellotriose (100 mg) in 50 mM acetate buffer (pH 4.0) was added 200 μL of enzyme solution (0.2 U) in the same buffer. The mixture was then incubated at 50°C. The amount of transglycosylation product as a function of time was examined on the 0.1 mL scale. Aliquots of 5 μL were taken and mixed with 145 μL of H_2O. The reaction was then immediately quenched by heating in a boiling water bath for 15 min and the mixture was clarified by filtration through a 0.45 μm filter unit. The reaction mixture (water soluble part) was subsequently analyzed by HPAEC-PAD.

4.4.2. MALDI-TOF mass spectrometry, solid-state ^{13}C NMR spectroscopy, and XRD analysis

Synthetic artificial cellulose was directly analyzed by MALDI-TOF mass spectrometry, solid-state ^{13}C NMR spectroscopy, and XRD analysis without derivatization.

4.5. *In vitro* preparation of cellulose-like substances

For the preparation of cellulose, a solution (200 μL) of cellotriose (100 mg) in 50 mM acetate buffer (pH 4.0) was added to 200 μL of enzyme solution (0.2 U) in the same buffer and the mixture was maintained at 50°C. After 1 h, the resulting insoluble substance was isolated by centrifugation and washed three times with 50 % methanol to afford 30 mg of substance, which was directly applied to MALDI-TOF mass spectrometry, solid-state ^{13}C NMR spectroscopy, and XRD analysis.

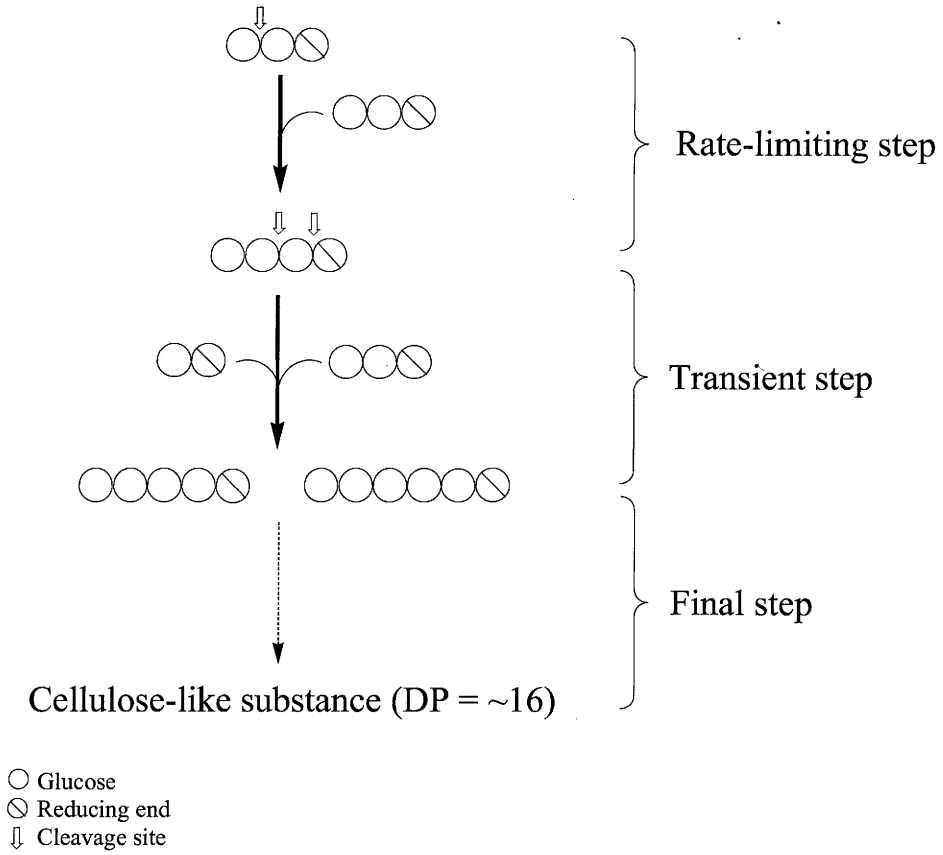

Scheme 1. Schematic outline for EG I-mediated formation of a cellulose-like substance from cellotriose in an aqueous system.

Table 1. ^{13}C Chemical shifts of residues A and B in the structure of cellulose II.

	^{13}C Chemical shifts/ppm					
	C1	C2	C3	C4	C5	C6
Residue A	107.4	73.4	76.0	87.9	74.4	62.7
Residue B	105.3	75.2	77.0	89.1	72.6	63.4
^{13}C Chemical shift difference	2.1	-1.8	-1.0	-1.2	1.8	-0.7

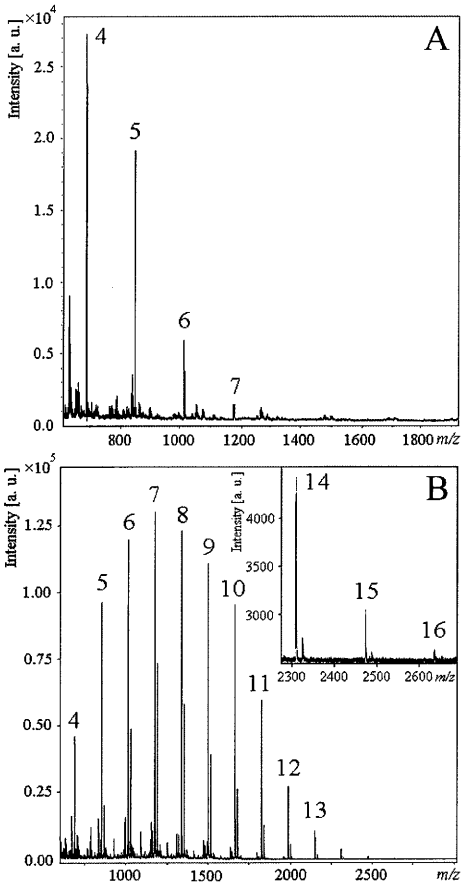

Figure 1. An EG I-mediated reaction was carried out using cellobiose or cellotriose as starting material. MALDI-TOF mass spectra of the reaction products are shown: (A) cellooligosaccharides from cellobiose and (B) a cellulose-like substance from cellotriose.

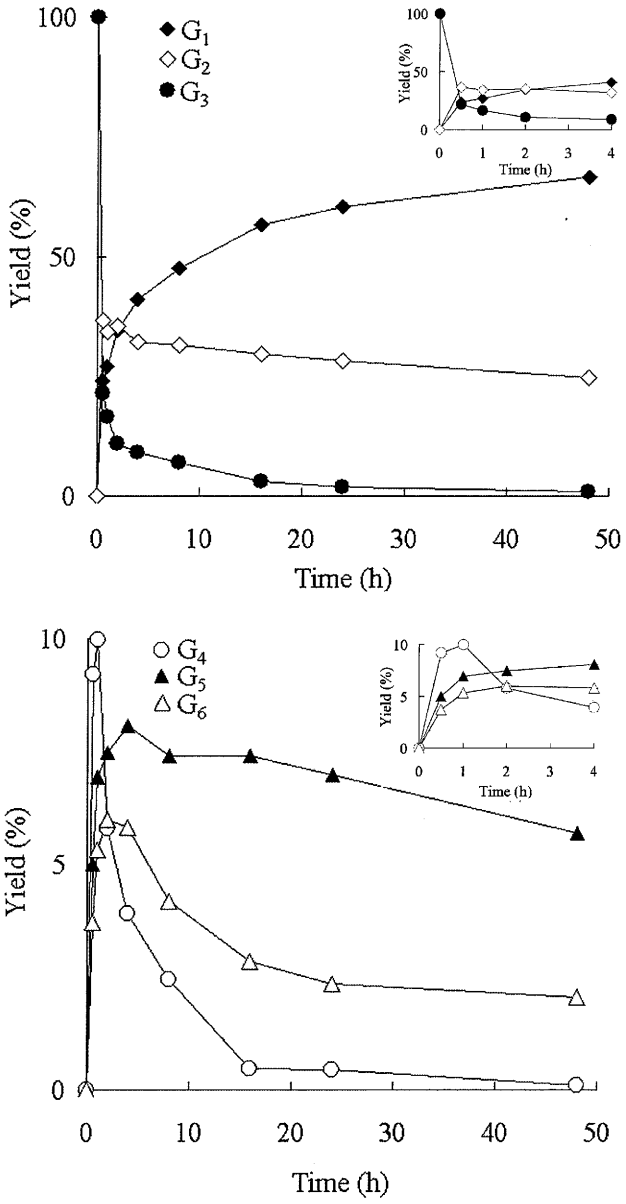

Figure 2. Time-course of products of the EG I-mediated reaction using cellotriose as substrate. Reaction conditions are described in the Experimental section. The water-soluble fraction of the reaction mixture was analyzed by HPAEC-PAD. G_1 and G_2-G_6 represent glucose and a series of cellooligosaccharides (DP 2 ~ 6), respectively.

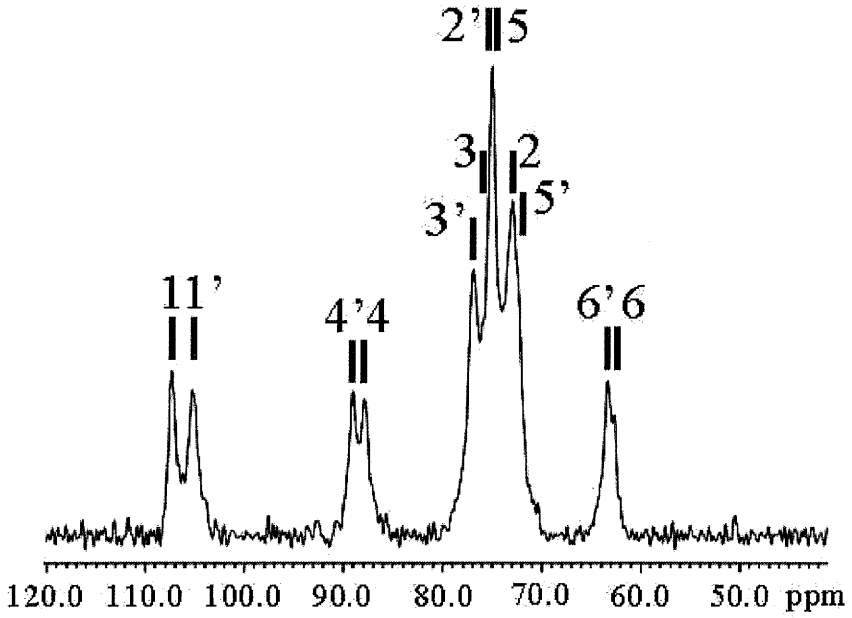

Figure 3. 1D CP/MAS ^{13}C NMR spectrum of the cellulose-like substance obtained by EG I-mediated transglycosylation using cellotriose as substrate.

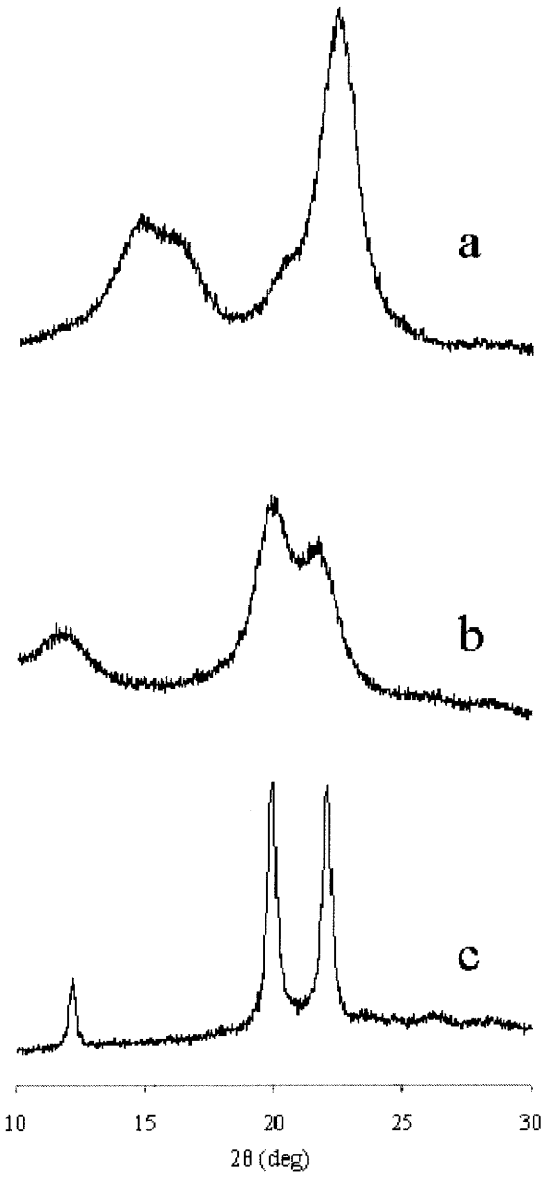

Figure 4. XRD patterns of (a) avicel, (b) mercerized cellulose and (c) cellulose-like substance.

Chapter III

Mode of action of a β-(1→6)-glucanase from *Penicillium multicolor*

1. Introduction

β-(1→6)-Glucan, which consists of glucose residues joined in a β-(1→6)-linkage, is a structurally important component of the cell wall of yeasts and fungi. It is produced in budding yeasts as a link between cell wall proteins and the main β-(1→3)-glucan/chitin polysaccharides.[1] However, the polymer is much less abundant in nature than other β-glucans, such as β-(1→4)- or β-(1→3)-glucan. Pustulan from *Umbilicaria papullosa* is well known as a typical linear β-(1→6)-glucan.[2] On the other hand, β-(1→6)-glucanase (EC 3.2.1.75) belongs to glycosyl hydrolase families 5 and 30 (http://www.cazy.org/).[3-6] Although β-(1→6)-glucanases are widely distributed among fungi,[7] few of them have been purified and characterized.[8-17] As a result, there are few studies on the hydrolytic mode of action of β-(1→6)-glucanase on β-(1→6)-glucan.[18-20] In general, enzymatic degradation of polysaccharides is considered to consist of *endo*-acting enzymes, which randomly hydrolyze glycosidic linkages in the polymers, and processive *exo*-acting enzymes, which degrade the polysaccharides from the polymer ends. For example, cellulose[21] and chitin[22] are hydrolyzed by the synergistic action of corresponding *endo*- and *exo*-acting enzymes. In starch hydrolysis, the reaction is performed through liquefaction (by an *endo*-type enzyme) and saccharification (by an *exo*-type enzyme).[23] During the first step, starch is solubilized in water and partially hydrolyzed with an α-amylase. In the second step, saccharifying enzymes such as β-amylase or glucoamylase transform the liquefied starch into final products that can be specific oligosaccharides such as glucose or maltose.

The present paper describes the hydrolytic mode of action of β-(1→6)-glucanase on pustulan based on kinetic and product analysis, together with specific purification of the enzyme and the methods for synthesizing a series of gentiooligosides using its transglycosylation activity.

2. Results

2.1. Purification of β-(1→6)-glucanase based on gentiotetraose (Gen_4)-immobilized affinity chromatography

To purify *P. multicolor* β-(1→6)-glucanase, the crude enzyme preparation was fractionated by ammonium sulfate precipitation. The desalted fraction was applied to cation-exchange chromatography using CM-Sepharose Fast Flow, yielding a single peak of β-(1→6)-glucanase activity that was completely devoid of β-glucosidase activity. This fraction was then subjected to substrate affinity chromatography on a Gen_4-coupled TOYOPEARL AF-Amino-650M column (Fig. 1A). β-(1→6)-Glucanase activity was strongly adsorbed on the column, and was subsequently easily eluted as a single peak by a salt gradient. The fraction was highly purified (244-fold relative to the crude enzyme preparation) with a specific activity of 164.1 U/mg (Table 1). It gave a single protein band by SDS-PAGE with a molecular mass of 51 kDa (Fig. 1B). Furthermore, the protein was analyzed by MALDI-TOF mass spectrometry, and a peak with an *m/z* value of 49,909 was observed. This suggests that the enzyme does take a monomer but not a unit structure. The isoelectric point (pI) was not determined because it was beyond the limit of detection (pI<3.5) (data not shown). The optimum temperature for the purified enzyme was 50 °C, and heat inactivation occurred above 60 °C. The optimum pH was pH 4.0, and more than 90% of the maximum enzyme activity was maintained in the pH range 2.0-9.0 at 4 °C and 24 h of incubation. The hydrolytic activity of the enzyme was prominent only for pustulan (a linear β-(1→6)-glucan) (Table 2). Little activity was detected toward soluble starch, Carboxymethyl cellulose or curdlan, enabling us to conclude that the enzyme is a specific β-(1→6)-glucanase.

2.2. Synthesis of methyl β-gentiooligosides and *p*-nitrophenyl β-gentiooligosides

A series of methyl β-gentiooligosides (DP 2-6, $Gen_{2\text{-}6}$ β-*O*Me) and *p*-nitrophenyl β-gentiooligosides (DP 2-6, $Gen_{2\text{-}6}$ β-*p*NP) were prepared as control samples for analyzing the hydrolytic mechanism of the

purified β-(1→6)-glucanase on the β-(1→6)-glucan linkage. We have recently reported that gentiooligosaccharides (DP 3-9) can be prepared from the starting substance Gen_2 by the sequential transglycosylation reactions of β-glucosidase and β-(1→6)-glucanase.[24] By following the reported methodology, a series of methyl β-gentiooligosides (DP 2-6) were enzymatically prepared in a similar way.

Gen_2 β-*O*Me was first synthesized from methyl β-D-glucoside (Glc β-*O*Me), which serves as both the donor and acceptor substrate, through the transglycosylation reaction of *Hypocrea jecorina* β-glucosidase. The resulting Gen_2 β-*O*Me was then used as a starting substance for obtaining methyl β-gentiooligosides (DP 3-6), utilizing the above-purified β-(1→6)-glucanase. The transglycosylation reaction was carried out at a high substrate concentration of Gen_2 β-*O*Me (4 M), which served as both the donor and acceptor. After terminating the enzyme reaction, the reaction mixture was subjected to pyridylamination with 2-amino-pyridine to give pyridylaminated gentiooligosyl derivatives because it proved difficult to separate the desired methyl β-gentiooligosides from gentiooligosaccharide by-products by chromatography. The reaction solution was applied to TOYOPEARL HW-40S chromatography to remove the excess of 2-aminopyridine. The fractions that showed color development with phenol-sulfuric acid were further subjected to charcoal-Celite chromatography with a linear gradient of ethanol (Fig. 2A and Scheme 1). The chromatogram showed six fractions (MG_1-MG_6), numbered according to their order of elution. Fractions MG_1 and MG_2 were recovered as Glc β-*O*Me and Gen_2 β-*O*Me, respectively. Fractions MG_3-MG_6 were obtained as the desired products Gen_3 β-*O*Me, Gen_4 β-*O*Me, Gen_5 β-*O*Me, and Gen_6 β-*O*Me in yields of 7.0%, 4.3%, 1.5%, and 0.8%, respectively. The structures of the synthesized products were analyzed by ^1H, ^{13}C NMR (Table 3), and ESIMS.

A series of *p*-nitrophenyl β-gentiooligosides (DP 2-6) were prepared in a similar way to the methyl β-gentiooligosides. *p*-Nitrophenyl β-D-glucoside (Glc β-*p*NP) was used as a starting material for the synthesis of Gen_2 β-*p*NP. The reaction was performed by using the transglycosylation activity of *H. jecorina* β-glucosidase with a high monomer concentration (100 mM). The reaction mixture was applied

to TOYOPEARL HW-40S chromatography to obtain the target dimer in 15.2% yield. The resulting Gen_2 β-*p*NP was used for the synthesis of Gen_{3-6} β-*p*NP. The gentiooligosides (DP 3-6) were synthesized by a β-(1→6)-glucanase-catalyzed transglycosylation reaction from the Gen_3 donor to a Gen_2 β-*p*NP acceptor. In this case, low temperature (4 °C) was effective for raising the transglycosylation rate (data not shown). The reaction mixture was applied to TOYOPEARL HW-40S chromatography. The chromatogram showed five peaks designated PG_2-PG_6 (Fig. 2B). Fraction PG_2 was recovered as Gen_2 β-*p*NP (57.4% recovery). Fractions PG_3 and PG_4 were obtained as the target products Gen_3β-*p*NP and Gen_4 β-*p*NP in yields of 2.1% and 14.2%, respectively. Fractions PG_5 and PG_6 were each further purified by reverse-phase ODS chromatography to remove the gentiooligosaccharide by-products. The target products Gen_5 β-*p*NP and Gen_6 β-*p*NP were obtained in yields of 2.6% and 1.7%, respectively. The structures of the synthesized products were identified by ^1H, ^{13}C NMR (Table 4), and ESIMS analyses. The synthetic gentiooligosaccharides and gentiooligosides were used to analyze the mechanism of action of β-(1→6)-glucanase on β-(1→6)-glucan as described below.

2.3. Hydrolysis of methyl β-gentiooligosides, *p*-nitrophenyl β-gentiooligosides, and gentiooligosaccharides: bond cleavage frequency

The mode of action of the purified β-(1→6)-glucanase on the gentiooligosides and gentiooligosaccharides prepared above were examined. The cleavage frequencies and relative hydrolytic rate of the enzyme were measured on the basis of the initial velocity of the hydrolytic reaction and are summarized in Tables 5 and 6.

2.3.1 Methyl β-gentiooligosides and *p*-nitrophenyl β-gentiooligosides

The cleavage frequencies and relative hydrolytic rate of the purified β-(1→6)-glucanase on methyl β-gentiooligosides (DP 2-6) were determined by high-pH anion-exchange chromatography with pulsed

amperometric detection (HPAEC-PAD) analysis (Table 5). As compared with Gen_3 β-*O*Me, Gen_{4-6} β-*O*Me acted as fairly good substrates. For Gen_3 β-*O*Me, the second glucosidic bond (bond 2) from the methyl group was cut preferentially. The major cleavage of Gen_4 β-*O*Me occurred at the second (bond 2) and third (bond 3) glucosidic bonds from the methyl group. The hydrolytic pattern of Gen_5 β-*O*Me was substantially similar to that of Gen_6 β-*O*Me: the major cleavages occurred at bonds 2, 3, and 4 in approximately equal proportion. It should be noted that the non-reducing end glucosyl residues of Gen_{4-6} β-*O*Me were either not or scarcely cleaved by the enzyme. Gen_3 β-*O*Me was hydrolyzed slowly to form Glc β-*O*Me and Gen_2 β-*O*Me in the ratio 91:9. The presence of a methyl group at the reducing end did not seem to prohibit the reaction. These results indicate that methyl β-gentiooligosides are cleaved through the terminal glycoside, and the number of the susceptible bond varies with the chain-length of substrate. Thus, the cleavage gradually shifts from bond 2 to bonds 3 and 4 with increasing DP. The cleavage frequencies of *p*-nitrophenyl β-gentiooligosides (DP 2-6) were similarly analyzed by HPLC. For Gen_4 β-*p*NP, the third bond (bond 3) from the *p*-nitrophenyl group was cut preferentially. The major cleavage of Gen_5 β-*p*NP occurred at bonds 3 and 4, whereas bond 2 was not completely cleaved. The hydrolytic pattern of Gen_6 β-*p*NP, which was found to be the best substrate for the enzyme, was substantially similar to that of Gen_5 β-*p*NP. Notably, glucose was not detected during any of the reactions with Gen_{4-6} β-*p*NP. This indicates that the non-reducing-end glucosyl terminus of the derivatives with DP 4 or higher is not subject to hydrolysis. The purified β-(1→6)-glucanase acted slightly on Gen_3 β-*p*NP (2% hydrolytic activity relative to 100% for Gen_6 β-*p*NP), which was a poor substrate. By contrast, the cleavage point of derivatives with DP 4 or higher shifted such that the enzyme kept away from the *p*-nitrophenyl group at the terminus. In all the tested substrates, release of *p*-nitrophenol was not observed by the HPLC-based assay and the result also confirmed colorimetrically by a standard end-point assay (data not shown). As a result, the relative enzyme activity for Gen_{4-6} β-*p*NP markedly increased in comparison to that for Gen_3 β-*p*NP.

2.3.2 Gentiooligosaccharides

The enzymatic cleavage of gentiooligosaccharides (DP 2-6) and the relative rate of hydrolysis by the purified enzyme were analyzed by HPAEC-PAD. However, the position of cleavage in the reducing oligosaccharides was not localized from the hydrolysate of the oligomers, because of the lack of aglycon. Taking into account the data for β-gentiooligosides, the frequencies of cleavage of gentiooligosaccharides with DP 4 or higher were proposed on the basis of the assumption that the glucosyl residue at the non-reducing end was not hydrolyzed by the enzyme (Table 6). The major cleavage of Gen_4 occurred at the first (bond 1) and second (bond 2) glucosidic bonds from the reducing terminus, and the activity was much lower relative to that of Gen_5, suggesting that gentiooligomers of DP 5 and higher are good substrates. Regarding Gen_5 and Gen_6, there was less cleavage at bond 1 as the DP increased, with cleavage shifting to bonds 2 and 3/4, respectively. Gen_2 was found to act only slightly as a substrate.

2.4. Hydrolytic mechanism of β-(1→6)-glucanase on pustulan

2.4.1 NMR analysis

To elucidate the mechanism of pustulan hydrolysis by the enzyme, the stereochemistry of the hydrolysis was investigated by ^1H NMR analysis. Figure 3 shows spectra of the time course of the hydrolysis reaction in the 4.6-5.3 ppm region. Before hydrolysis, no signal was observed (Fig. 3A). During the early stage of hydrolysis, doublets at 4.66-4.68 ppm (J=8 Hz), characteristic of H-1β from gentiooligosaccharides with different chain lengths, appeared and rapidly increased in intensity over time (Fig. 3B-C). Instead of these signals, a small doublet at 5.25 ppm (J=4 Hz), characteristic of H-1α from the corresponding gentiooligosaccharides, appeared at 1 h after addition of the enzyme and gradually increased over time (Fig. 3C-E). These observations suggest that the β-anomer is initially formed and then easily converted into the α-anomer by mutarotation.

2.4.2 HPAEC-PAD analysis

The manner of the hydrolysis of β-(1→6)-glucan (pustulan) by the purified β-(1→6)-glucanase was analyzed in real time by HPAEC-PAD. Pustulan was shown to have an average degree of polymerization ($\overline{DP}$) of 320, within the DP 200 to 550 range (Fig. 4A). In the early stage (after 3 minutes) of incubation, the glucan was quickly hydrolyzed to form a broad peak corresponding to $\overline{DP}$ 45 in DP 15 to 100 range, which was designated a short-chain glucan (Fig 4B). After 10 min of incubation, the peak corresponding to $\overline{DP}$ 45 had decreased to afford a main broad peak of $\overline{DP}$ 15 with minor peaks of DP 2-4 (Fig. 4C). After 30 min of incubation, the resulting oligomer ($\overline{DP}$ 15) was further distributed into two peak groups corresponding to $\overline{DP}$ 10 and DP 2-4 (Fig. 4D). One should remark that the peak of DP 2-4 increased in proportion with great regularity over time, while a low level of glucose was detected during the reaction. The resulting oligomers ($\overline{DP}$ 10) were slowly degraded over time to two peak groups corresponding to $\overline{DP}$ 7 and DP 2-4 after 2 h of incubation (Fig. 4E). In the final stage of the reaction, the cleavage of oligomers (DP 3-4) into glucose and Gen_2 proceeded extremely slowly, and it took prolonged incubation (96 h) to reach this stage (Fig. 4F).

Lastly, the hydrolytic profiles of Gen_8 and Gen_9 (Fig. 5) as reference compounds were compared with the time course of the hydrolysis of pustulan (Fig. 4). Gen_8 was hydrolyzed in the order of DP 2 and DP 6 > DP 3 and DP 5 > DP 4, and Gen_9 in the order of DP 2 and DP 7 > DP 3 and DP 6 > DP 4 and DP 5 (Fig. 5). This indicates that the major cleavages occur at bonds 2, 3 and 4 through a reducing terminus. The cleavage pattern was substantially similar to that of $\overline{DP}$ 10 derived from pustulan (Fig. 4D).

3. Discussion

The aim of the present work was to elucidate the hydrolytic mode of action of purified β-(1→6)-glucanase on a typical linear β-(1→6)-glucan pustulan. For this purpose, the enzyme was purified from

the culture filtrate of *P. multicolor*. In this process, substrate affinity chromatography using Gen_4 as a ligand was shown to be a powerful technique for the purification of β-(1→6)-glucanase. The highly purified enzyme (244-fold purified, 164.1 U/mg) gave a single protein band at 51 kDa by SDS-PAGE and was used for analysis of its hydrolytic mode of action on pustulan. The enzyme showed activity only against substrates with a β-(1→6)-glycosidic linkage.

The present method for obtaining a series of gentiooligosides (DP 3-6) starting from pre-prepared gentiooligoside (DP 2) incorporated a simple one-pot reaction process and ensured the regioselectivity of glycosylation, although it was not always sufficient. The resulting synthetic methyl β-gentiooligosides and *p*-nitrophenyl β-gentiooligosides were very useful as substrates for providing analytical insight into how the enzyme actually cleaves pustulan. From the cleavage frequencies, it was shown that methyl β-gentiooligosides (DP 2-6) and *p*-nitrophenyl β-gentiooligosides (DP 2-6) were cleaved through the terminal glycoside and that the number of the susceptible bond varied with the chain length of substrate. However, the cleavage pattern of methyl β-gentiooligosides (DP 4-6) was somewhat different from that of *p*-nitrophenyl β-gentiooligosides (DP 4-6). For example, the cleavage of Gen_5 β-*O*Me occurred in almost equal proportion at bonds 2, 3, and 4, whereas Gen_5 β-*p*NP was preferentially cleaved at bonds 3 and 4, but not cleaved at all at bond 2. This indicates that the presence of a methyl group does not influence enzyme action, whereas that of a *p*-nitrophenyl group shifts the cleavage position for one glucosyl residue to the non-reducing end. Taking these data into account, the cleavage frequencies of gentiooligosaccharides were proposed on the basis of the assumption that the glucose residue at the non-reducing terminus of gentiooligosaccharides with DP 4 or higher is not hydrolyzed by the enzyme. The cleavage pattern of gentiooligosaccharides is approximated to that of Gen_n β-*O*Me rather than Gen_n β-*p*NP. Thus, cleavage at bond 1 gradually decreases with extension of the DP and the cleavage location shifts to bonds 2 and 3.

As mentioned above, our purpose was to elucidate the mechanism of the hydrolysis of pustulan by β-(1→6)-glucanase based on kinetic and product analysis. Enzymatic hydrolysis of glycosidic bonds

usually occurs with two possible stereochemical outcomes namely, inversion or retention of the anomeric configuration at the cleavage site.[25] The hydrolytic mechanism of the enzyme was first evaluated by ^{1}H NMR. In the initial stage of the reaction, the β-anomer was formed and was then easily converted into the α-anomer by mutarotation. This indicates that the hydrolysis of pustulan occurs with retention of the anomeric configuration. Pitson and co-workers[14] have reported that β-(1→6)-glucanase from *Acremonium persicinum* acts with retention of the anomeric center, releasing products in the β-configuration. Furthermore, the pathway of the hydrolysis of pustulan by the purified enzyme could be proposed on the basis of HPAEC-PAD analysis of the time course of hydrolysate production (Scheme 2). The enzyme was shown to achieve complete hydrolysis of the glucan in three steps as follows. In the initial stage, the enzyme cleaved the glucan with a pattern resembling that of an *endo*-hydrolase to quickly produce a short-chain glucan ($\overline{DP}$ 45) as an intermediate after 3 min of incubation. In the midterm stage, the resulting short-chain glucan was further cleaved into two peak fractions corresponding to DP 15-10 and DP 2-4 within 30 min. During this process, it can be envisaged how the enzyme initially attacks the glucan so quickly. Notably, the relative hydrolytic activity of the enzyme towards Gen_8 was 3, whereas that towards pustulan was 100, representing a 33-fold difference. Once the chain length of DP 15-10 was reached, the preferred cleavage occurred at bonds 2, 3 and 4 from the reducing terminus of the chain to afford DP 2-4 with great regularity. Only a low level of glucose was detected despite the subsequent reaction. In the midterm stage, the cleavage pattern of $\overline{DP}$ 10 derived from pustulan (Fig. 4D) was substantially similar to those of Gen_8 and Gen_9 (Fig. 5). In the final stage of the reaction, the lower oligomers (DP 3 and DP 4) underwent hydrolysis extremely slowly to produce glucose and Gen_2 as the main products, because of the lower hydrolytic activity of the enzyme on Gen_3 and Gen_4. It took prolonged incubation to reach this stage (Fig. 4F). In this way, the enzyme varies its mode of action depending on the chain length derived from the glucan during the whole course of the reaction. Montero and co-workers[20] demonstrated that a β-(1→6)-glucanase from *T. harzianum*, namely BGN16.3, has an *endo*-hydrolytic mode of action by HPLC analysis of the products from pustulan.

In conclusion, β-(1→6)-glucanase from *P. multicolor* was purified and the hydrolytic manner of the enzyme toward β-(1→6)-glucan was elucidated in real time during the whole course of the reaction. Longer polymers are initially hydrolyzed by an *endo*-hydrolytic mode of action. In the subsequent reaction, the resulting short-chain glucan is hydrolyzed by a pattern resembling a saccharifying-hydrolase to produce DP 2-4 with great regularity; ultimately, DP 2-4 are cut up to produce glucose and Gen_2. As a result, it has been revealed that the hydrolytic cooperation of both an *endo*-type and a saccharifying-type reaction of a single enzyme, which plays in a bifunctional role, leads to complete hydrolysis of the β-(1→6)-glucan pustulan.

4. Experimental

4.1. Materials

A crude enzyme preparation from *P. multicolor* IAM7153 (Institute of Molecular and Cellular Biosciences, The University of Tokyo) was kindly supplied by Amano Enzyme, Inc. (Gifu, Japan). Cellulase from *H. jecorina* was purchased from NagaseChemteX Co. (Osaka, Japan). Gentiobiose, methyl β-D-glucopyranoside, *p*-nitrophenyl β-D-glucopyranoside, glucan from *Saccharomyces cerevisiae*, carboxymethylcellulose, and curdlan from *Alcaligenes faecalis* were purchased from Sigma Chemical Co. (St. Louis, MO, USA). Pustulan was purchased from Calbiochem (San Diego, CA, USA) and prepared for the removal of insoluble material as follows: the pustulan was dissolved in water (10 mg/mL) and boiled for 10 min. After cooling, the resulting precipitate was removed by centrifugation (5,000 *g*, 15 min). The supernatant was then lyophilized and used as substrate for the β-(1→6)-glucanase assay. The lyophilized pustulan was also fractionated by 50% ethanol precipitation to afford a water-soluble pustulan for hydrolytic analysis. All other commonly used chemicals were obtained from commercial sources.

4.2. Analytical methods

MALDI-TOF mass spectra were obtained on an AutoFlex instrument (Bruker Daltonics, Bremen, Germany). The spectra were measured in positive linear mode with 2,5-dihydroxybenzoic acid (10 mg/mL) in H_2O/ethanol (70:30) as the matrix solution. The sample solutions were mixed with the matrix solution (1:4 v/v), and then a 1-μL droplet was applied to a stainless target plate and dried at room temperature. A mass calibration procedure was carried out before the analysis of samples by using protein calibration standard II (Bruker Daltonics). The HPLC analysis was carried out on an Asahipak GS-220 HQ column (7.5 × 300 mm, Japan) with a Jasco Intelligent system liquid chromatograph and detection at 300 nm. The bound material was eluted with H_2O at a flow rate of 0.9 mL/min at 40 °C. HPAEC-PAD analysis was carried out using a DIONEX DX-500 system (Dionex, Sunnyvale, CA) fitted with a PAD (ED-40) and a CarboPac PA1 column (4.0 × 250 mm). Bound material was eluted by the following gradients. Condition 1: 0-40 min, the ratio of eluent A was decreased from 60% (v/v) to 45% (v/v), the ratio of eluent B was increased from 0% (v/v) to 15% (v/v), and eluent C was kept at 40% (v/v); 40-50 min, 100% (v/v) eluent B; 50-60 min, 60% (v/v) eluent A, and 40% (v/v) eluent C. Condition 2: 0-50 min, the ratio of eluent A was decreased from 60% (v/v) to 0% (v/v), the ratio of eluent B was increased from 0% (v/v) to 60% (v/v), and eluent C was kept at 40% (v/v); 50-60 min, 100% (v/v) eluent B; 60-70 min, 60% (v/v) eluent A and 40% (v/v) eluent C. In both conditions, eluents A, B, and C were deionized water, 0.1 M NaOH containing 1 M sodium acetate, and 0.2 M NaOH, respectively. The flow rate was 1.0 mL/min. ^1H and ^{13}C NMR spectra of each sample in D_2O were recorded on a JEOL JNM-LA 500 spectrometer. Chemical shifts (δ) were expressed relative to sodium 3-(trimethylsilyl)-propionate (TPS) as an external standard. ESIMS spectra were recorded on a JMS-T100LC mass spectrometer. The samples were injected in methanol (0.2-0.5 mg/mL) directly into the spectrometer.

4.3. Enzyme assays

β-(1→6)-Glucanase was assayed as follows. A mixture containing 180 μL of substrate (5 mg/mL of pustulan) in 50 mM sodium acetate buffer (pH 5.5) and 20 μL of an appropriate amount of enzyme was incubated for 15 min at 40 °C. The reducing sugars produced were determined directly by Somogyi-Nelson's method.[26, 27] One unit was determined as that amount of enzyme catalyzing the formation of 1 μmol of D-glucose per min from the substrate under the conditions of the assay. β-Glucosidase was measured as follows: 100 μL of 10 mM *p*-nitrophenyl β-D-glucoside solution, 250 μL of 100 mM sodium acetate buffer (pH 4.0) and 125 μL of H_2O were premixed. Then, enzyme solution (25 μL) was added to the solution, which was kept at 40 °C for 15 minutes. One-tenth of the reaction mixture was removed at 5-min intervals and immediately transferred to a microplate containing 50 μL of 1 M Na_2CO_3 to stop the reaction, and the *p*-nitrophenol liberated was determined spectrophotometrically at 420 nm. One unit of activity was defined as the amount of enzyme releasing 1 μmol of *p*-nitrophenol per min.

4.4. Preparation of Gen_4-coupled gel

Gen_4-coupled Toyopearl AF-Amino-650M was prepared as follows: Gen_4 (580 mg in 2 mL of 0.2 M K_2HPO_4) was added to pre-swollen gel (1 g) and then $NaCNBH_3$ (200 mg) was added. The gel in the solution was incubated at 60 °C overnight with gentle agitation, and then washed with water (20 mL) three times and sodium borate buffer (20 mL, pH 8.2) three times. For acetylation of the free amino group, 0.2 M sodium acetate (8 mL) and acetic anhydride (4 mL) were added to the gel and allowed to react for 30 min at 0 °C. Next, acetic anhydride (4 mL) was added to the solution containing the gel, which was then kept for 30 min at room temperature with gentle agitation. The gel was washed successively with H_2O, 0.1 M NaOH, and H_2O (three times for each) and packed into a column (1 mL).

4.5. Purification of β-(1→6)-glucanase

Unless otherwise indicated, all steps were carried out at 4 °C. The *P. multicolor* crude enzyme (720 mg) was dissolved in 50 mM sodium acetate buffer (pH 5.5), brought to 60% saturation with solid ammonium sulfate, and left to stand for 30 min. The precipitate was removed by centrifugation (5000 *g*, 10 min). The supernatant was brought to 80% saturation with solid ammonium sulfate and left to stand for 30 min. The precipitate was dissolved in 50 mM sodium acetate buffer (10 mL, pH 5.5), dialyzed against H_2O, and lyophilized. The enzyme powder (80 mg) was dissolved in 20 mM sodium acetate buffer (1 mL, pH 4.0), applied to a CM-Sepharose Fast Flow column (2.5 × 30 cm) equilibrated with 20 mM sodium acetate buffer (pH 4.0), and eluted with the same buffer (200 mL) at flow rate of 1 mL/min. The eluent was collected in 10-mL fractions. β-(1→6)-Glucanase activity was measured by a standard assay using each fraction as an enzyme solution. Fractions showing β-(1→6)-glucanase activity (tubes 6-10) were pooled and concentrated with an Amicon PM-30 membrane. The concentrated enzyme fraction was applied to a Gen_4-coupled affinity column (1 mL) equilibrated with 20 mM sodium acetate buffer (pH 5.5) containing 45 mM NaCl. After the column was washed with 20 mL of equilibration buffer, the adsorbed material was eluted with a linear gradient from 45 to 800 mM NaCl in the same buffer over a volume of 20 mL, and then with 800 mM NaCl in the same buffer at flow rate of 0.1 mL/min. The eluent was collected in 0.5-mL fractions. Fractions showing β-(1→6)-glucanase activity (tubes 52-54) were combined and concentrated with a Nanosep 10k Omega membrane. The enzyme purity was checked by SDS-PAGE.

4.6. Characterization of β-(1→6)-glucanase

The effect of pH on the activity of the purified β-(1→6)-glucanase was measured under the standard conditions of pustulan hydrolysis while changing the pH of the 50 mM buffers used in the reaction mixture. The pH stability was determined by incubating the enzyme at 4 °C for 24 h at each pH, and then measuring the activity under the standard conditions. The buffers used were Tris-HCl (pH 2.0-3.0), sodium acetate (pH 3.0-6.0), and sodium phosphate (pH 7.0-9.0). The optimum temperature of the

activity was measured under the standard conditions at various temperatures (4-80 °C). Thermostability was determined by incubating the enzyme at each temperature for 1 h in 50 mM sodium acetate buffer (pH 5.5), and then measuring the activity under the standard conditions.

4.7. Enzymatic synthesis of methyl β-gentiooligosides (DP 2-6, Gen_{2-6} β-*O*Me)

Glcβ-*O*Me (15 g, 77.2 mmol) was dissolved in 21.2 mL of 100 mM sodium acetate buffer (pH 4.0) and β-glucosidase (17.4 mL, 776 U) in crude cellulase from *H. jecorina* was added. The solution was incubated without stirring for 23 h at 40°C, and the reaction was terminated by boiling for 5 min. The reaction mixture was applied to a charcoal-Celite column (4.5 × 50 cm) equilibrated with water. The column was washed with 1.5 L of water and eluted with a linear gradient of 0% (3 L) to 7.5% (3 L) ethanol (flow rate 7 mL/min; a fraction size 50 mL/tube). Elution was monitored at 485 nm, with carbohydrate content determined by the phenol-H_2SO_4 method. The eluate (550-4,115 mL) was concentrated and applied to charcoal-Celite chromatography again. The eluate (850-1,550 mL) was concentrated and lyophilized, and afforded 770 mg of Gen_2 β-*O*Me[28] in 5.6% yield based on the Glcβ-*O*Me added. As an acceptor and a donor, the synthetic Gen_2 β-*O*Me (627 mg, 1.8 mmol) was dissolved in 340 μl of 50 mM sodium acetate buffer (pH 4.0) and purified β-(1→6)-glucanase (100 μl, 28.3 mU) was added. After the solution was incubated for 60 h at 50 °C, the reaction mixture was boiled for 15 min. To remove reducing sugar in the reaction mixture by chromatography, pyridylamination was performed as follows: Solution A was prepared by dissolving 0.5 g of 2-aminopyridine in 380 μl of 35% HCl. Solution B was prepared by dissolving 40 mg of $NaBH_3CN$ in Solution A and adding 100 μl of H_2O. Solution A was added to the reaction mixture, kept at 100°C for 15 min, and then 295 μl of solution B was added. The mixture was incubated for 24 h at 70°C. After pyridylamination, the mixture was loaded onto a TOYOPEARL HW-40S column (4.5×90 cm) equilibrated with 25% methanol at a flow rate of 1.5 mL/min. The eluate (1,125-2,475 mL) was collected, evaporated to remove methanol, and loaded onto a charcoal-Celite column (4.5×90 cm) equilibrated with H_2O. The column was washed

with 1.5 L of water and then eluted with a linear gradient of 5% (5 L) to 35% (5 L) ethanol (flow rate, 7 mL/min; fraction size, 50 mL/tube). The eluate showed six main peaks, MG_1 (tubes 18–26), MG_2 (tubes 62-73), MG_3 (tubes 95-103), MG_4 (tubes 108-115), MG_5 (tubes 120-125), and MG_6 (tubes 129-134), which were concentrated and lyophilized. Fraction MG_1 was recovered as Glc β-*O*Me (142.3 mg), and fraction MG_2 was recovered as Gen_2 β-*O*Me (242.2 mg, 38.6% recovery). Fractions MG_3, MG_4, MG_5 and MG_6 gave Gen_3 β-*O*Me (63.4 mg, 7.0%), Gen_4 β-*O*Me (51.5 mg, 4.3%), Gen_5 β-*O*Me (22.9 mg, 1.5%), and Gen_6 β-*O*Me (15.0 mg, 0.8%), respectively.

The structures of synthetic Gen_2-Gen_6 β-*O*Me were evaluated by ^1H and ^{13}C NMR analyses in D_2O (Figs. 6-15). Characteristic signals were commonly observed in the region 4.20-4.55 ppm. H-1β signals of the products were observed at 4.39-4.42 ppm (d, $J_{1,2}$=8 Hz). The peaks of internal anomeric protons were observed as overlapping signals at 4.55-4.51 ppm (d, $J_{1,2}$=8Hz), characteristic of the β-(1→6)-linkage from the corresponding methyl β-gentiooligosides. Furthermore, overlapping signals at 4.21-4.25 ppm were observed. The signals were indicative of low-field shifts of internal H-6 protons. In addition, peaks of methyl group were observed at 3.58-3.60 ppm (s, 3H). The structures of these methyl β-gentiooligosides were further confirmed by ^{13}C NMR analysis, as shown in Table 3. Each peak could be assigned to the corresponding carbon atom of a methyl β-oligoside with a β-(1→6) linkage. No signals derived from other linkages were detected. In addition, ESIMS analysis of Gen_2 β-*O*Me, Gen_3 β-*O*Me, Gen_4 β-*O*Me, Gen_5 β-*O*Me, and Gen_6 β-*O*Me showed molecular ions at *m/z* 379.12125 (calcd. for $C_{13}H_{24}NaO_{11}$, 379.12163), 541.17498 (calcd. for $C_{19}H_{34}NaO_{16}$, 541.17445), 703.22668 (calcd. for $C_{25}H_{44}NaO_{21}$, 703.22728), 865.28050 (calcd. for $C_{31}H_{54}NaO_{26}$, 865.28010), and 1027.33524 (calcd. for $C_{37}H_{64}NaO_{31}$, 1027.33292), respectively, arising from the $[M+Na]^+$ ions.

4.8. Enzymatic synthesis of *p*-nitrophenyl β-gentiooligosides (DP 3-6, Gen_{3-6} β-*p*NP)

Glc β-*p*NP (1356 mg, 4.5 mmol) was dissolved in 33.7 mL of 83 mM sodium acetate buffer (pH 4.0) and β-glucosidase (11.3 mL, 24.9 U) in crude cellulase from *H. jecorina* was added. The mixture was incubated without stirring for 6 h at 40 °C. The reaction was terminated by boiling for 15 min, and the solution was loaded onto a Toyopearl HW-40S column (6×100 cm) equilibrated with 25% (v/v) methanol at a flow rate 1.5 mL/min. The eluate was collected in 25-mL fractions and monitored by measuring the absorbance at 300 nm (*p*-nitrophenyl group). Peak fractions (3150-3400 mL) containing the target product were pooled, concentrated and lyophilized. Gen_2 β-*p*NP[29] (158.1 mg) was obtained in 15.2% yield based on the initial substrate. The synthetic Gen_2 β-*p*NP (278 mg, 0.6 mmol) and Gen_3 (757 mg, 1.5 mmol) were dissolved in 2.8 mL of 55 mM sodium acetate buffer (pH 5.5) and *P. multicolor* β-1,6-glucanase solution (0.2 mL, 2.4 U) was added. The mixture was incubated for 116 h at 4 °C. The reaction was terminated by boiling for 15 min and loaded onto a Toyopearl HW-40S column (6×100 cm) equilibrated with 25% methanol at a flow rate 1.5 mL/min (25 mL/tube). The chromatogram showed five peaks eluted in the following order: PG_6 (1700-1800 mL), PG_5 (1850-1950 mL), PG_4 (2075-2200 mL), PG_3 (2450-2550 mL), and PG_2 (3300-3525 mL). Fractions PG_4, PG_3, and PG_2 were individually concentrated and lyophilized to afford Gen_4 β-*p*NP (66.9 mg), Gen_3 β-*p*NP (7.7 mg), and Gen_2 β-*p*NP (159.7 mg), respectively, in 14.2%, 2.1% and 57.4% yield based on the acceptor. PG_6 and PG_5 were separately concentrated and loaded onto a reverse-phase ODS column (1.5×3.1 cm) equilibrated with H_2O. After washing the column with H_2O (30 mL), the adsorbed glucoside was eluted with methanol (30 mL), and the eluate was collected in 2-mL fractions and monitored by measuring the absorbance at 300 nm (*p*-nitrophenyl group). Peak fractions (32-50 mL) were individually combined, concentrated, and lyophilized to afford Gen_6 β-*p*NP (7.8 mg) and Gen_5 β-*p*NP (14.9 mg) in 1.7% and 2.6% yield, respectively, based on the acceptor.

The structures of synthetic Gen_2-Gen_6 β-*p*NP were evaluated by ^1H NMR and ^{13}C NMR as in Table 4 and Figs. 16-25. ESIMS analysis of Gen_2 β-*p*NP, Gen_3 β-*p*NP, Gen_4 β-*p*NP, Gen_5 β-*p*NP, and Gen_6 β-*p*NP showed molecular ions at *m/z* 486.12527 (calcd. for $C_{18}H_{25}NNaO_{13}$, 486.12236), 648.17548 (calcd. for $C_{24}H_{35}NNaO_{18}$, 648.17518), 810.22788 (calcd. for $C_{30}H_{45}NNaO_{23}$, 810.22800), 972.28091 (calcd.

for $C_{36}H_{55}NNaO_{28}$, 972.28083), and 1134.33385 (calcd. for $C_{42}H_{65}NNaO_{33}$, 1134.33365), respectively, arising from the $[M+Na]^+$ ions.

4.9. Action of β-(1→6)-glucanase

The hydrolytic activity of purified β-(1→6)-glucanase was evaluated by using several glucans and an oligosaccharide (Gen_8) under standard conditions. Before the assay, Gen_8 was dissolved in H_2O and then the reducing power in the solution was adjusted by H_2O to match that of the pustulan solution (5 mg/mL). The hydrolysate and enzyme activity on these substrates was determined by measuring the amount of reducing sugar by the Somogyi-Nelson method.[26, 27] Methyl β-gentiooligosides (DP 2-6), *p*-nitrophenyl β-gentiooligosides (DP 2-6) and gentioligosaccharides (DP 2-6) were used to analyze the frequency of the enzymatic cleavage of the β-(1→6)-linkage and relative hydrolytic rate. Each substrate was dissolved in H_2O (25 μl, 10 mM) and mixed with 25 mM sodium acetate buffer (200 μl, pH4.0) and then added to the enzyme solution (25 μl, 59 mU). The reaction was conducted at 40°C. The amount of each product formed at an early stage (within 27% hydrolysis) from the initial substrate during incubation with the enzyme was analyzed by HPAEC-PAD (Gen_{2-6} β-*O*Me and Gen_{2-6}, condition 1) and HPLC (Gen_{2-6} β-*p*NP). From the peak areas on the chromatogram of the digest of each substrate with enzyme, the amount of the products was calculated. The amount of each product increased linearly with time in the initial stage of the reaction. On the basis of these data, the frequency and relative hydrolytic rate of the β-(1→6)-glucanase-catalyzed cleavage of glycosidic linkages were determined.

The pattern of pustulan hydrolysis by the enzyme was analyzed as follows: purified pustulan was dissolved in H_2O (900 μl, 5 mg/mL) and then added to enzyme solution (100 μl, 53 mU) in 50 mM sodium acetate buffer (pH 5.5). The reaction was performed at 40°C and monitored by HPAEC-PAD analysis (condition 2). The hydrolytic profile of Gen_8 and Gen_9 was analyzed as follows: each substrate was dissolved in H_2O (25 μl, 10 mM), mixed with 25 mM sodium acetate buffer (200 μl, pH 4.0) and

then added to enzyme solution (25 μl, 59 mU). The reaction was conducted at 40°C. The amount of each product formed at an early stage (Gen_8; 10% hydrolysis, Gen_9; 35% hydrolysis) was analyzed by HPAEC-PAD (condition 1)

DP of pustulan was estimated as follows: purified pustulan was hydrolyzed by β-(1→6)-glucanase and the hydrolysate was analyzed by HPAEC-PAD (condition 2). Standard curve was generated from the retention time of clearly resolved peaks and corresponding DPs that have less than 56. Higher DPs were calculated from the extrapolated standard curve.

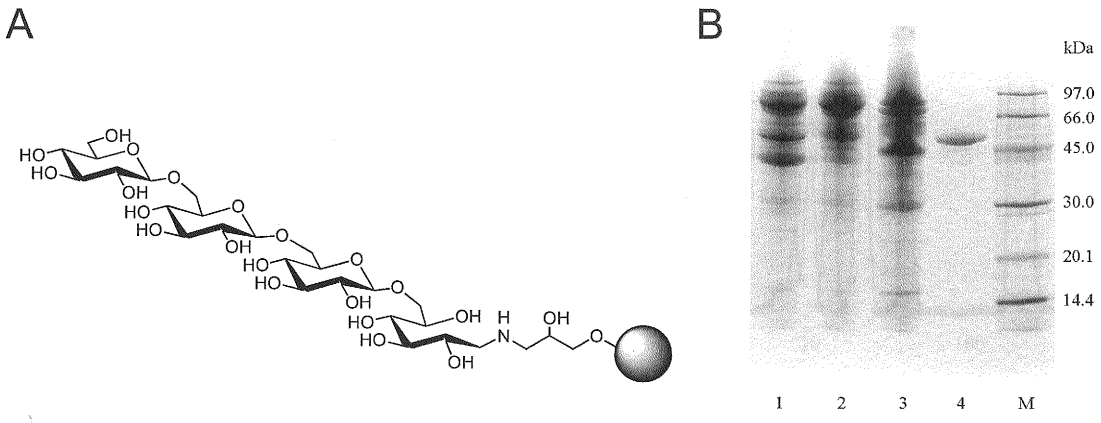

Figure 1. (A) Structure of the Gen_4-coupled affinity gel. (B) SDS-PAGE of purified *P. multicolor* β-(1→6)-glucanase using a 12.5% gel under reducing conditions. Proteins were stained with CBB. Lane 1, crude enzyme; Lane 2, ammonium sulfate precipitation; Lane 3, cation-exchange elute; Lane 4, affinity elute. Numbers on the right indicate the molecular mass of the protein standards. (Lane M).

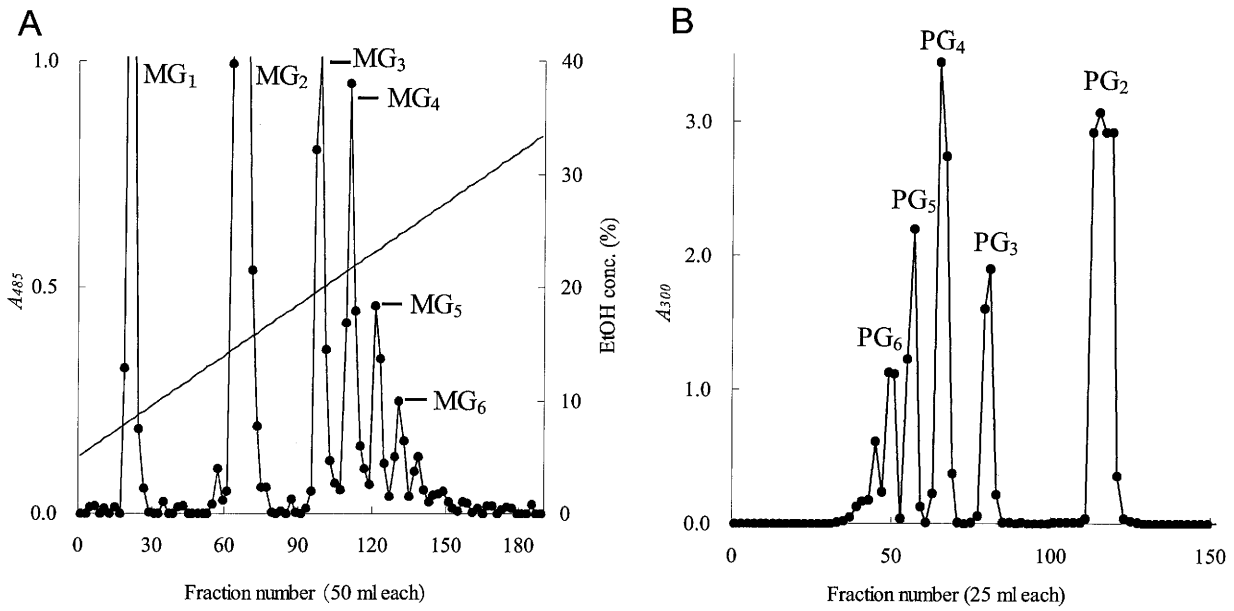

Figure 2. (A) Charcoal-Celite chromatography of transglycosylation products formed by the action of β-(1→6)-glucanase on methyl β-gentiobioside. The elution positions of MG_1 and MG_2-MG_6 correspond to methyl β-D-glucoside and methyl β-gentiooligosides (DP 2-6), respectively. The straight line indicates ethanol concentration (%). (B) TOYOPEARL HW-40S chromatography of transglycosylation products formed by the action of β-(1→6)-glucanase on gentiotriose and *p*-nitrophenyl β-gentiobioside. The elution positions of PG_2-PG_6 correspond to *p*-nitrophenyl β-gentiooligosides (DP 2-6), respectively.

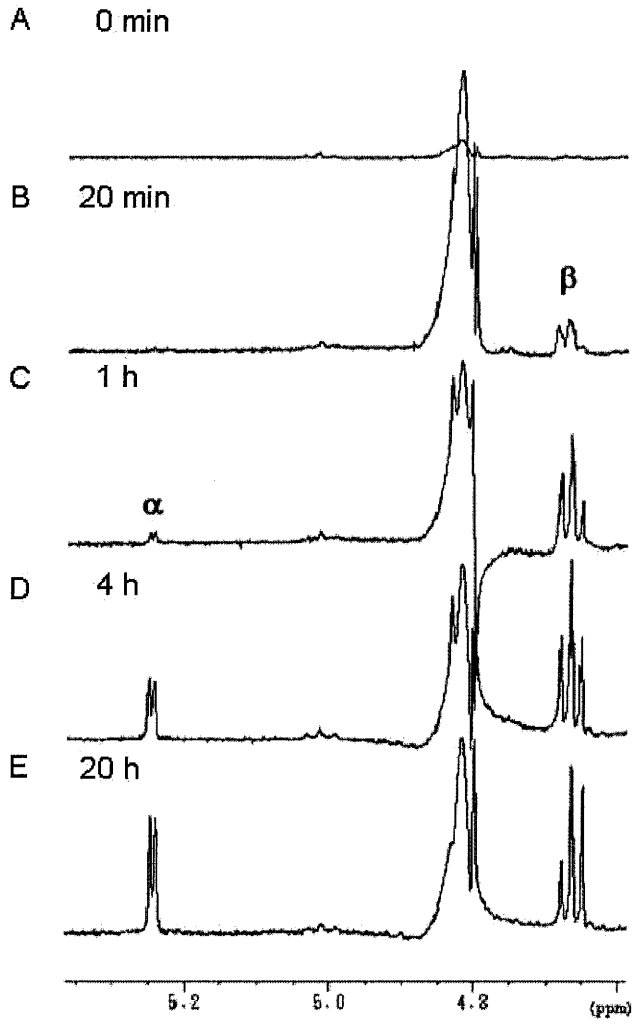

Figure 3. ^{1}H NMR spectra of the time course of pustulan hydrolysis by the purified β-(1→6)-glucanase. (A) Initial substrate; (B) 20 min, (C) 1 h, (D) 4 h, and (E) 20 h incubation after addition of the enzyme. α and β indicate signals from H-1α and H-1β protons, respectively, of gentiooligosaccharides produced by pustulan hydrolysis by the enzyme. The enzyme reaction was performed in a 3-mm sample tube at 25 °C. Pustulan was dissolved in D_2O (0.65%, w/v) and then the enzyme solution (10 μl, 72 mU) was added.

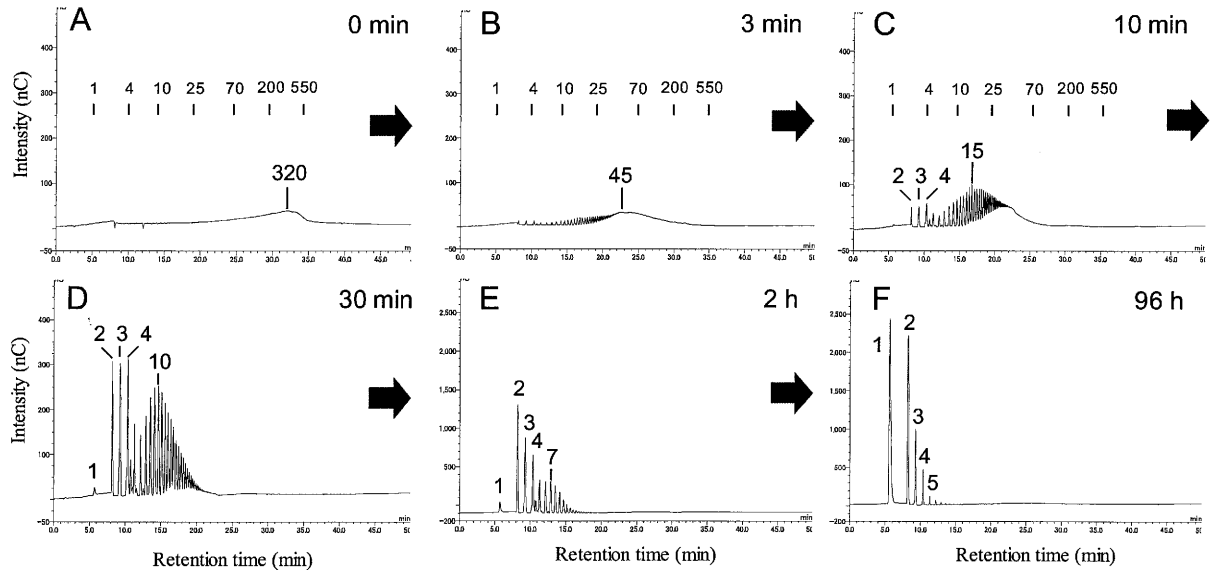

Figure 4. HPAEC-PAD analysis of the hydrolytic products of pustulan obtained with the purified β-(1→6)-glucanase. (A) Initial substrate; (B) 3 min, (C) 10 min, (D) 30 min, (E) 2 h, and (F) 96 h after incubation after the addition of enzyme. Numbers indicate the DP of gentiooligosaccharides.

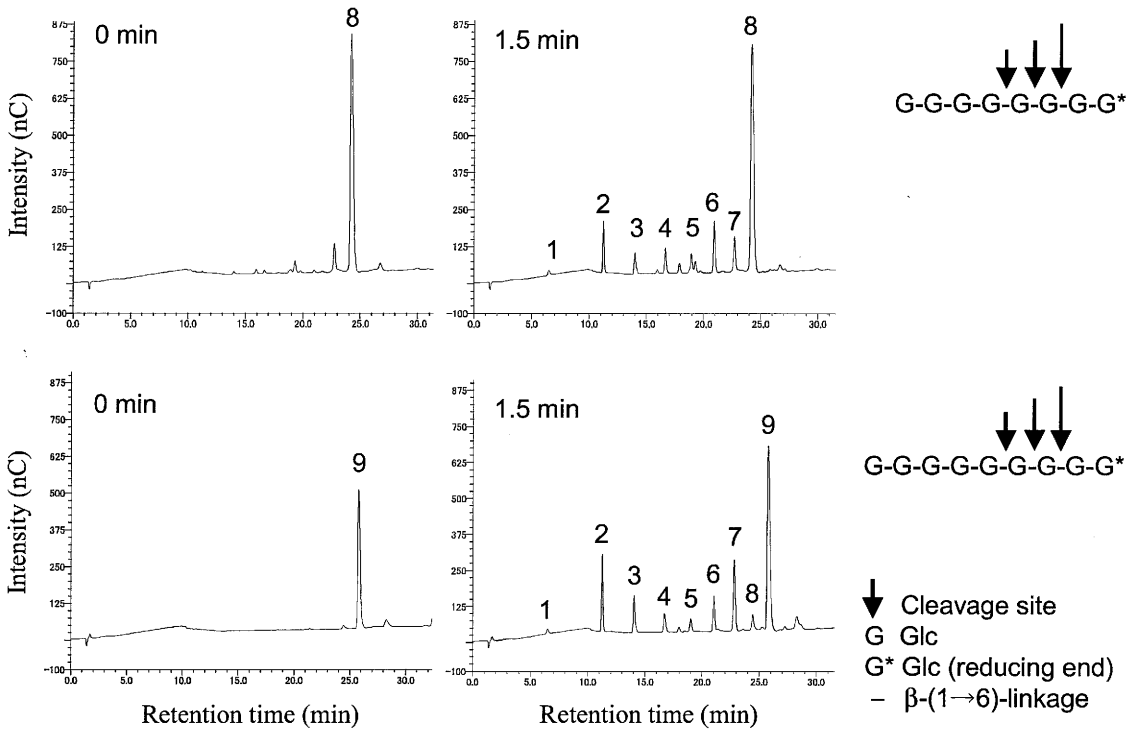

Figure 5. HPAEC-PAD analysis of the hydrolytic products of Gen_8 (top) and Gen_9 (bottom) obtained with the purified β-(1→6)-glucanase. Left, initial substrate; right, 1.5 min after the addition of enzyme. Numbers indicate the DP of gentiooligosaccharides.

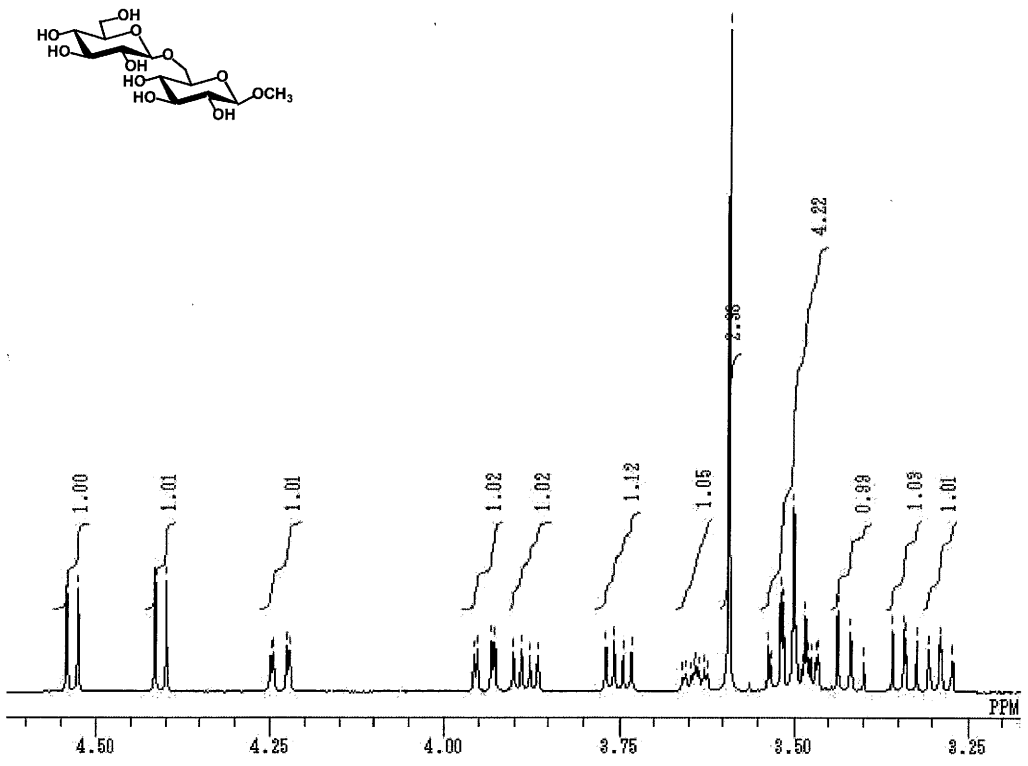

Figure 6. ^{1}H NMR spectrum of Gen_2 β-*O*Me in D_2O (500 MHz).

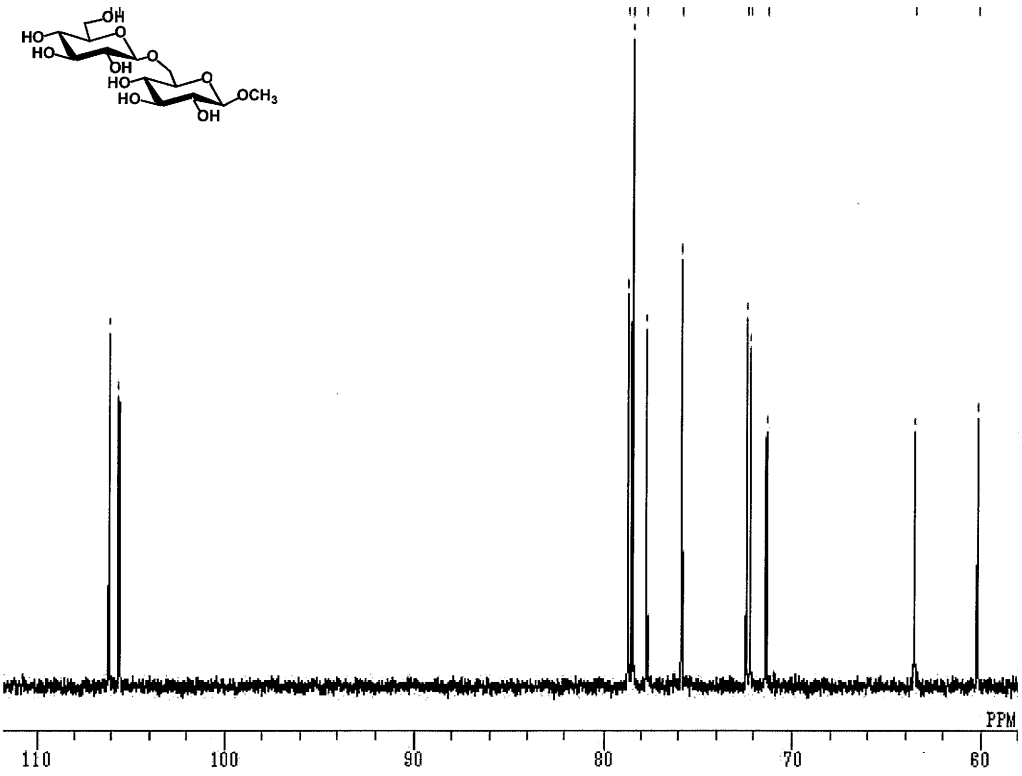

Figure 7. ^{13}C NMR spectrum of Gen_2 β-*O*Me in D_2O (125 MHz).

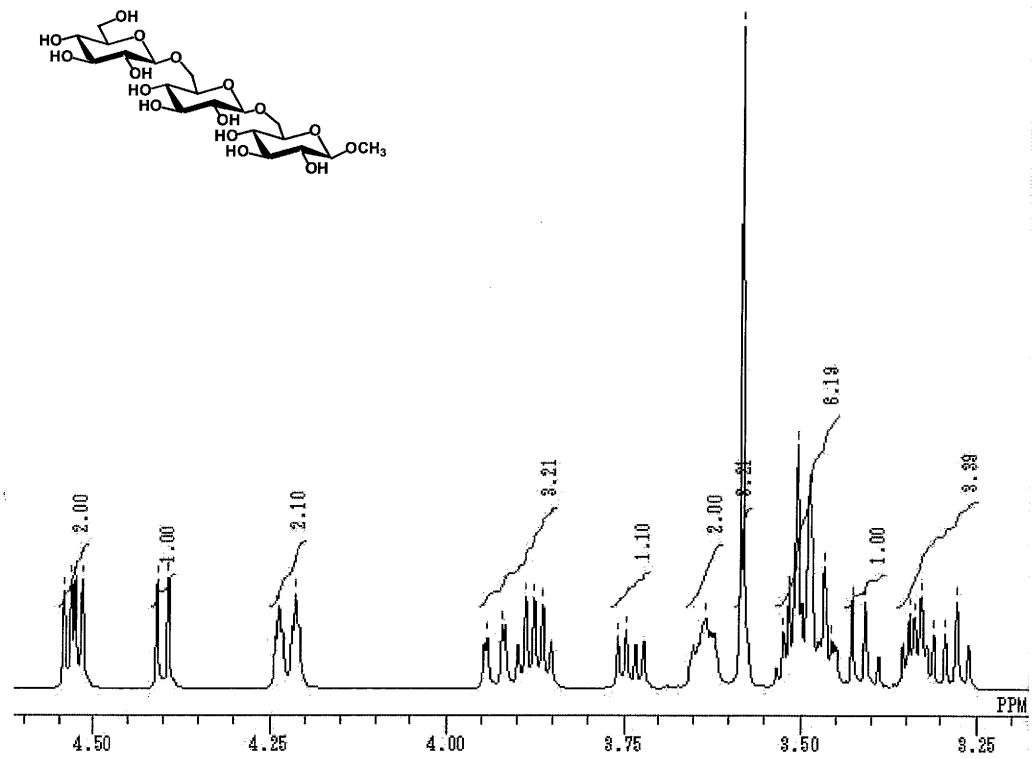

Figure 8. ^{1}H NMR spectrum of Gen_3 β-*O*Me in D_2O (500 MHz).

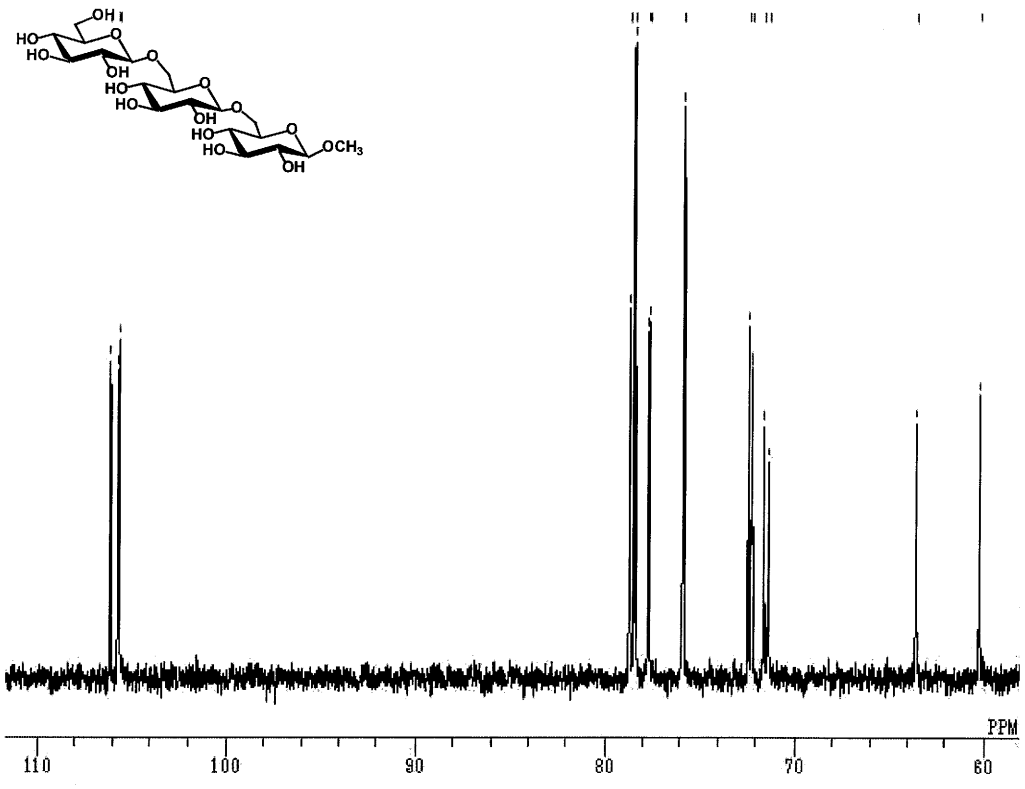

Figure 9. ^{13}C NMR spectrum of Gen_3 β-*O*Me in D_2O (125 MHz).

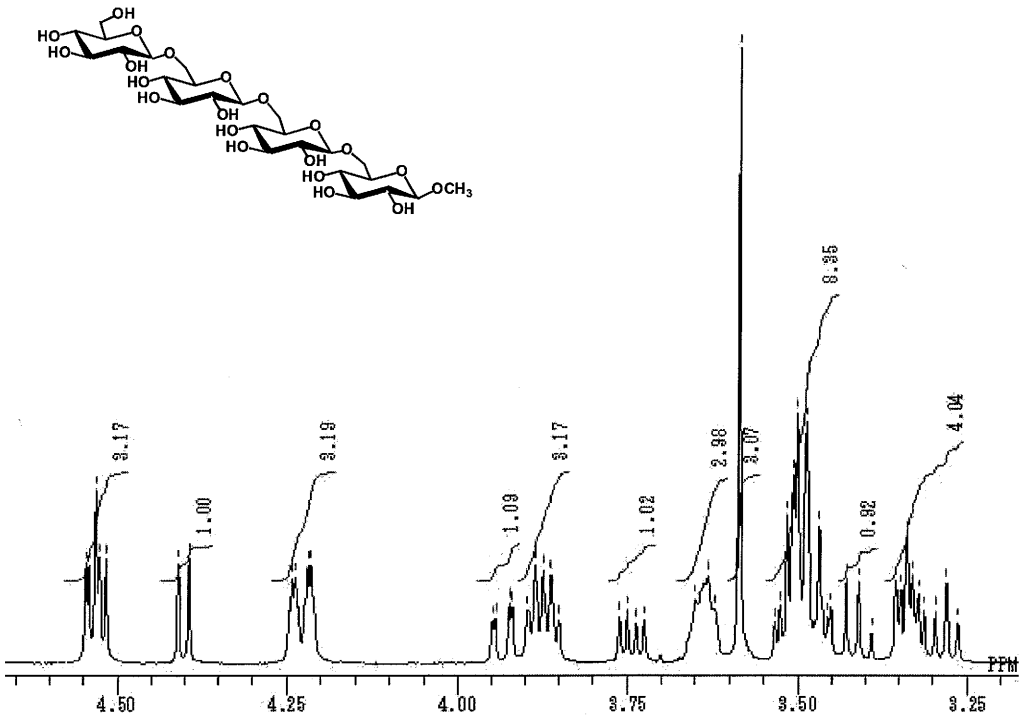

Figure 10. ^{1}H NMR spectrum of Gen_4 β-*O*Me in D_2O (500 MHz).

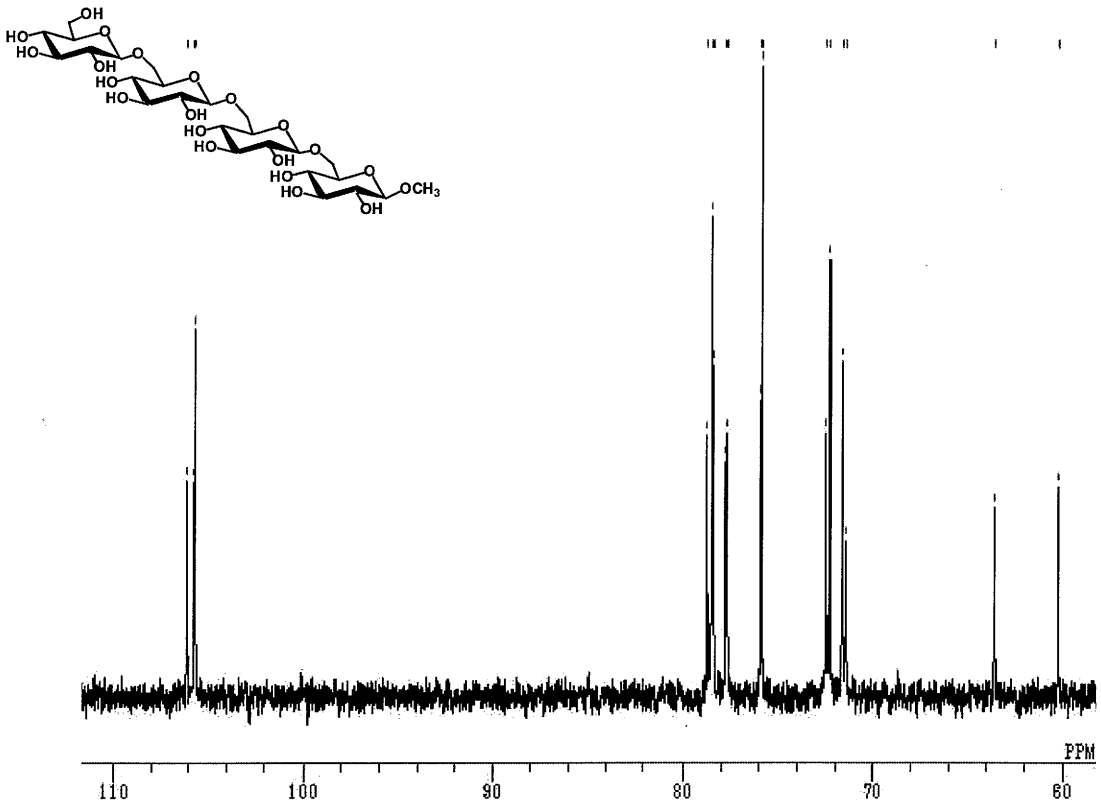

Figure 11. ^{13}C NMR spectrum of Gen_4 β-*O*Me in D_2O (125 MHz).

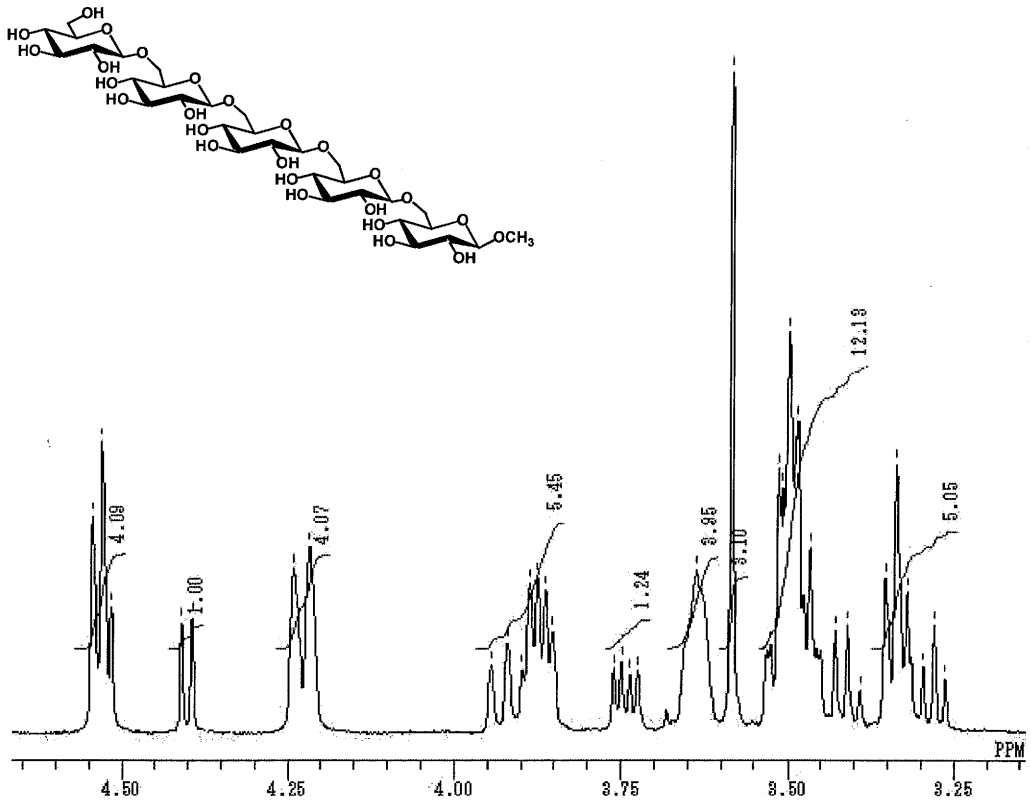

Figure 12. ^{1}H NMR spectrum of Gen_5 β-*O*Me in D_2O (500 MHz).

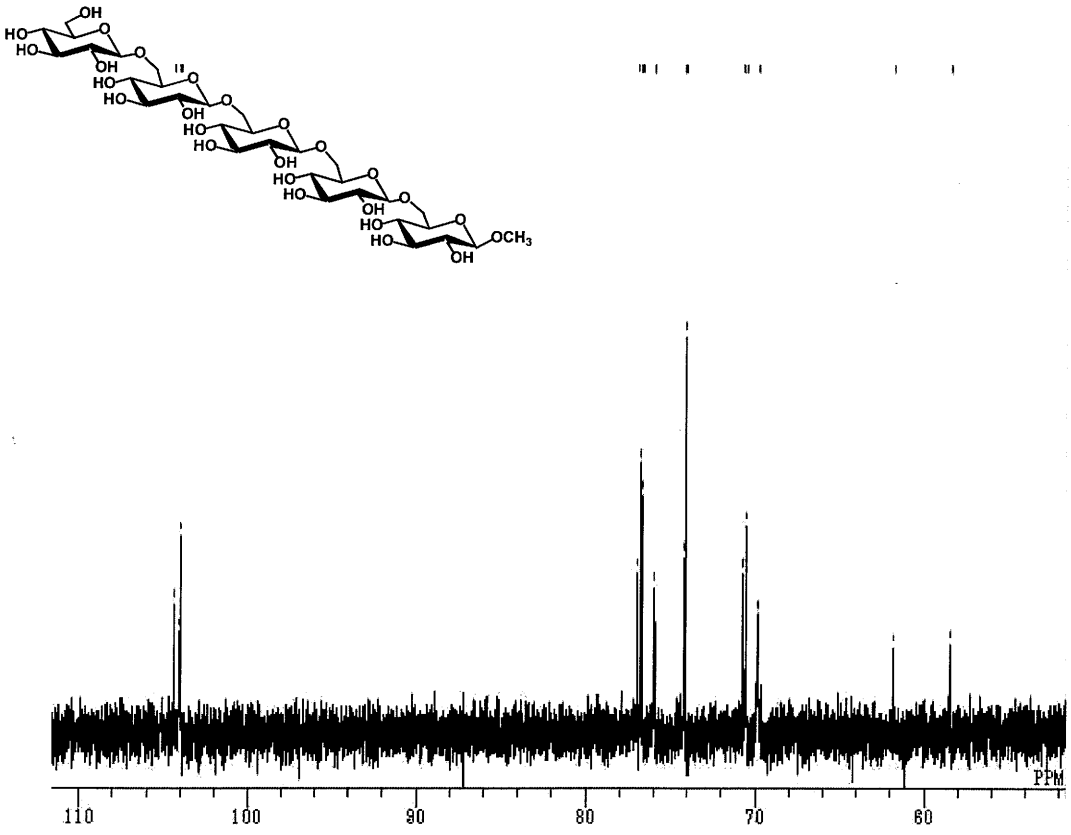

Figure 13. ^{13}C NMR spectrum of Gen_5 β-*O*Me in D_2O (125 MHz).

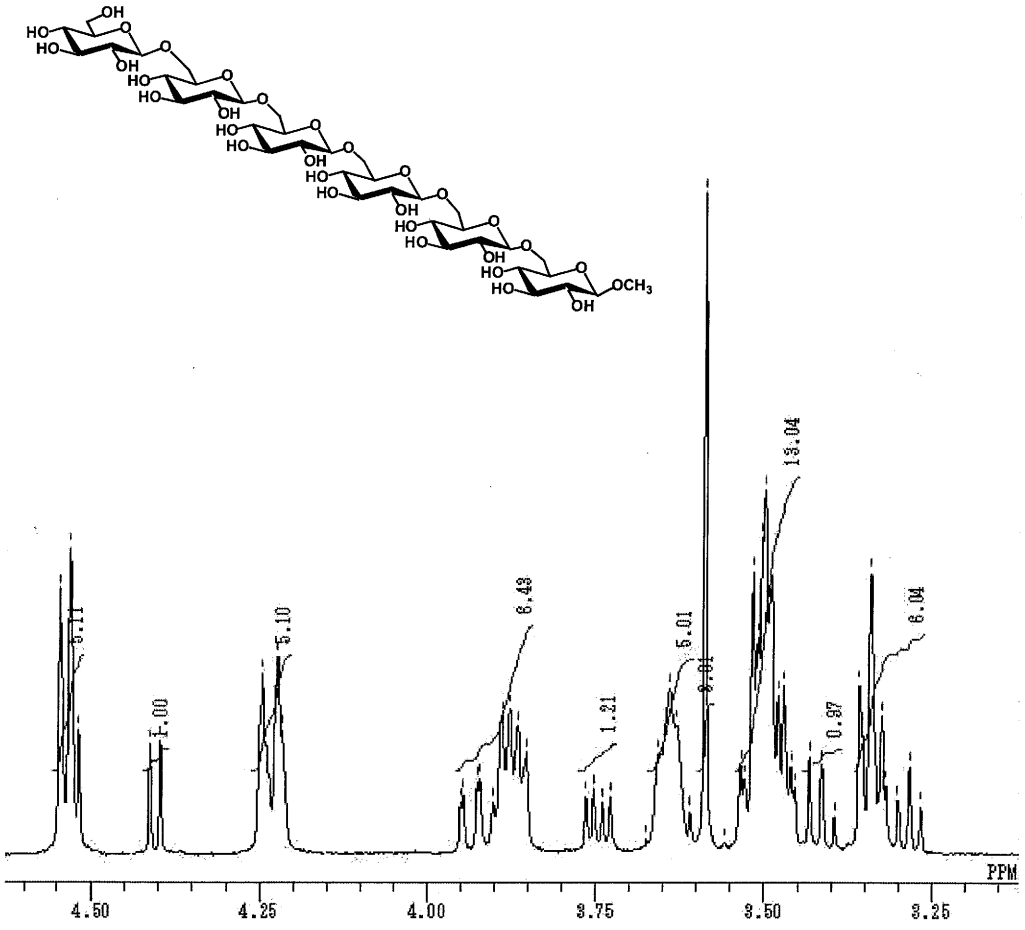

Figure 14. ^{1}H NMR spectrum of Gen_6 β-*O*Me in D_2O (500 MHz).

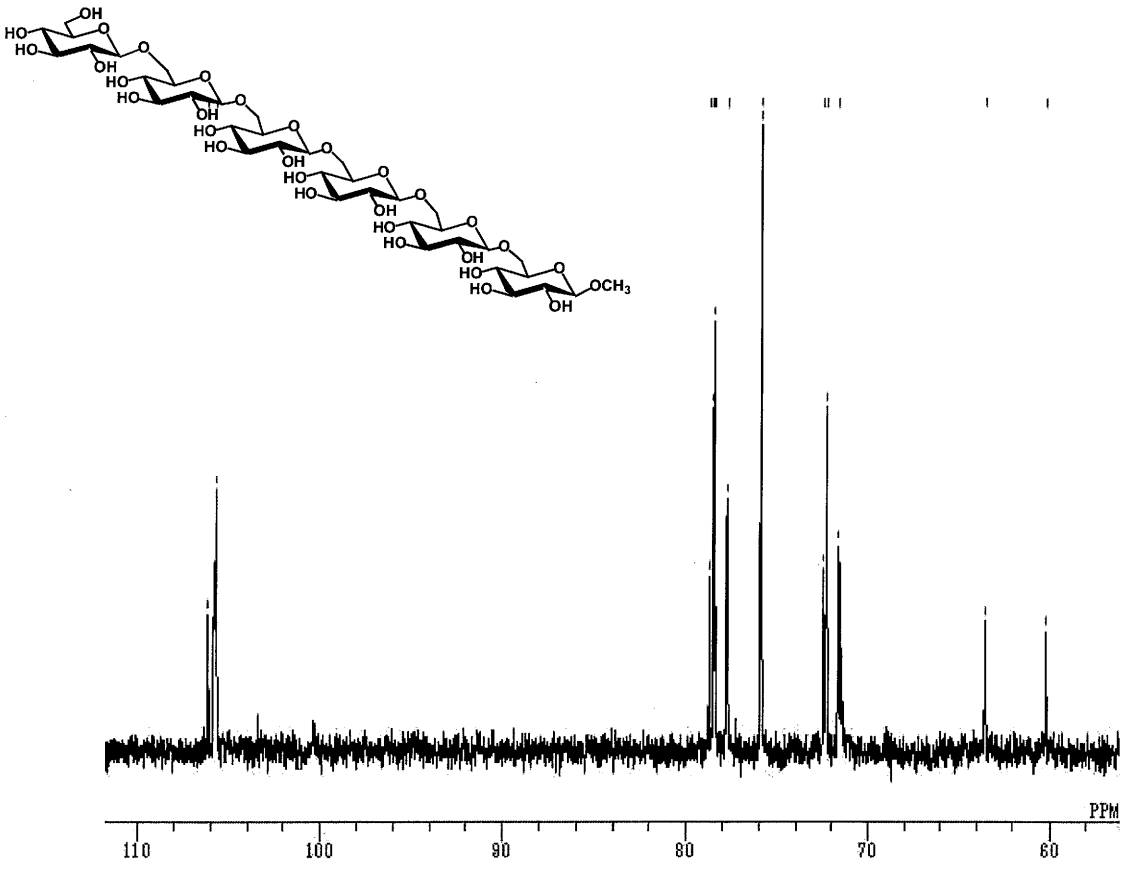

Figure 15. ^{13}C NMR spectrum of Gen_6 β-*O*Me in D_2O (125 MHz).

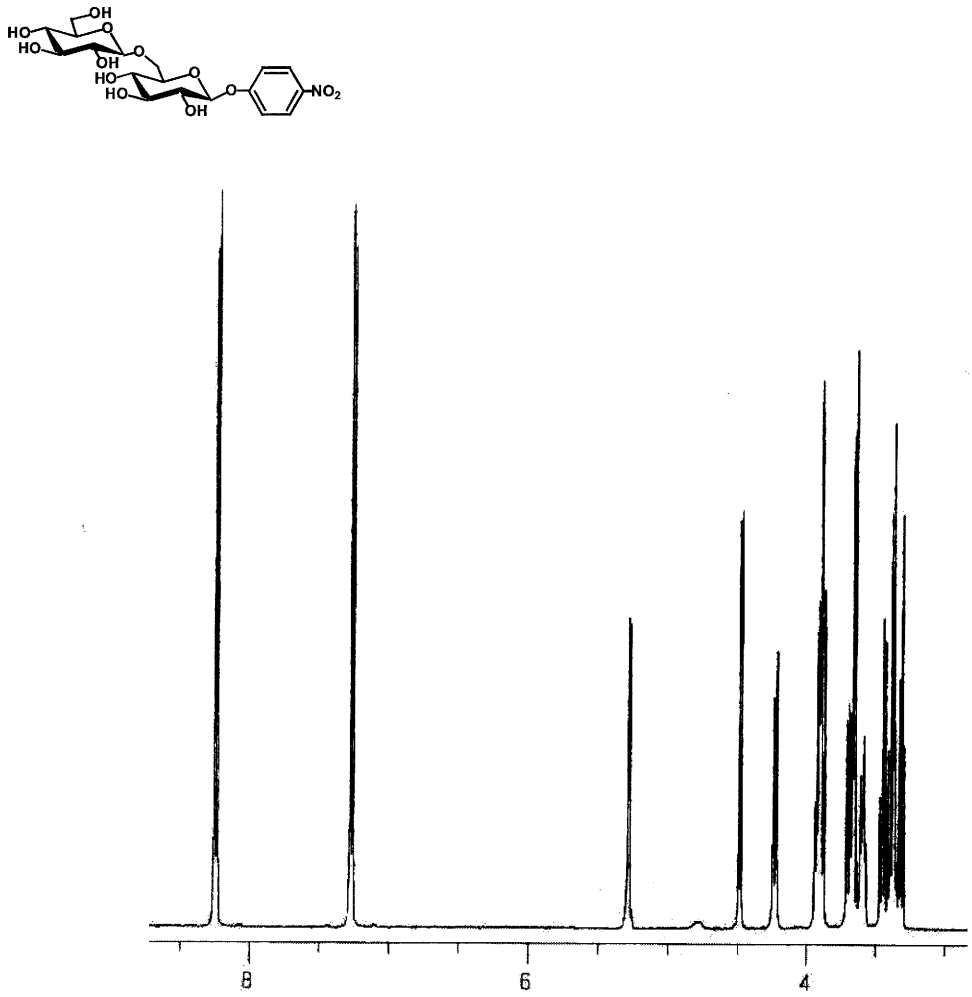

Figure 16. ^{1}H NMR spectrum of Gen_2 β-*p*NP in D_2O (500 MHz).

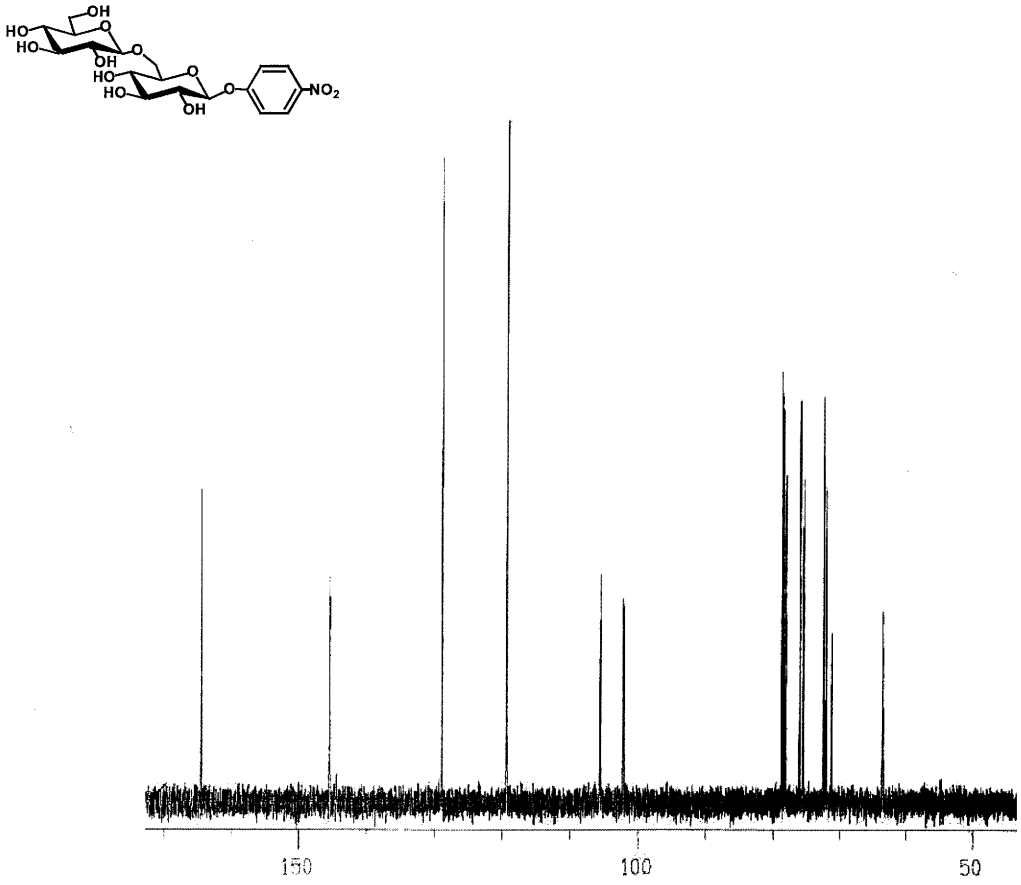

Figure 17. ^{13}C NMR spectrum of Gen_2 β-*p*NP in D_2O (125 MHz).

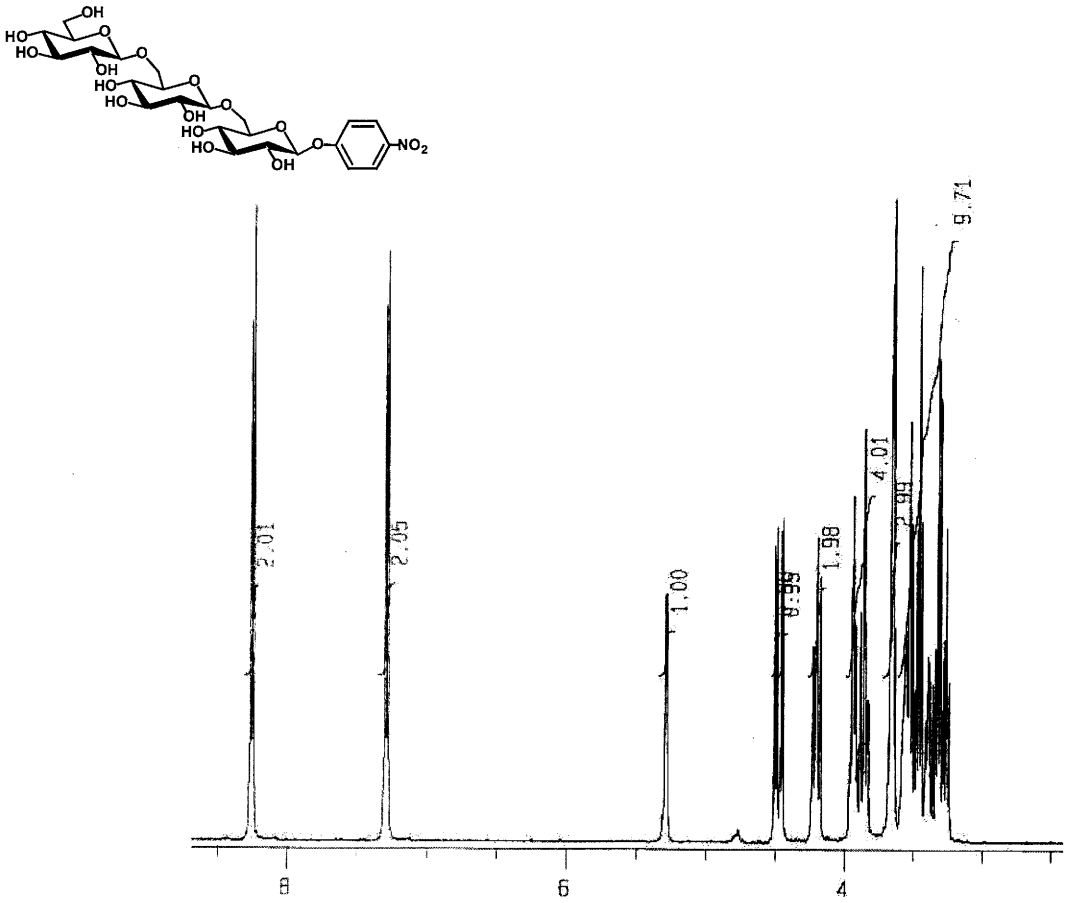

Figure 18. ^{1}H NMR spectrum of Gen_3 β-*p*NP in D_2O (500 MHz).

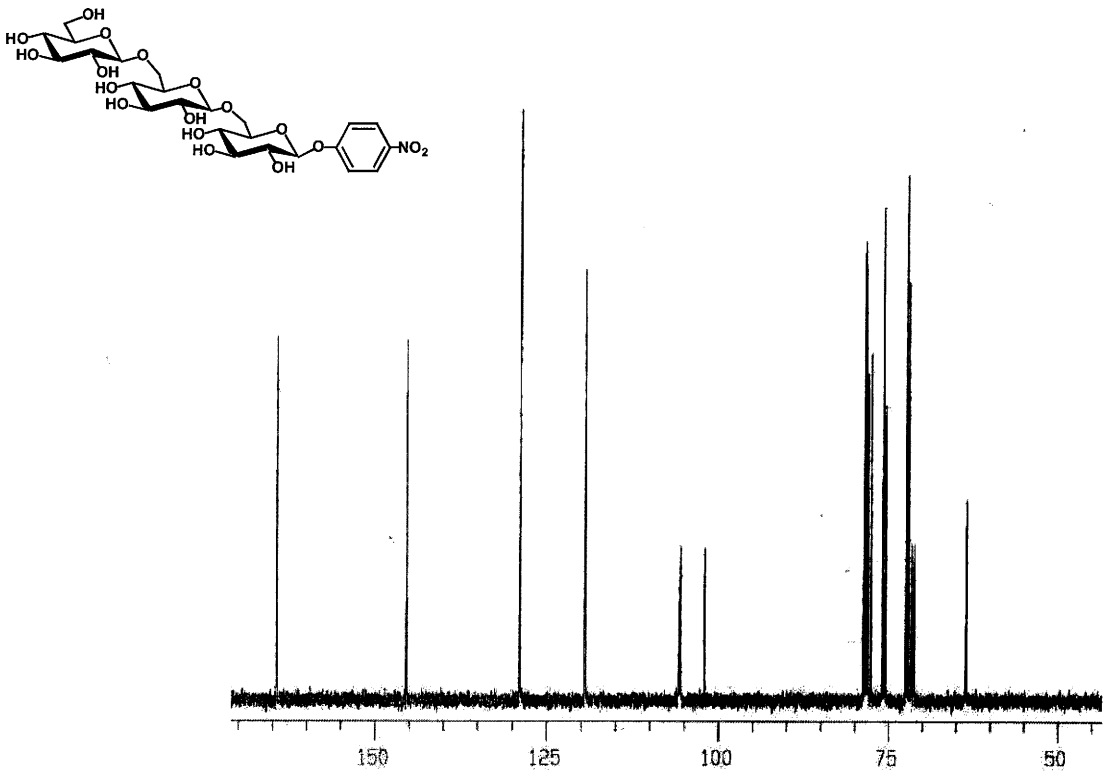

Figure 19. ^{13}C NMR spectrum of Gen_3 β-*p*NP in D_2O (125 MHz).

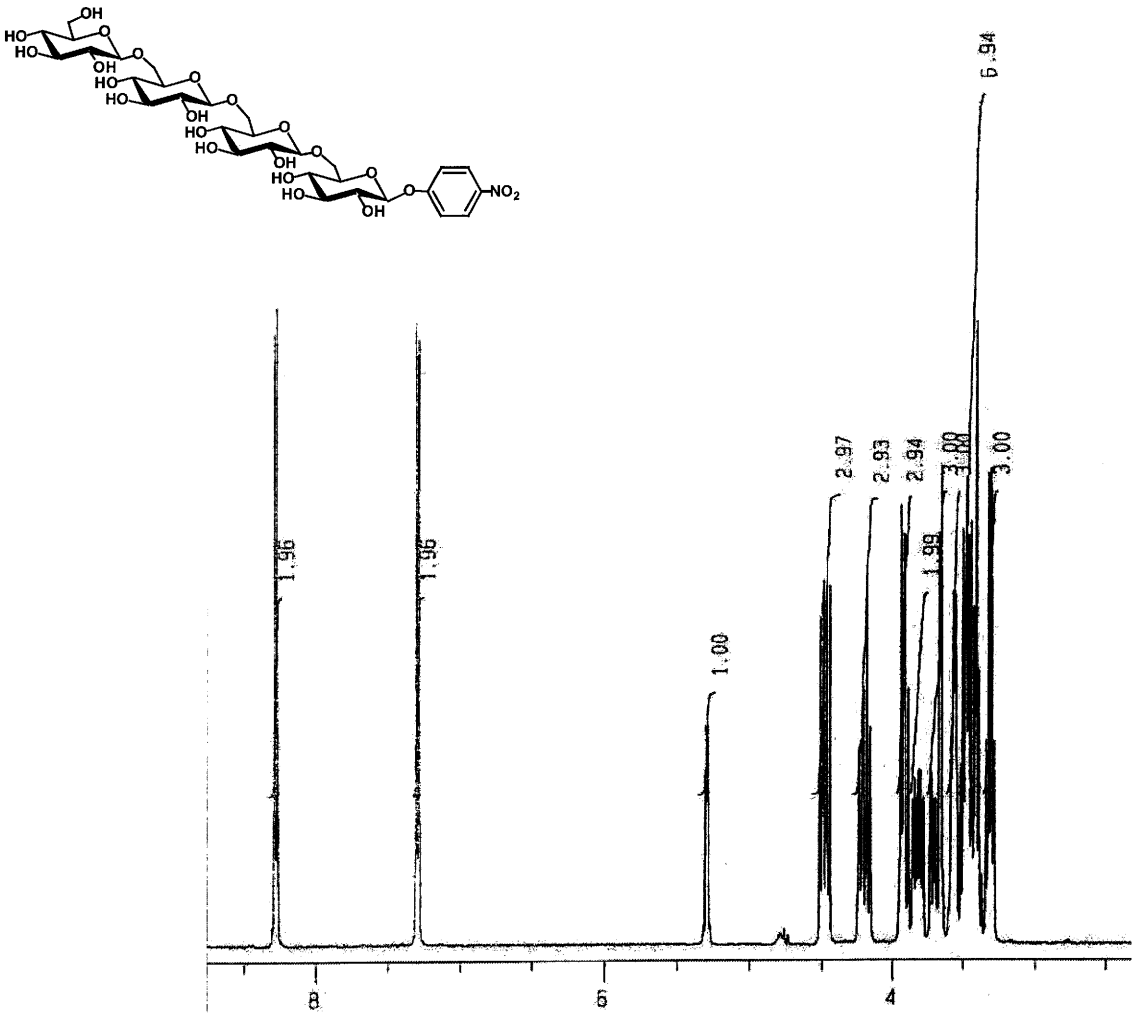

Figure 20. ^{1}H NMR spectrum of Gen_4 β-*p*NP in D_2O (500 MHz).

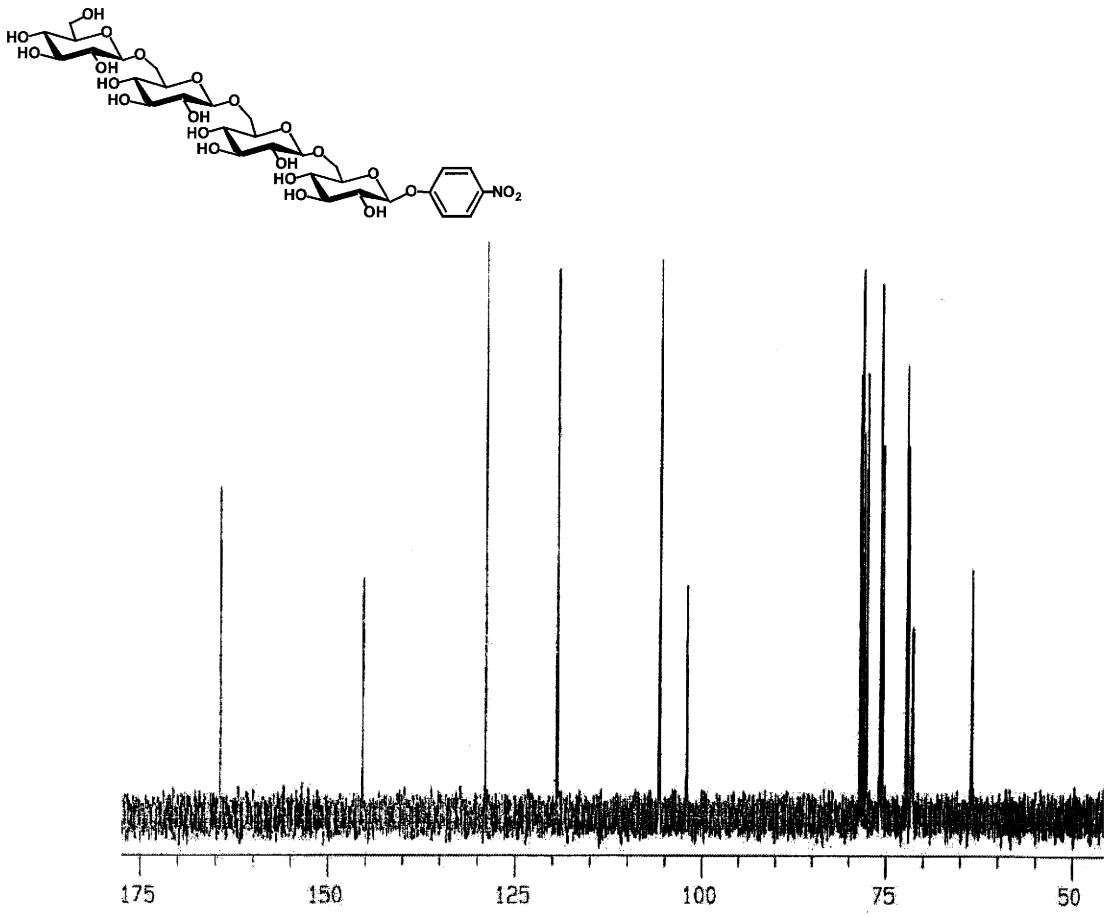

Figure 21. ^{13}C NMR spectrum of Gen_4 β-*p*NP in D_2O (125 MHz).

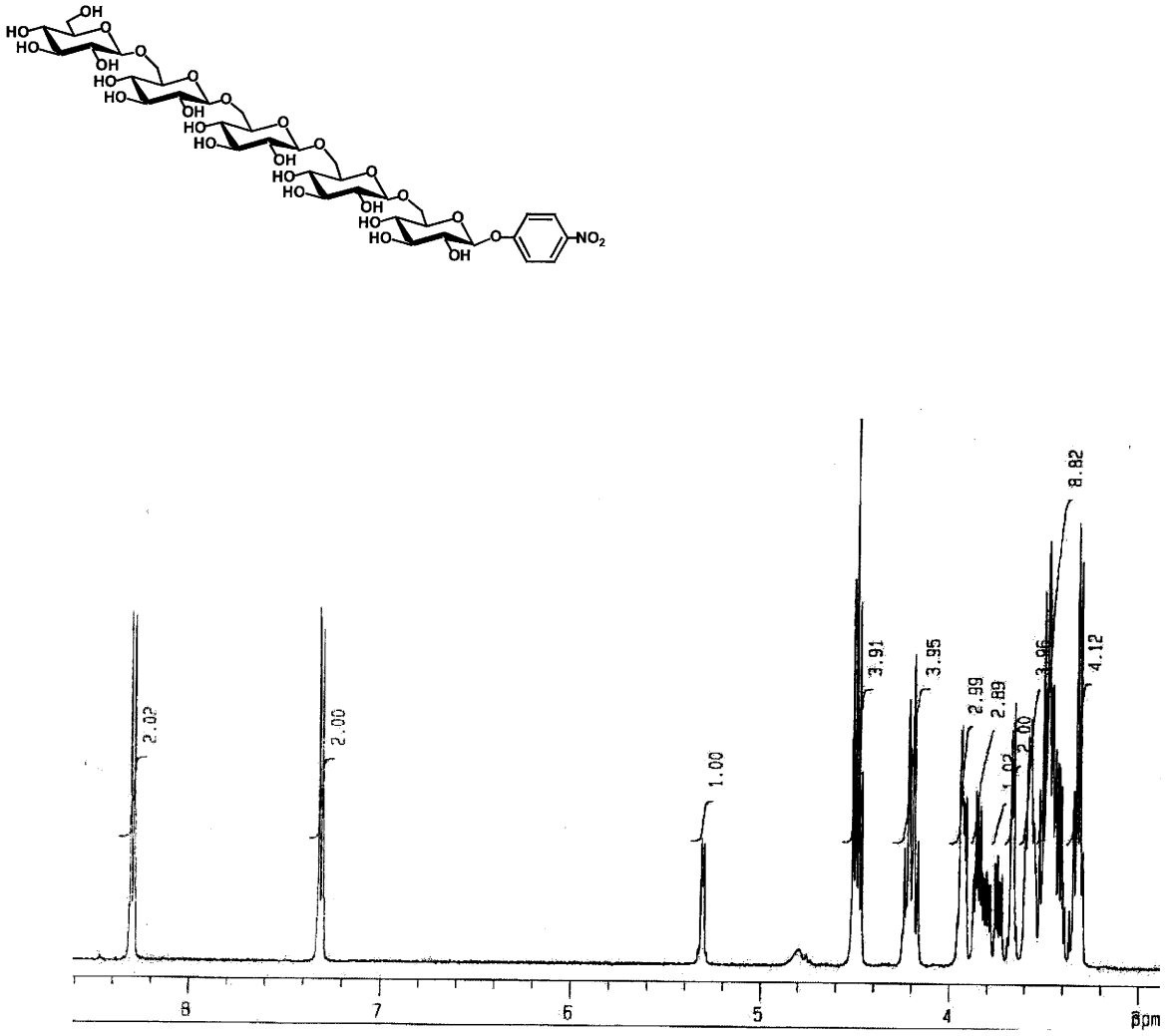

Figure 22. ^{1}H NMR spectrum of Gen_5 β-*p*NP in D_2O (500 MHz).

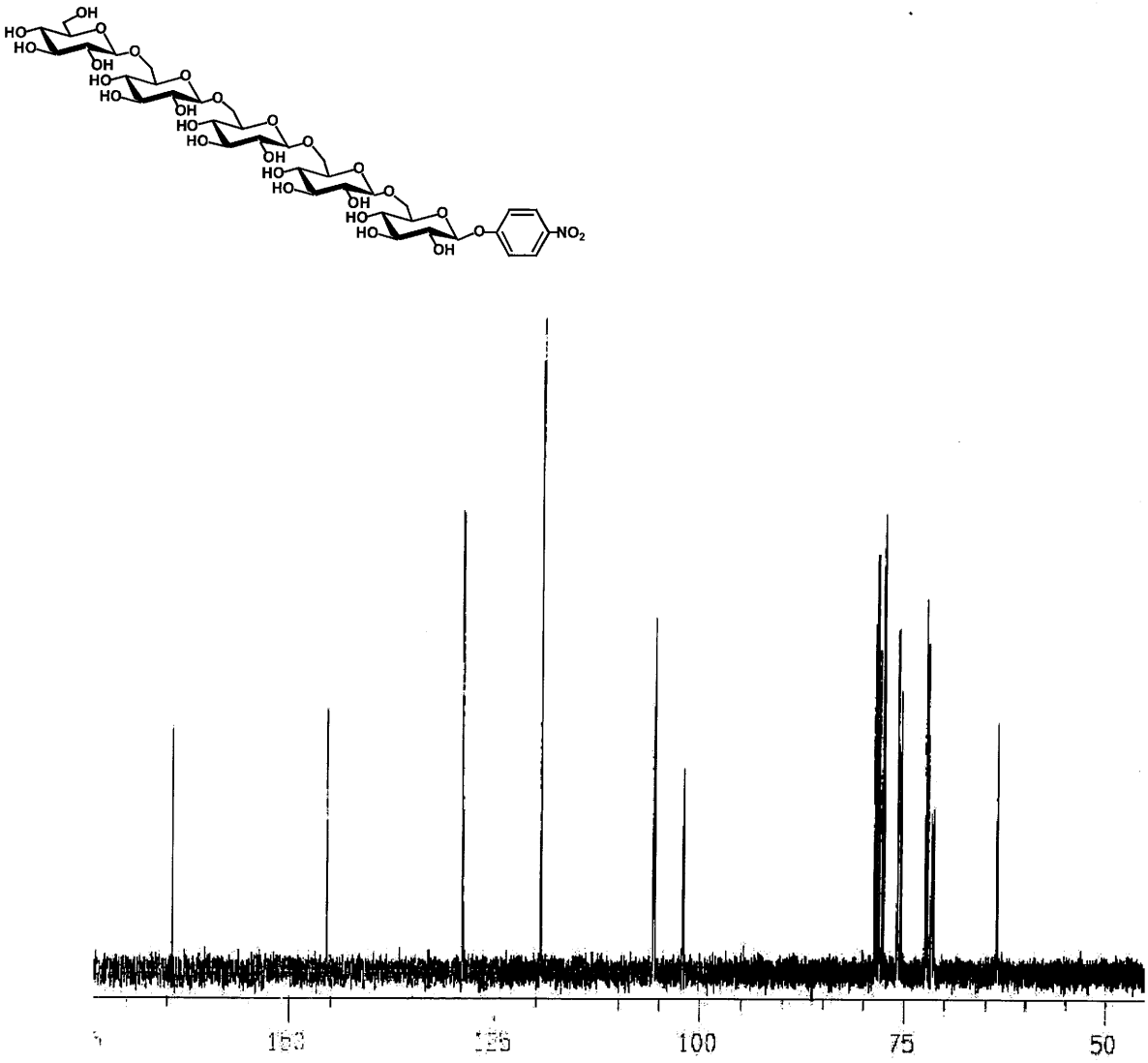

Figure 23. ^{13}C NMR spectrum of Gen_5 β-*p*NP in D_2O (125 MHz).

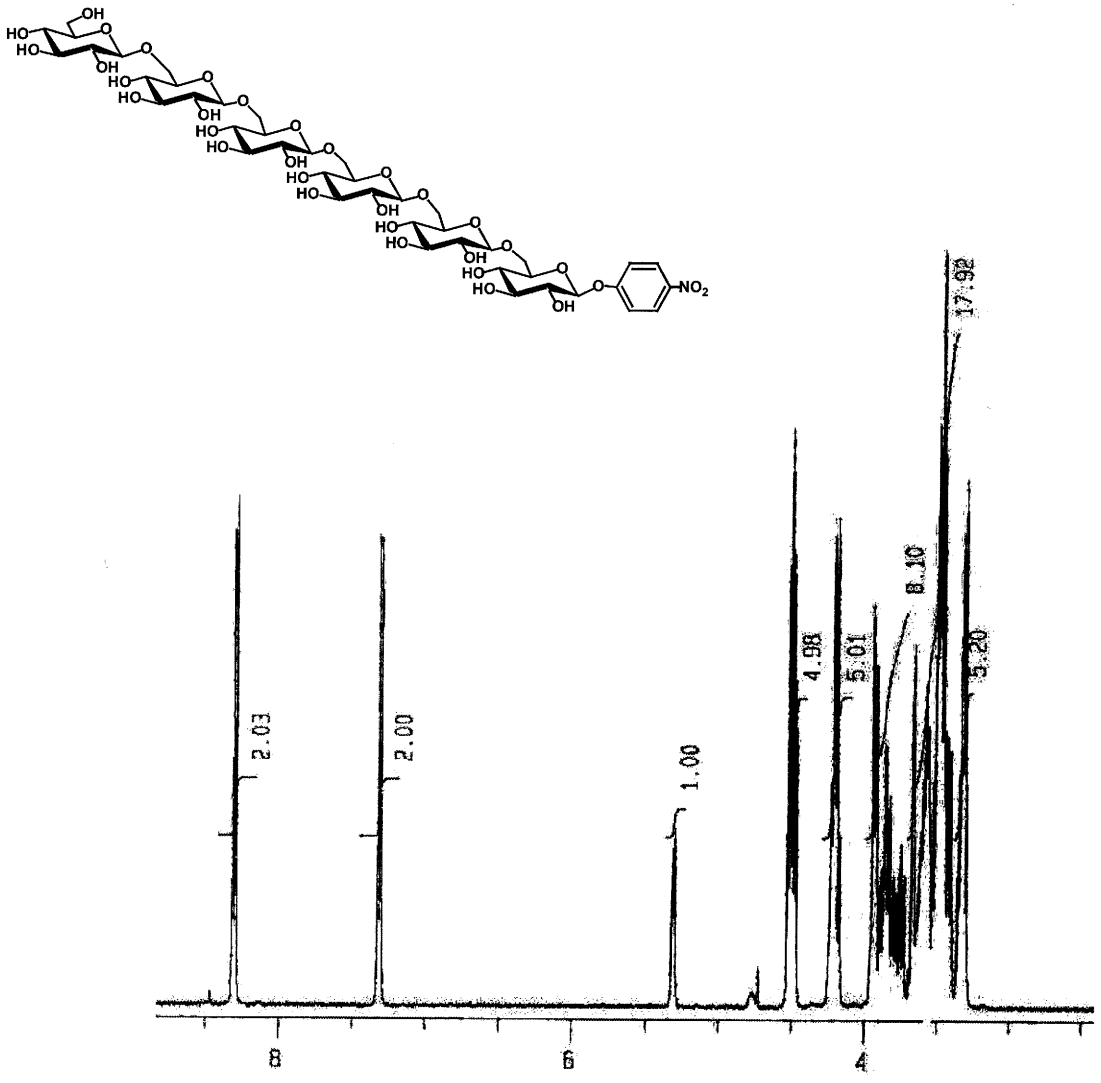

Figure 24. ^{1}H NMR spectrum of Gen_6 β-*p*NP in D_2O (500 MHz).

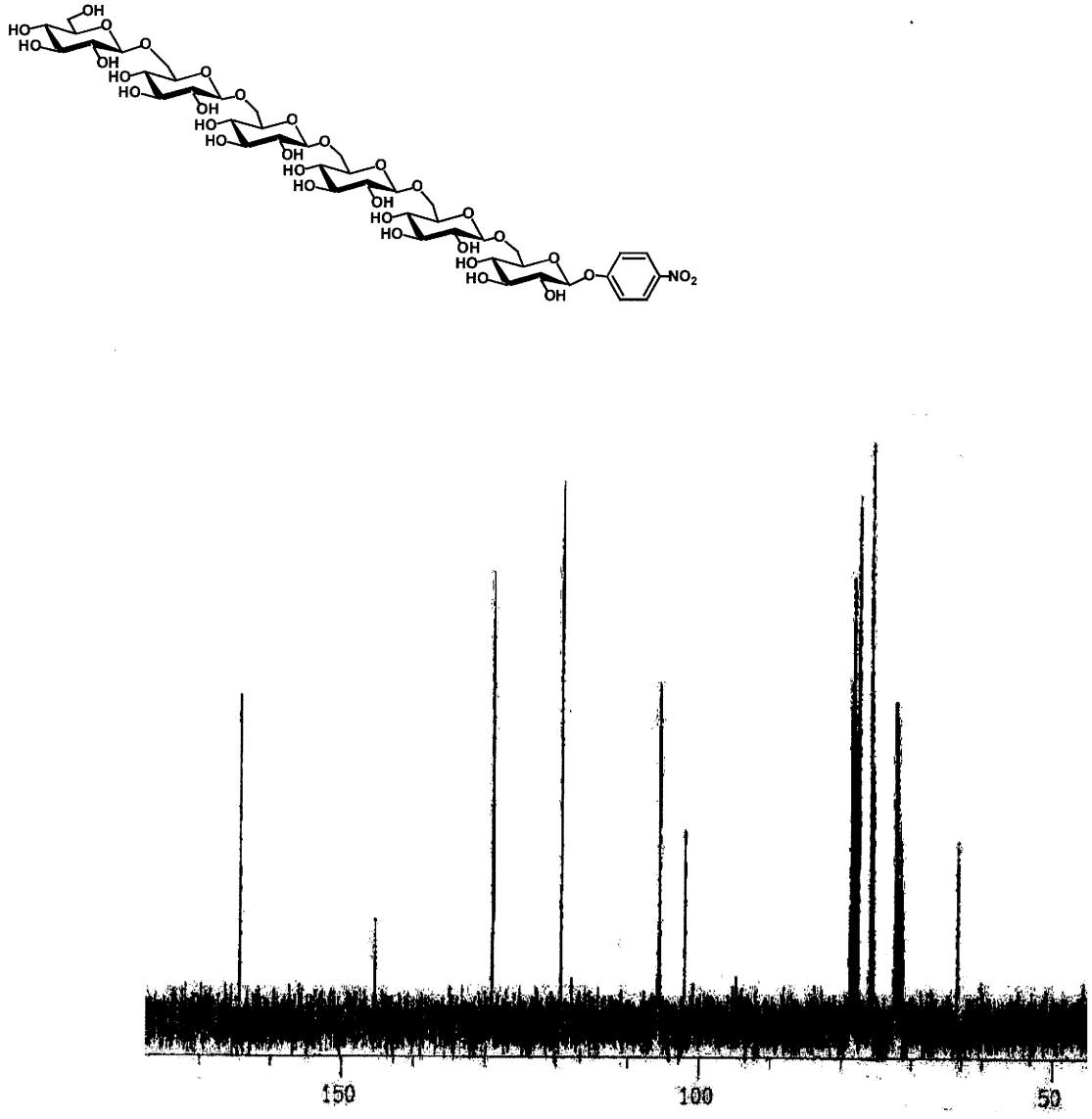

Figure 25. ^{13}C NMR spectrum of Gen_6 β-*p*NP in D_2O (125 MHz).

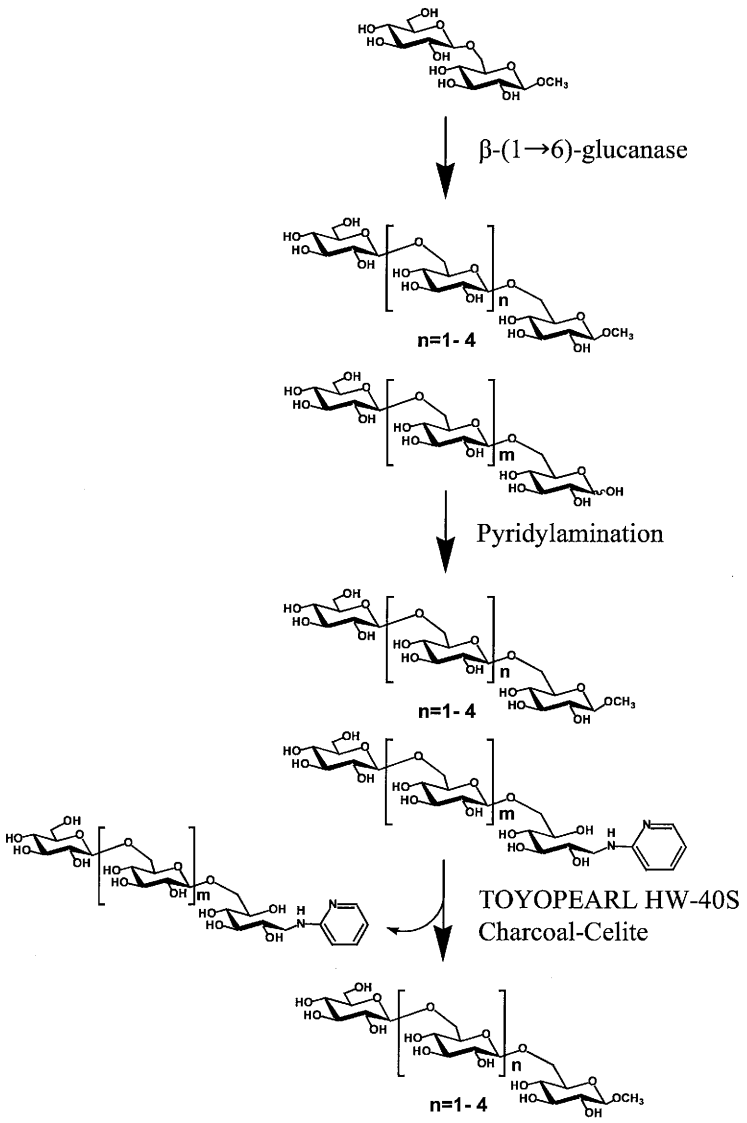

Scheme 1. Synthesis and purification of methyl β-gentiooligosides.

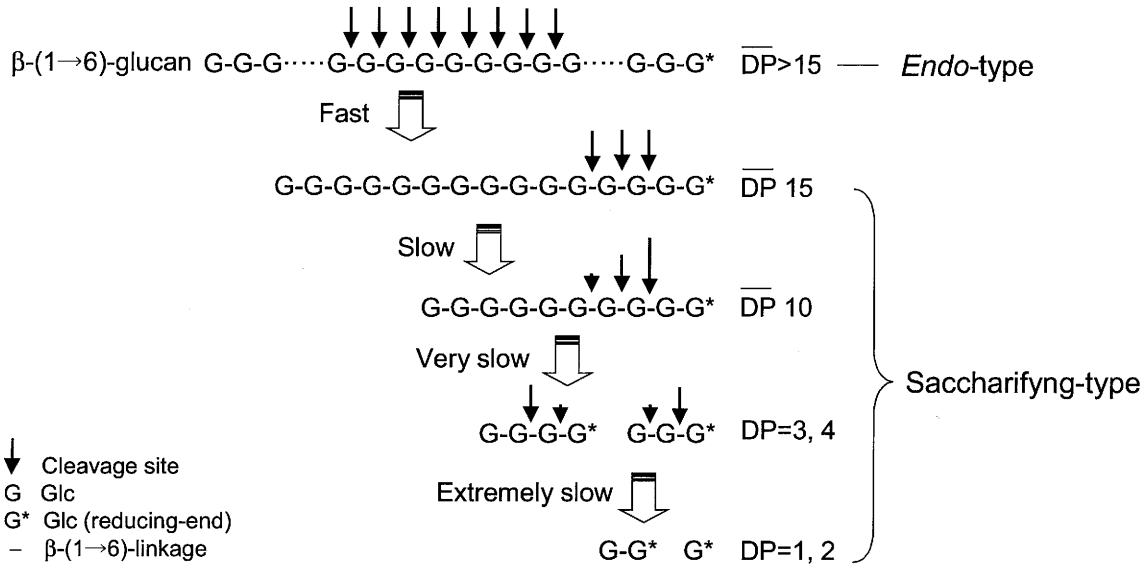

Scheme 2. Proposed mechanism of the hydrolytic action of β-(1→6)-glucanase from *P. multicolor* on pustulan.

Table 1. Summary of the purification and yield of β-(1→6)-glucanase from *P. multicolor*

Purification step	Total protein (mg)	Total activity (U)	Specific activity (U/mg)	Yield (%)	Purification (fold)
Crude enzyme	73.0	49.1	0.7	100.0	1.0
$(NH_4)_2SO_4$ precipitation	29.7	33.3	1.1	67.8	1.7
CM Sepharose F.F.	0.8	3.7	4.5	7.6	6.7
Affinity	0.007	1.1	164.1	2.2	244.3

Table 2. Substrate specificity of purified β-(1→6)-glucanase toward selected glucans and oligosaccharides

Substrate	Linkage type	Activity (U/mg)
Pustulan	β-1,6	164.1
Yeast glucan	β-1,3: β-1,6	1.4
Soluble starch	α-1,4: α-1,6	0
Carboxymethyl cellulose	β-1,4	0
Curdlan (*Alcaligenes faecalis*)	β-1,3	0
Gen_8	β-1,6	4.2

Table 3. ^{13}C-chemical shifts of methyl β-gentiooligosides (DP 2-6) in D_2O solution (30 °C)

		Chemical shift (δ)						
Compound	Residue [a]	C-1	C-2	C-3	C-4	C-5	C-6	$\underline{C}H_3$
Gen_2 β-*O*Me	CH_3							60.2
	1	106.2	75.87	78.5	72.3	77.7	71.4	
	2	105.7	75.91	78.5	72.5	78.7	63.6	
Gen_3 β-*O*Me	CH_3							60.2
	1	106.2	75.87	78.5	72.3	77.7	71.6	
	2	105.74	75.87	78.4	72.2	77.8	71.4	
	3	105.69	75.93	78.5	72.5	78.7	63.6	
Gen_4 β-*O*Me	CH_3							60.2
	1	106.2	75.88	78.5	72.3	77.70	71.6	
	2	105.7	75.88	78.4	72.3	77.74	71.6	
	3	105.7	75.88	78.4	72.3	77.77	71.5	
	4	105.8	75.93	78.5	72.5	78.8	63.6	
Gen_5 β-*O*Me	CH_3							60.3
	1	106.2	75.89	78.53	72.3	77.7	71.6	
	2	105.7	75.89	78.45	72.3	77.7	71.6	
	3	105.7	75.89	78.45	72.3	77.7	71.6	
	4	105.84	75.89	78.45	72.3	77.7	71.5	
	5	105.77	75.94	78.53	72.5	78.8	63.6	
Gen_6 β-*O*Me	CH_3							60.3
	1	106.2	75.88	78.5	72.3	77.7	71.6	
	2	105.7	75.88	78.4	72.3	77.7	71.6	
	3	105.7	75.88	78.4	72.3	77.7	71.6	
	4	105.8	75.88	78.4	72.3	77.7	71.6	
	5	105.8	75.88	78.4	72.3	77.7	71.5	
	6	105.8	75.92	78.5	72.5	78.8	63.6	

[a] Numbers indicate the position of the glucose residues; the glucose residue that is attached to the methyl group is represented as 1.

Table 4. ^{1}H- and ^{13}C-chemical shifts of *p*-nitrophenyl β-gentiooligosides (DP 2-6) in D_2O solution (25 °C).

		Chemical shift (δ)											
ompound	Residue [a]	C-1	C-2	C-3	C-4	C-5	C-6	*o*-ph	*m*-ph	*p*-ph	C-O	H-1	$J_{1,2}$ [b]
en_2 β-*p*NP	*p*NP							119.4	128.9	145.4	164.4		
	1	102.2	75.5	78.2	72.0	78.3	71.2					5.29	6.7
	2	105.6	75.9	78.5	72.5	78.7	63.6					4.48	8.0
en_3 β-*p*NP	*p*NP							119.5	129.0	145.4	164.4		
	1	102.1	75.6	78.2	72.2	78.1	71.7					5.29	5.5
	2	105.8	75.94	78.4	72.2	77.7	71.3					4.50	8.0
	3	105.6	75.89	78.5	72.5	78.7	63.6					4.46	7.9
en_4 β-*p*NP	*p*NP							119.5	129.0	145.4	164.5		
	1	102.1	75.5	78.2	72.16	78.1	71.7					5.30	7.6
	2	105.7	75.92	78.4	72.20	77.7	71.6					4.51	7.9
	3	105.8	75.88	78.4	72.3	77.7	71.5					4.48	7.9
	4	105.7	75.86	78.5	72.4	78.7	63.6					4.46	8.0
en_5 β-*p*NP	*p*NP							119.5	129.0	145.5	164.5		
	1	102.2	75.6	78.2	72.19	78.1	71.7					5.31	7.4
	2	105.73	75.91	78.4	72.25	77.72	71.6					4.51	7.9
	3	105.80	75.87	78.4	72.33	77.72	71.8					4.49	8.3
	4	105.83	75.83	78.4	72.21	77.75	71.4					4.47	8.0
	5	105.68	75.93	78.5	72.5	78.7	63.6					4.51	7.9
en_6 β-*p*NP	*p*NP							119.5	129.1	145.5	164.5		
	1	102.2	75.6	78.2	72.20	78.1	71.70					5.31	7.7
	2	105.74	75.91	78.4	72.25	77.72	71.65					4.51	7.4
	3	105.8	75.87	78.4	72.34	77.72	71.8					4.49	9.2
	4	105.8	75.84	78.4	72.21	77.74	71.65					4.48	8.0
	5	105.8	75.93	78.4	72.31	77.8	71.4					4.52	7.6
	6	105.71	75.87	78.5	72.5	78.7	63.6					4.52	7.6

Numbers indicate the position of the glucose residues; the glucose residue that is attached to *p*-nitrophenyl group is represented as 1.

$J_{1,2}$, coupling constants given in Hz.

Table 5. Frequency and relative activity of the β-(1→6)-glucanase-catalyzed hydrolysis of methyl β-gentiooligosides and *p*-nitrophenyl β-gentiooligosides

Compound	Frequency of hydrolysis (%)[a]	Relative activity (%)[b]
Gen_2 β-*O*Me	100 G — G — CH_3	4
Gen_3 β-*O*Me	9 91 G — G — G — CH_3	13
Gen_4 β-*O*Me	5 39 56 G — G — G — G — CH_3	67
Gen_5 β-*O*Me	31 30 39 G — G — G — G — G — CH_3	81
Gen_6 β-*O*Me	12 31 30 27 G — G — G — G — G — G — CH_3	100
Gen_2 β-*p*NP	100 G — G — *p*NP	1
Gen_3 β-*p*NP	39 61 G — G — G — *p*NP	2
Gen_4 β-*p*NP	90 10 G — G — G — G — *p*NP	22
Gen_5 β-*p*NP	38 62 G — G — G — G — G — *p*NP	39
Gen_6 β-*p*NP	25 29 46 G — G — G — G — G — G — *p*NP	100

[a] The frequency of the enzymatic cleavage of the indicated glycosidic linkages was estimated by measuring the amount of lower methyl β-gentioligosides and *p*-nitrophenyl gentiooligosides liberated from the corresponding methyl β-gentiooligosides and *p*-nitrophenyl β-gentiooligosaccharides, respectively. [b] The hydrolytic rate of Gen_6 β-*PNP* and Gen_6 β-*p*NP was arbitrarily set to 100. G, glucose residue.

Table 6. Frequency and relative activity of the β-(1→6)-glucanase-catalyzed hydrolysis of

Compound	Frequency of hydrolysis (%)[a]	Relative activity (%)[b]
Gen_2	100 G — G*	<1
Gen_3	a A a + A = 100 (a<A) G — G — G*	15
Gen_4	68 32 G — G — G — G*	21
Gen_5	a A 22 a + A = 78 (a<A) G — G — G — G — G*	77
Gen_6	a 22 A 13 a + A = 65 (a<A) G — G — G — G — G — G*	100

[a] The frequency of the enzymatic cleavage of the indicated glycosidic linkages was estimated by measuring the amount of lower gentiooligosaccharides liberated from the corresponding gentiooligosaccharides.

[b] The hydrolytic rate of Gen_6 was arbitrarily set at 100.

G, glucose residue; G*, glucose residue with a reducing end.

References

General Introduction

1. Berg, J. M.; Tymoczko, L. J.; Stryer, L. *Biochemistry*, 6th International ed., W. H. Freeman & Co.: New York, 2006; Chapter 11.

2. Schuerch, C. *Polysaccharides in Encyclopedia of Polymer Science and Engineering*, 2nd ed.; John Wiley & Sons: New York, 1986; Vol. 13, 87-162.

3. *Carbohydrates in Chemistry and Biology*; Ernst, B., Hart, G. W., Sinaÿ, P., Eds.; Wiley-VCH: Weinheim, Germany, 2000.

4. *Glycoscience*, 2nd ed.; Fraser-Reid, B. O., Tatsuta, K., Thiem, J., Coté, G. L., Flitsch, S., Ito, Y., Kondo, H., Nishimura, S.-I., Yu, B., Eds.; Springer: Berlin, 2008.

5. Essentials of Glycobiology, 2nd ed.; Varki, A, Cummings, R. D., Esko, J. D., Freeze, H. H., Stanley, P., Bertozzi, C. R., Hart, G. W., Etzler, M. E., Eds.; Cold Spring Harbor Laboratory Press: New York, 2009.

6. Raman, R; Raguram, S.; Venkataraman, G.; Paulson, J. C.; Sasisekharan. R.; *Nat. Methods* **2005**, 2, 817–24.

7. Seeberger, P. H. *Carbohydr. Res.* **2008**, 343, 1889-1896.

8. Varki, A. *Cell* **2006**, 126, 841–5.

9. Ohtsubo, K *Cell* **2006**, 126, 855–67.

10. Cote, G. L.; Tao, B. Y. *Glycoconjugate J.* **1990**, 145-162

11. Murata, T.; Usui T. *Biosci. Biotechnol. Biochem.* **2006,** 70, 1049-1059.

12. Wang, L. X.; Huang, W. *Curr. Opin. Chem. Biol.* **2009**, *13*, 592-600.

13. Peat, S.; Whelan, W. J.; Hinson, K. A. *Nature* **1952**, 170, 1056-7.

14. Bojarova, P.; Kren, V.; *Trends Biotechnol.* **2009**, 27, 199-209.

15. Kadokawa, J. *Chem. Rev.* **2011**, 111, 4308-4345.

Chapter I - Enzymatic synthesis of an α-chitin-like substance *via* lysozyme-mediated transglycosylation

1. Kurita, K. *Polym. Degrad. Stab.* **1995**, *59*, 117-120.

2. Hirano, S. *Biotechnol. Annu. Rev.* **1996**, *2*, 237-258.

3. Jayakumar, R.; Prabaharan, M.; Nair, S. V.; Tamura, H. *Biotechnol. Adv.* **2010**, *28*, 142-150.

4. Yoshiike, Y.; Yokota, S.; Tanaka, N.; Kitaoka, T.; Wariishi, H. *Carbohydr. Polym.* **2010**, *82*, 21-27.

5. Sato, H.; Mizutani, S.; Tsuge, S.; Ohtani, H.; Aoki, K.; Takasu, A.; Okada, M.; Kobayashi, S.; Kiyosada, T.; Shoda, S. *Anal. Chem.* **1998**, *70*, 7-12.

6. Kang, M. S.; Narayasamy, E.; Mattia, E.; Au-Young, J.; Robbins, P. W.; Cabib, E. *J. Biol. Chem.* **1984**, *259*, 14966-14972.

7. Muthanaa, S.; Caoa, H.; Chen, X. *Curr. Opin. Chem. Biol.* **2009**, *13*, 573-581.

8. Wang, L. X.; Huang, W. *Curr. Opin. Chem. Biol.* **2009**, *13*, 592-600.

9. Kobayashi, S.; Kiyosada, T.; Shoda, S. *J. Am. Chem. Soc.* **1996**, *118*, 13113-13114.

10. Sakamoto, J.; Sugiyama, J.; Kimura, S; Imai, T.; Itoh, T.; Watanabe, T.; Kobayashi, S. *Macromolecules* **2000**, *33*, 4155-4160.

11. Usui, T.; Hayashi, Y.; Nanjo, F.; Sakai, K.; Ishido, Y. *Biochim. Biophys. Acta* **1987**, *923*, 302-309.

12. Usui, T.; Matsui, H.; Isobe, K. *Carbohydr. Res.* **1990**, *203*, 65-77.

13. Minke, R.; Blackwell, J. *J. Mol. Biol.* **1978**, *120*, 167-181.

14. Rinaudo, M. *Prog. Polym. Sci.* **2006**, *31*, 603-632.

15. Dweltz, N. E. *Biochim. Biophys. Acta* **1961**, *51*, 283-294.

16. Kobayashi, S.; Kashiwa, K.; Kawasaki, T.; Shoda, S. *J. Am. Chem. Soc.* **1991**, *113*, 3079-3084.

17. Nanjo, F.; Sakai, K.; Usui, T. *J. Biochem.* **1988**, *104*, 255-258.

18. Rupley, J. A. *Proc. R. Soc. Lond. B* **1967**, *167*, 416-428.

19. Kurita, K.; Ishii, S.; Tomioka, K.; Nishimura, S.; Shimoda, K. *J. Polymer. Sci., Polym. Chem.* **1994**, *32*, 1027.

20. Fujimoto, Y.; Hattori, T.; Uno, S.; Murata, T.; Usui, T. *Carbohydr. Res.* **2009**, *344*, 972-978.

21. Saint-Blancard, J.; Chuzel, P.; Mathieu, Y.; Perrot, J.; Jollès, P. *Biochem. Biophys. Acta* **1970**, *220*, 300-306.

Chapter II - Enzymatic synthesis of cellulose II-like substance *via* cellulolytic enzyme-mediated transglycosylation in an aqueous medium

1. Liungdahl, L. G.; Eriksson, K. Ecology of microbial cellulose degradation. VIII. In *Advances in Microbial Ecology*, **1985**, 237-299, Edited by K. C. Marshall. New York.

2. Atalla, R. H.; VanderHart, L. D. *Science* **1984**, *223*, 283-285.

3. Heux, L.; Dinand, E.; Vignon, M. R. *Carbohydr. Polym.* **1999**, *40*, 115-124.

4. Katharine, S. *Nature* **2011**, *474*, 12-14.

5. Siró, I.; Plackett D. *Cellulose*, **2010**, *17*, 459-494.

6. Eichhorn, S. J.; Dufresne, A.; Aranguren, M.; Marcovich, N. E.; Capadona, J. R.; Rowan, S. J.; Weder, C.; Thielemans, W.; Roman, M.; Renneckar, S.; Gindl, W.; Veigel, S.; Keckes, J.; Yano, H.; Abe, K.; Nogi, M.; Nakagaito, A. N.; Mangalam, A.; Simonsen, J.; Benight, A. S.; Bismarck, A.; Berglund, L. A.; Peijs, T. *J. Mater. Sci.*, **2010**, *45*, 1-13.

7. John, M. J.; Thomas, S. *Carbohydr. Polym.* **2008**, *71*, 343-364.

8. Lin, F. C.; Brown, R. M., Jr.; Cooper, J. B.; Delmer, D. P. *Science* **1985**, *230*, 822-825.

9. Bureau, T. E.; Brown, R. M., Jr. *Proc. Natl. Acad. Sci. USA* **1987**, *84*, 6985-6989.

10. Okuda, K.; Li, L., Kudlicka, K.; Brown, R. M., Jr. *Plant Physiol.* **1993**, *101*, 1131-1142.

11. Lai-Kee-Him, J.; Chanzy, H.; Müller, M.; Putaux, J-L.; Imai, T.; Bulone, V. *J. Biol. Chem.* **2002**, *277*, 36931-36939.

12. Colombani, A.; Djerbi, S.; Bessueille, L.; Blomqvist, K.; Ohlsson, A.; Berglund, T.; Teeri, T. T.; Bulone, V. *Cellulose* **2004**, *11*, 313-327.

13. Cifuentes, C.; Bulone, V.; Emons, A. M. C. *J. Integr. Plant Biol.* **2010**, *52*, 221-233.

14. Sugiyama, J.; Persson, J.; Chanzi, H. *Macromolecules* **1991**, *24*, 2461-2466.

15. Saxena, I. M.; Brrown, R. M. J. *Ann. Bot.* **2005**, *96*, 9-21.

16. Rånby, B.G. *Acta Chem. Scand.* **1952**, *6*, 101-115.

17. Sisson, W. *Science* **1938**, *87*, 350.

18. Kadokawa, J. *Chem. Rev.* **2011**, *111*, 4308-4345.

19. Kobayashi, S.; Kashiwa, K.; Kawasaki, T.; Shoda, S. *J. Am. Chem. Soc.* **1991**, *113*, 3079–3084.

20. Fort, S.; Boyer, V.; Gerffe, L.; Davies, G. J.; Moroz, O.; Christiansen, L.; Schülein, M.; Cottaz, S.; Driguez, H. *J. Am. Chem. Soc.* **2000**, *122*, 5429-5437.

21. Lee, J. H.; Brown, R. M., Jr.; Kuga, S.; Shoda, S.; Kobayashi, S. *Proc. Natl. Acad. Sci. USA* **1994**, *91*, 7425-7429.

22. Egusa, S; Kitaoka, T; Goto, M.; Wariishi, H. *Angew. Chem. Int. Edit.* **2007**, *46*, 2063-2065.

23. Egusa, S.; Kitaoka, T.; Igarashi, K.; Samejima, M.; Goto, M.; Wariishi, H. *J. Mol. Catal. B: Enzym.* **2010**, *67*, 225-230.

24. Hiraishi, M.; Igarashi, K.; Kimura, S.; Wada, M.; Kitaoka, M.; Samejima, M. *Carbohydr. Res.* **2009**, *344*, 2468-2473.

25. Kono, H.; Numata, Y.; Erata, T.; Takai, M. *Polymer* **2004**, *45*, 2843-2852.

26. Kono, H.; Numata, Y. *Polymer* **2004**, *45*, 4541-4547.

27. Malm, E.; Bulone, V.; Wickholm, K.; Larsson, P. T.; Iversen, T. *Carbohydr. Res.* **2010**, *345*, 97-100.

28. Yasutake, N.; Totani, K.; Harada, Y.; Haraguchi, S.; Murata, T.; Usui, T. *Biosci. Biotechnol. Biochem.* **2003**, *67*, 1530-1536.

29. Yasutake, N.; Totani, K.; Harada, Y.; Haraguchi, S.; Murata, T.; Usui, T. *Biochem. Biophys. Acta* **2003**, *1620*, 252-258.

30. Biely, P.; Vršanskă, M.; Claeyssens, M. *Eur. J. Biochem.* **1991**, *200*, 157-163.

31. Kleywegt, G. J.; Zou, J. Y.; Divne, C.: Davies, G. J.; Sinning, I.; Stâhlberg, J.; Reinikainen, T.; Srisodsuk, M.; Teeri, T. T.; Jones, T. A. *J. Mol. Biol.* **1997**, *272*, 383-397.

32. Nishiyama, Y.; Langan, P.; Chanzy, H. *J. Am. Chem. Soc.* **2002**, *124*, 9074-9082.

33. Nishiyama, Y.; Sugiyama, J.; Chanzy, H.; Langan. P. *J. Am. Chem. Soc.* **2003**, *125*, 14300-14306.

34. Wada, M.; Chanzy, H.; Nishiyama, Y.; Langan. P. *Macromolecules*, **2004**, *37*, 8548-8555.

35. Langan, P.; Sukumar, N.; Nishiyama Y.; Chanzy, H. *Cellulose*, **2005**, *12*, 551-562.

36. Dinand, E.; Vignon, M.; Chanzy, H.; Heux, L. *Cellulose* **2002**, *9*, 7-18.

37. Ogata, M.; Kameshima, Y.; Hattori, T.; Michishita, K.; Suzuki, T.; Kawagishi, H.; Totani, K.; Hiratake, J.; Usui, T. *Carbohydr. Res.* **2010**, *345*, 2623-2629.

Chapter III - Mode of action of a β-(1→6)-glucanase from *Penicillium multicolor*

1. Kapteyn, J. C.; Montijn, R. C.; Vink, E.; De la Cruz, J; Llobell, A.; Douwes, J. E.; Shimoi, H.; Lipke, P. N.; Klis, F. M. *Glycobiology* **1996**, 6, 337-345.

2. Lindberg, B.; McPherson, J. *Acta Chem. Scand.* **1954**, *8*, 985-988.

3. Henrissat, B.; Bairoch, A. *Biochem. J.* **1993**, *293*, 781-788.

4. Davies, G.; Henrissat, B. *Structure* **1995**, *3*, 853-859.

5. Henrissat, B.; Bairoch, A. *Biochem. J.* **1996**, *316*, 695-696.

6. Henrissat, B.; Davies, G. J. *Curr. Op. Struct. Biol.* **1997**, *7*, 637-644.

7. Reese, E. T.; Parrish, F. W.; Mandels, M. *Can. J. Microbiol.* **1962**, *8*, 327-334.

8. Shibata, Y.; Fukimbara, T. *J. Ferment. Technol.* **1973**, *51*, 216-226.

9. Yamamoto, S.; Kobayashi, R.; Nagasaki, S. *Agric. Biol. Chem.* **1974**, *38*, 1493-1500.

10. Santos, T.; Villanueva, J. R.; Nombela, C. *J. Bacteriol.* **1977**, *129*, 52-58.

11. Katohda, S.; Suguki, F.; Katsuki, S.; Sato, T. *Agric. Biol. Chem.* **1979**, *43*, 2029-2034.

12. Hiura, N.; Nakajima, T.; Matsuda, K. *Agric. Biol. Chem.* **1987**, *51*, 3315-3321.

13. Lora, J. M.; De la Cruz, J.; Llobell, A.; Benítez, T.; Pintor-Toro, J. A. *Mol. Gen. Genet.* **1995**, *247*, 639-645.

14. Pitson, S. M.; Seviour, R. J.; McDougall, B. M.; Stone, B. A.; Sadek, M. *Biochem. J.* **1996**, *316*, 841-846.

15. Martin, K. L.; Unkles, S. E.; McDougall, B. M.; Seviour R. J. *Enzyme Microb. Technol.* **2006**, *38*, 351-357.

16. Montero, M.; Sanz, L., Rey, M.; Llobell, A.; Monte, E. *J. Appl. Microbiol.* **2007**, *103*, 1291-1300.

17. Konno, N.; Sakamoto, Y. *Appl. Microbiol. Biotechnol.* **2011**, *91*, 1365-1373.

18. De La Cruz, J.; Pintor-Toro, J. A.; Benítez, T.; Llobell, A. *J. Bacteriol.* **1995**, *177*, 1864-1871.

19. De La Cruz, J.; Llobell, A. *Eur. J. Biochem* **1999**, *265*, 145-151.

20. Montero, M.; Sanz, L.; Rey, M.; Monte, E.; Llobell, A *FEBS J.* **2005**, *272*, 3441-3448.

21. Himmel, M. E.; Ding, S. Y.; Johnson, D. K.; Adney, W. S.; Nimlos, M. R.; Brady, J. W.; Foust, T. D. *Science* **2007**, *315*, 804-807.

22. Vaaje-Kolstad, G.; Westereng, B; Horn, S. J.; Liu Z.; Zhai H.; Sørlie, M.; Eijsink, V. G.. H. *Science* **2010**, *330*, 219-222.

23. A. Reeve, in: F.W. Schenck, R. Hebeda (Eds.), Starch Hydrolysis Products, VCH Publishers, New York, 1992, p. 79.

24. Fujimoto, Y.; Hattori, T.; Uno, S.; Murata, T.; Usui, T. *Carbohydr. Res.* **2009**, *344*, 972-978.

25. McCarter, J. D.; Withers, G. S. *Curr. Opin. Struct. Biol.* **1994**, *4*, 557-564.

26. Somogyi, M. *J. Biol. Chem.* **1952**, *195*, 19-23.

27. Nelson, N. J. *Methods Enzymol.* **1955**, *3*, 85-86.

28. Jansson, P. E.; Kenne, L.; Kolare, I. *Carbohydr Res.* **1994**, *257*, 163-74.

29. Hrmova, M.; MacGregor, A. E.; Biely, P.; Stewart, R. J.; Fincher, G. B. *J. Biol. Chem.* **1998**, *273*, 11134-11143.

Summary of Thesis

Chapter I - Enzymatic synthesis of an α-chitin-like substance *via* lysozyme-mediated transglycosylation

The enzymatic synthesis of α-chitin-like substance *via* a non-biosynthetic pathway has been achieved by transglycosylation in an aqueous system of the corresponding substrate, tri-*N*-acetyl chitotriose [$(GlcNAc)_3$] for lysozyme. A significant amount of water-insoluble product precipitated out from the reaction system. MALDI-TOF mass analysis showed that the resulting precipitate had a degree of polymerization (DP) of up to 15 from $(GlcNAc)_3$. Solid-state ^{13}C NMR analysis revealed that the resulting water-insoluble product is chitin-like substance consisted of *N*-acetylglucosamine (GlcNAc) residues joined exclusively in a β-(1→4)-linked chain with stringent regio-/stereo selection. X-ray diffraction (XRD) measurement as well as ^{13}C NMR analysis showed that the crystal structure of synthetic product corresponds to α-chitin with a high degree of crystallinity. We propose that the multiple oligomers form a α-chitin-like substance as a result of self-assembly *via* oligomer-oligomer interaction when they precipitate.

Chapter II - Enzymatic synthesis of cellulose II-like substance *via* cellulolytic enzyme-mediated transglycosylation in an aqueous medium

The enzymatic synthesis of cellulose-like substance *via* a non-biosynthetic pathway has been achieved by transglycosylation in an aqueous system of the corresponding substrate, cellotriose for cellulolytic enzyme endo-acting endoglucanase I (EG I) from *Hypocrea jecorina*. A significant amount of water-insoluble product precipitated out from the reaction system. MALDI-TOF mass analysis showed that the resulting precipitate had a degree of polymerization (DP) of up to 16 from cellotriose. Solid-state ^{13}C-NMR spectrum of the resulting water-insoluble product revealed that all carbon resonance lines were assigned to two kinds of anhyroglucose residues in the corresponding structure of cellulose II. X-ray

diffraction (XRD) measurement as well as ^{13}C NMR analysis showed that the crystal structure corresponds to cellulose II with a high degree of crystallinity. We propose the multiple oligomers form highly crystalline cellulose II as a result of self-assembly *via* oligomer-oligomer interaction when they precipitate.

Chapter III - Mode of action of a β-(1→6)-glucanase from *Penicillium multicolor*

β-(1→6)-glucanase from the culture filtrate of *Penicillium multicolor* LAM7153 was purified by ammonium sulfate precipitation, followed by cation-exchange and affinity chromatography using gentiotetraose (Gen_4) as ligand. The hydrolytic mode of action of the purified protein on β-(1→6)-glucan (pustulan) was elucidated in real time during the reaction by HPAEC-PAD analysis. Gentiooligosaccharides (DP 2-9, Gen_{2-9}), methyl β-gentiooligosides (DP 2-6, Gen_{2-6} β-*PNP*), and *p*-nitrophenyl β-gentiooligosides (DP 2-6, Gen_{2-6} β-*p*NP) were used as substrates to provide analytical insight into how the cleavage of pustulan ($\overline{DP}$ 320) is actually achieved by the enzyme. The enzyme was shown to completely hydrolyze pustulan in three steps as follows. In the initial stage, the enzyme quickly cleaved the glucan with a pattern resembling an *endo*-hydrolase to produce a short-chain glucan ($\overline{DP}$ 45) as an intermediate. In the midterm stage, the resulting short-chain glucan was further cleaved into two fractions corresponding to DP 15-7 and DP 2-4 with great regularity. In the final stage, the lower oligomers corresponding to DP 3 and DP 4 were very slowly hydrolyzed into glucose and gentiobiose (Gen_2). As a result, the hydrolytic cooperation of both an *endo*-type and saccharifying-type reaction by a single enzyme, which plays a bifunctional role, led to complete hydrolysis of the glucan. Thus, β-(1→6)-glucanase varies its mode of action depending on the chain length derived from the glucan.

Acknowledgments

I feel privileged to express deep sense of appreciation to my supervisor Professor Taichi Usui of the Faculty of Agriculture, Shizuoka University, for his valuable guidance, kind assistance, constant encouragement, and great endurance throughout the course of this study. I would like to express my hearty thanks to Professor Hirokazu Kawagishi, Associate Professor Takeomi Murata, and Associate Professor Hirofumi Hirai of the Faculty of Agriculture, Shizuoka University for their helpful and critical suggestions on this research.

I also extend my sincere thanks to Makoto Ogata Research Assistant Professor of the Faculty of Agriculture, Shizuoka University for his valuable comments during this study. I would like to express my deep gratitude to Associate Professor Hideo Dohra of Institute for Genetic Research and Biotechnology, Shizuoka University for the measurements of MALDI-TOF mass spectrometry. I would like to express my deep gratitude to Professor Kazuhide Totani and Professor Mitsuru Nikaido of Department of Chemical Engineering, Ichinoseki National College of Technology for the measurements of XRD. Further, I also would like to express my deep gratitude to Professer Takashi Nakamura and Dr. Hiroyuki Koshino of Molecular Characterization Team, RIKEN Advanced Science Institute for the measurements of solid-state ^{13}C NMR spectroscopy. I thank Mr. Akihito Yagi of the Faculty of Agriculture, Shizuoka University for the measurements of ESI-MS spectrometry.

I am also grateful to Mr. Shuji Uno, Ms. Yasuna Kato, Ms. Yumiko Kameshima, Ms. Yoko Sakabe, Mr. Kousuke Michishita, Mr. Yuichi Tami, Mr. Naohiro Sugiyama, Mr. Daichi Mori, and Mr. Yoshinori Yasumoto of the Faculty of Agriculture, Shizuoka University.

I would like to thank Dr. Kazuo Sakai, Mr. Kazuhiro Yamamoto, Mr. Shigeru Saito and Dr. Yoshiharu Matahira for an opportunity that made it possible to complete this study. I am also grateful to Mr. Masaaki Tonaka, Dr. Yoshinori Misawa, Mr. Masayoshi Yamamoto, Dr. Daiki Kubomura, Ms.

Kanako Shibata, Ms. Ayano Masui, Ms. Junko Mitsuishi, Mr. Takashi Nakatomi, and Yaizu Suisankagaku Industry Co., Ltd. R&D Members.

I am grateful to Amano Enzyme Inc. for generously presenting a crude enzyme preparation from *Penicillum multicolor* IAM7153 and Nihon Shokuhin Kako Co., Ltd. for kindly presenting gentiobiose.

Finally, I thank my wife Chieko Hattori and my family for their generous support over the past years.

Takeshi Hattori